Master's thesis

NTNU
Norwegian University of Science and Technology

Tore Kolstad Linløkken

Development of a Test Method for Evaluating Durability of Adhesive Tapes in Construction

Master's thesis in Civil and Environmental Engineering
Supervisor: Bozena Hrynyszyn
Co-supervisor: Stig Geving, Malin Sletnes
June 2023

NTNU
Norwegian University of Science and Technology

SINTEF

Tore Kolstad Linløkken

Development of a Test Method for Evaluating Durability of Adhesive Tapes in Construction

Master's thesis in Civil and Environmental Engineering
Supervisor: Bozena Hrynyszyn
Co-supervisor: Stig Geving, Malin Sletnes
June 2023

Norwegian University of Science and Technology

NTNU
Norwegian University of
Science and Technology

Abstract

Achieving adequate airtightness in a building envelope is crucial for enhancing its overall energy efficiency and preventing moisture-related damages in a Nordic climate. Air leakages typically arise from joints and perforations in air and vapour barriers installed within exterior walls and roofs. Sealing such building details with durable solutions is essential for ensuring sufficient airtightness overall. In recent years, adhesive tapes have increasingly been used for this application. However, there remains uncertainty regarding its performance in the long-term.

The purpose of this thesis is to contribute to the development of a new test method with sufficient accuracy, reproducibility, and repeatability fit for use in the development and certification of tape products and systems for air-sealing application in buildings. The thesis offers theoretical background on the topics of airtightness and moisture transfer, along with relevant technical requirements which currently apply to the Norwegian construction industry. The thesis presents an overview of the current state of the art by incorporating findings from a literature review. This includes an analysis of established methods currently being used for evaluation of tape joint durability, as well as other experimental test methods.

The test method in development is based on air permeability measurements using a Test Stand made from welded-together steel plates. The effective leakage area of the test specimens measures approximately 450x1000 mm, and each includes four joints, made by applying tape over 900 mm long cuts in the substrate material. The durability of products is assessed by measuring and comparing permeability rates before and after artificial ageing. The aptness of the method is assessed through a measurement program involving six different material samples, each made by combining an adhesive tape with a substrate material. Two substrate materials were involved, a vapour barrier and a roofing membrane, along with three different adhesive tapes. Parallel to the air permeability tests, the material samples were tested for peel resistance according to the Norwegian standard NS-EN 12316-2:2013, before and after the same artificial ageing procedures to examine how the two methods compare with regard to durability assessment.

The artificial ageing procedures led to significant degradation of air permeability across all material samples. Changes in peel resistance were comparatively small, and three out of six material samples even exhibited increased peel resistance after ageing. Fluctuating system leakage contributed to uncertainty in the permeability measurements and made it difficult to determine what share of air leakage could be attributed to the tape joints themselves. Additionally, as permeability rates seemingly depended on the implementation quality of individual specimens, the method in its current form is not perceived as reliable enough to precisely determine the airtightness inherent to distinctive tape products. However, the method is considered applicable for verifying that permeability rates remain below relevant threshold values after ageing.

Although the method in development displays limitations in terms of reproducibility, accuracy, and repeatability, it is regarded as a promising concept. Through further development, the method is believed to be suitable for potential integration into wider evaluation programs addressing adhesive tape durability, supplementary to existing methods such as NS-EN 12316-2:2013.

Sammendrag

Tilstrekkelig lufttetthet i bygningers klimaskall er sentralt i forbindelse med energieffektivitet og forebygging av fuktskader. Luftlekkasjer kan typisk oppstå i sammenheng med skjøter, overganger og punkteringer i vind- og dampsperresjikt i yttervegger og tak. Å sikre god tetting i forbindelse med slike detaljer er nødvendig for å oppnå tilfredsstillende lufttetthet i bygget som helhet. Bruk av teip til tetteløsninger har blitt mer og mer vanlig de siste årene, men det er ennå usikkerhet knyttet til produktenes bestandighet i et langtidsperspektiv.

Denne masteroppgaven har til hensikt å bidra til utvikling av en ny testmetode for evaluering av bestandighet i teipede skjøter brukt til lufttetting av klimaskall. Metodens potensielle bruksområde tenkes på sikt å omfatte produktutvikling og sertifisering. Oppgaven omfatter et måleprogram som tar i bruk den nyutviklede testmetoden, med hensikt å evaluere dens nøyaktighet, etterprøvbarhet og repeterbarhet. En litteraturstudie er gjennomført for å kartlegge teoretisk bakgrunn, samt relevante tekniske krav i norsk byggenæring. I tillegg presenteres flere eksisterende evalueringsmetoder. Herunder etablerte testmetoder som på nåværende tidspunkt brukes i forbindelse med produktsertifisering, samt fire alternative, eksperimentelle tilnærminger.

Den nyutviklede testmetoden er basert på luftpermeabilitetsmålinger, som gjennomføres ved hjelp av et trykkammer bestående av sammensveisede stålplater. Prøvestykker består av et substratmateriale, med effektivt prøveareal på 450x1000 mm, hvor skjøter er laget ved å påføre teip over fire 900 mm lange kutt. Bestandigheten til skjøtene evalueres ved å måle luftpermeabiliteten til prøvestykkene før og etter akselerert aldring. Måleprogrammet involverer seks materialkombinasjoner, satt sammen av tre ulike teipprodukter og to ulike substrat; en dampsperrefolie og en undertaksmembran. Parallelt med luftpermeabilitetsmålingene, er de samme materialkombinasjonene testet for spaltestyrke iht. standardmetoden NS-EN 12316-2:2013 før og etter akselerert aldring. Dette er gjort for å undersøke hvordan resultater fra den nyutviklede metoden samsvarer med etablerte testmetoder.

Etter akselerert aldring utviste samtlige materialprøver betydelig reduksjon i lufttetthet. Endring i spaltestyrke var derimot liten. Tre av de seks materialprøvene viste økning i spaltestyrke etter aldringsprosessen. På grunn av usikkerhet knyttet til trykkammerets egenlekkasje og måleutstyrets nøyaktighet, var det vanskelig å fastslå nøyaktig permeabilitet i de tetteste prøvestykkene. Prøvestykkenes utførelse virket også å ha stor innvirkning på målingene. På bakgrunn av disse observasjonene anses metoden, i sin nåværende form, som lite egnet for å nøyaktig tallfeste luftpermeabilitet til enkeltprodukter. Imidlertid vurderes den som velegnet til å undersøke om skjøtene møter relevante minimumskrav, ved å dokumentere at permeabiliteten forblir under relevante terskelverdier.

Til tross for begrensninger med hensyn til reproduserbarhet, nøyaktighet og repeterbarhet, vurderes metodens overordnede konsept likevel som en hensiktsmessig tilnærming til evaluering av bestandighet i teipede skjøter. Ved å videreutvikle konseptet antas metoden å være egnet som en integrert del av et helhetlig evalueringsprogram, i kombinasjon med eksisterende metoder som NS-EN 12316-2:2013.

Preface

This master's thesis marks the end of a 5-year master's program in Civil and Environmental Engineering at NTNU Trondheim, with a major in Building Technology. The thesis has been written in collaboration with SINTEF Community as part of the research project TightEN.

The thesis focuses on the development of an experimental test method aimed at evaluating the durability of adhesive tape joints based on air permeability measurements. The suitability and reliability of the test method have subsequently been assessed based on laboratory experiments conducted at the laboratories of SINTEF Community in Trondheim.

I would like to express my sincere gratitude to my supervisor, Bozena Dorota Hrynyszyn, as well as co-supervisors Stig Geving and Malin Sletnes for their academic input, assistance with writing the thesis, and other contributions that have been necessary to complete the work. Furthermore, I would like to thank Ole Aunrønning and Stig Rudolfsen for their practical assistance in the laboratory. Despite occasional delays and unforeseen events, accompanied by moderate frustration and worry, the work has brought forth valuable experience.

Finally, I would like to thank my mother, father, and brother Harald for their moral support throughout this period.

Trondheim

June 8, 2023

Contents

List of Figures

List of Tables

Nomenclature

List of abbreviations

EPDM	Ethylene propylene diene monomer
DPT	Differential pressure transmitter
PE	Polyethylene
PEF	Polyethylene foil
PP	Polypropylene
PU	Polyurethane
ROM	Roofing membrane
RQ	Research question
TEK	Norwegian regulations on technical requirements for construction works

Symbol index

Symbol	Description	Unit
A_E	Envelope area	m^2
C	Air flow coefficient	$m^3/(h \cdot Pa^n)$
l	Joint length	m
n	Pressure exponent	-
n_{pr}	Air change rate at reference pressure difference	h^-1
p	Pressure	Pa
Δp_r	Reference pressure difference	Pa
q	Air permeability	$m^3/(h \cdot m^2)$
q_{Epr}	Air leakage rate per envelope area at reference pressure	$m^3/(h \cdot m^2)$
q_{pr}	Air permeability at reference pressure difference	$m^3/(h \cdot m^2)$
q_{50}	Air permeability at 50 Pa pressure difference	$m^3/(h \cdot m^2)$
RH	Relative humidity	%
s_x	Standard deviation of variable x	-
s_{xy}	Covariance of variables x and y	-
Sd	Vapour diffusion thickness	m
V	Volume	m^3
$\dot{V}$	Air flow rate	m^3/h
$\dot{V}_{pr}$	Air flow rate at reference pressure difference	m^3/h

1 Introduction

1.1 Background

In the face of climate change, the construction industry is facing increasingly stringent energy efficiency requirements. In the EU, buildings were responsible for 40% of the total energy consumption and 36% of greenhouse gas emissions as of 2020 (European Commission, 2020). In Norway, the building stock accounts for around a third of domestic energy consumption and 40% of greenhouse gas emissions (Forskningsrådet, 2021).

The Energy Performance of Buildings Directive (EPBD) was initiated by the EU to provide a legislative framework for promoting energy efficiency in buildings. Among its stated goals is to "achieve a highly energy efficient and decarbonised building stock by 2050" (Commission, 2021). The latest proposal for a revision of the EPBD from 2021 establishes a vision for achieving a zero-emission building stock by 2050. In Norway, technical requirements regarding energy efficiency are defined in the *Regulations on technical requirements for construction works* i.e. TEK, with its newest edition TEK17 taking effect in 2017 (Direktoratet for Byggkvalitet, 2017). TEK is guided by EPBD in posing stricter requirements to the overall energy efficiency of buildings and emphasizing building airtightness in Norway.

Airtightness requirements are established to prevent the influx of cold outdoor air and the escape of humid indoor air into the internal structures of the building envelope. Sufficient airtightness is thus important, both to ensure the overall energy efficiency of the building, and to prevent moisture-related damages to the structure, like mold and rot. Air and vapour barriers are installed in external walls and roofs to inhibit air from moving through the building envelope. However, air leakage commonly occurs in joints and perforations in these barriers. It is essential to give proper attention to these details, during design and construction, to achieve sufficient airtightness.

In recent years, adhesive tapes have gained popularity as a mean of air-sealing joints and perforations in the building envelope. Early on, these tapes had a reputation for having poor adhesive properties and durability. More recently, along with further product development, adhesive tapes have been recognized for their ability to provide adequate air tightness (Skogstad, Kvalvik and Jelle, 2010). The use of tape also allows for innovative solutions, along with a simple and quick application, making it a highly convenient option for air-sealing details.

However, as adhesive tapes represent a relatively recent way of air-sealing buildings, there are concerns and uncertainty regarding the long-term durability of the products and solutions. Current evaluation methods used in the certification of products and systems are primarily based on assessing the mechanical and adhesive properties of products, rather than addressing the airtightness directly. The usefulness and validity of these established evaluation methods may seem to depend on the existence of a direct correlation between the airtightness and adhesion of the tape joints. However, research results have suggested otherwise, as while adhesive properties in many cases remain unchanged or even improve over time, the airtightness is in most cases reduced (Møller and Rasmussen, 2020).

The aforementioned uncertainty has led research communities to recognize the need for new test methods. The Norwegian Institute of applied research (SINTEF), among others, initiated the research project TightEN in 2019 to enhance expertise and understanding regarding the airtightness and long-term durability of sealing systems utilizing adhesive tapes (SINTEF, 2019).

1.2 Purpose

This master's thesis is written in collaboration with SINTEF and the research project TightEN. TightEN seeks to develop reliable methods for testing and evaluating the airtightness of self-adhesive products, as well as full-scale testing of systems. Such methods are to be used in product development and certification, helping to ensure and document a technical lifetime of at least 25 years (SINTEF, 2019).

The purpose of this thesis is to develop and evaluate the usefulness of a medium-scale test method for assessing the airtightness of joints sealed with adhesive tapes. In this context, the term "medium-scale" is used to differentiate the method from full-scale tests evaluating larger and more complex building components.

The aim is to contribute to the development of a new test method with sufficient accuracy, reproducibility and repeatability to be used during the development and certification of adhesive tape products and systems in the future.

The proposed test method utilizes a Test Stand consisting of a steel box to pressurize different test samples simulating taped joints between barriers in a wall or roof construction, and subsequently measure their air leakage rates. Test samples are made up of a substrate, such as sheets of membrane, with cuts sealed with tape to imitate joints. The method is described further in detail in Chapter 3.

To address the purpose of the thesis, the following research questions have been formulated:

- RQ1: How does the method in development perform in providing reproducible, accurate and repeatable results in the assessment of airtightness in tape joints?
- RQ2: How do the method and its measurement results compare to other existing evaluation methods?
- RQ3: How can the method potentially be implemented in the context of product certification and development?

1.3 Limitations

The method in development is intended to evaluate the air permeability of adhesive tapes used for permanent air-sealing of joints and perforations in building envelopes. The durability of the tapes is assessed based on the change in air permeability after an accelerated ageing process. The test method does not evaluate the water tightness or vapour diffusion resistance of tape joints, and can therefore only account for moisture transfer through convection.

The tape joints featured in the experiments are comprised of simple cuts in membrane sheets, unto which tape is applied. However, in practical applications, overlapping joints are more commonly used to join such sheets together. Consequently, the specimen layout deviates somewhat from the typical application of tape in air and vapour barriers. It remains unclear how this factor affects the validity of the test method.

In the experiments conducted in this thesis, the durability of products is evaluated by measuring the change in performance following artificial ageing procedures. These procedures aim to accelerate deterioration by exposing the materials to simulated climatic strains. It is important to note that there is considerable uncertainty associated with these ageing procedures, as they do not necessarily replicate the effects of natural ageing.

1.4 Structure

In Chapter 2, the thesis presents the results from a literature review, providing a theoretical background as well as an overview of currently established evaluation practises and experimental test methods. Chapter 3 presents the test method in development, and describes a measurement program used to assess the aptness of the method and to examine its potential limitations. The test program involves measuring the system leakage of the test apparatus before the test method is used to measure the air permeability of material samples comprised of combinations of commercially available tapes and substrate materials. The same material samples are evaluated based on peel resistance measurements in accordance with NS-EN 12316-2. Results from the tests are presented in Chapter 4 and are discussed and analyzed in Chapter 5, to answer the research questions before a final conclusion is drawn in Chapter 6.

2 Literature review

2.1 Airtightness in buildings

Air enters and leaves buildings through ventilation or infiltration. Ventilation constitutes the intended airflow which is necessary for providing satisfactory indoor air quality. In modern buildings, ventilation is often provided through balanced ventilation with heat recovery. This makes the airflow predictable and controllable and allows for outdoor air to be heated before it is supplied to the indoor environment, improving thermal comfort. Modern ventilation systems also make it possible for heat batteries to reclaim energy from the exhaust air to limit heat loss (Thue, 2016, p. 284).

Thue (2016) defines infiltration as air flowing in and out of a building as a result of leakages in the building envelope (p. 284). Unlike ventilation, air leakages constitute undesirable and uncontrollable movement of air through openings in the building envelope. These openings occur in many different locations and in a range of sizes. For instance, a punctured air barrier can allow cold outdoor air to penetrate into a layer of insulation, subsequently reducing its insulating properties. Cold air can also penetrate further, into occupied space, causing excessive heat loss and thermal discomfort for building occupants. Likewise, humid indoor air can leak into the insulation through holes in the vapour barrier, entailing risks of condensation and consequentially the formation of mold and rot. Ensuring the building envelope is airtight is thus important to reduce unwanted leakages and consequential excessive heat loss and risk of damage to the structure (Blom and Uvsløkk, 2012).

Infiltration is driven by differences in air pressure, Δp, between the inside and the outside of the building envelope. This results in an airflow, $\dot{V}$, moving from areas with high air pressure to areas where it is comparatively lower. Pressure differences are typically caused by wind pressure and pressurization from mechanical ventilation. Temperature differences will simultaneously contribute to pressurization through the stack effect, as warm air rises up through the building and creates a higher pressure in its upper levels compared to its base (Thue, 2016, p. 266).

A building envelope will never be entirely airtight, as it is virtually impossible to eliminate leakages and infiltration completely. Building air permeability is instead used as a physical property in order to measure and describe airtightness (Boberach, 2022). Achieving airtightness thus becomes a matter of sufficiently reducing the air permeability of the building. The standard NS-EN ISO 9972:2015 defines building air permeability as the "air leakage rate per the envelope area across the building envelope" (ISO, 2015). This measure is quantified as the specific leakage rate of a building, q_{Epr}, referring to the airflow rate per square meter of the envelope area at a given reference pressure:

$$q_{Epr} = \frac{\dot{V}_{pr}}{A_E} \quad [m^3/(h \cdot m^2)] \tag{1}$$

Here, $\dot{V}_{pr}$ represents the total air leakage rate through the envelope in m^3/h at a given reference pressure difference Δp_r between the inside and outside of the building. The enveloping area, A_E, accounts for the total area of walls, floors and ceilings bordering the internal volume of the building (ISO, 2015). The airtightness of a building can alternatively be expressed by its air change rate n_{pr}, taking into account the internal volume of the building, V:

$$n_{pr} = \frac{\dot{V}_{pr}}{V} \quad [h^-1] \tag{2}$$

NS-EN ISO 9972:2015 describes a standardized method for measuring the air permeability of a building using a blower-door test. This method involves controlled pressurization of the building using a fan, while simultaneously measuring the airflow required to sustain the induced pressure difference, Δp. The relationship between the airflow rate through the building envelope and the pressure difference can then be described by the power law equation (ISO, 2015):

$$\dot{V}_{env} = C_{env} \cdot (\Delta p)^n \quad [m^3/h] \tag{3}$$

The flow coefficient, C, expresses the resistance the leaks are facing, with a small C indicating high resistance. The pressure exponent, n, describes the dominant mode of airflow among the leakages, where a value of 1 corresponds to laminar flow, while 0.5 indicates turbulent flow (Boberach, 2022). The flow coefficient and the pressure exponent are both determined by a regression analysis of measurement results from the blower-door test (Thue, 2016, p. 284).

2.2 Moisture transfer

Moisture can transfer through the building envelope by convection and vapour diffusion. Convective moisture transfer is the result of water molecules moving along with an airflow caused by differences in air pressure. The airflow is enabled through leakages, such as holes and crevices or porous materials. The rate at which moisture is transported through convection depends on the airflow and the humidity of the air. Convective moisture transfer can thus be prevented or reduced by rendering the building envelope sufficiently airtight, preventing airflow (Thue, 2016, p. 326).

However, it is possible for a material to be airtight, yet permeable to water vapour diffusion. Vapour diffusion occurs when water molecules permeate through a material as a result of differences in vapour pressure. In this case, water molecules move from a location of higher vapour concentration towards areas with lower concentrations. The rate of vapour diffusion through a material depends on the permeability of the material as well as the gradient in vapour concentration (Thue, 2016, p. 324).

Both mechanisms of moisture transfer are illustrated in Figure 2.1. Convection will typically have a greater potential for transferring moisture compared to diffusion. This is because convection of humid air can occur at relatively small differences in air pressure.

Vapour diffusion, on the other hand, faces greater resistance, requiring comparatively large differences in vapour pressure in order to transfer the same amount of moisture. As a consequence, air leakages generally pose a larger risk of moisture-related damage than vapour diffusion (Thue, 2016, p. 326).

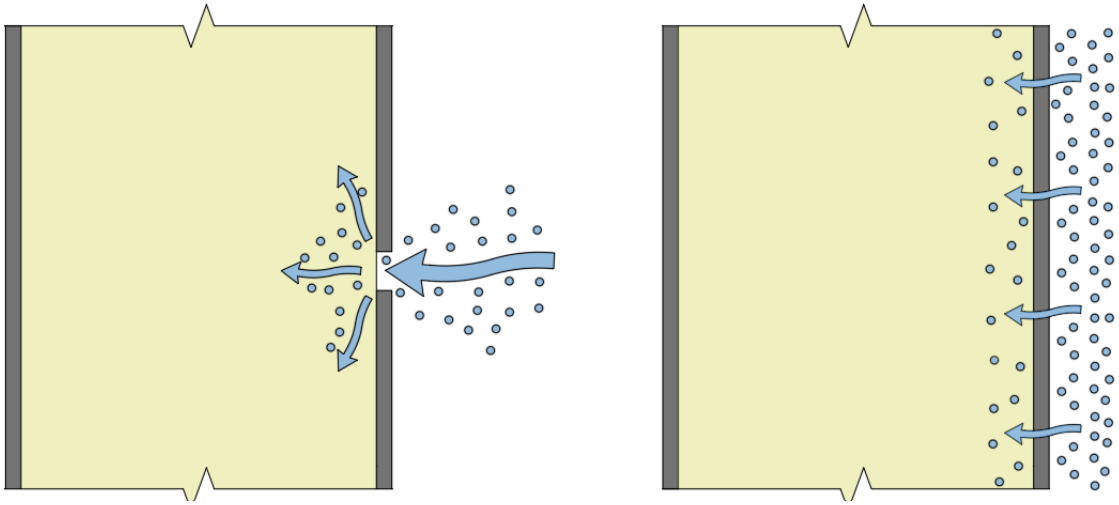

Figure 2.1: Convective moisture transfer (left) and vapour diffusion (right) in a wall construction.

2.3 Norwegian regulations

Norwegian construction projects must meet the *Regulations on technical requirements for construction works*, TEK17. This building code determines requirements regarding a building's overall energy efficiency, including its airtightness through upper limit values concerning the air change rate, $n50$. The air change rate is herein defined as the volumetric airflow, $\dot{V}_{50}$, leaking through the building envelope divided by the internal volume of the building, V, when an air pressure difference of 50 Pa occurs between the inside and outside environment (Direktoratet for Byggkvalitet, 2017):

$$n_{50} = \frac{\dot{V}_{50}}{V} \quad [h^{-}1] \tag{4}$$

All new Norwegian building projects must be built according to the minimum requirements in TEK17. These requirements also apply when performing a complete renovation of existing buildings, in cases where only structural elements are reused. Using the minimum requirements, buildings must also be designed according to an energy budget depending on the building type. "Energy-saving measures" constitute an alternative way of ensuring energy efficiency in residential buildings. This method disregards the overall energy budget, but includes stricter requirements to the U-values of different components, as well as demanding a lower air change rate.

Buildings can be built with an even higher level of energy efficiency than required by TEK17. This can be achieved by designing the building according to the Passive House Standards NS 3700 or NS 3701, for residential and non-residential buildings respectively (Standard Norge, 2013*a*). These standards involve more ambitious requirements to the

building's overall energy efficiency. However, the airtightness requirements are currently the same for passive houses as when applying the energy-saving measures in TEK17.

Table 2.1 shows the different airtightness requirements that are relevant to the construction of new buildings and the total renovation of existing buildings in Norway. As of January 1, 2013, the air leakage rates of new buildings are required to be verified by an independent controller (Direktoratet for byggkvalitet, 2012). Verification can be carried out by performing the aforementioned blower-door test described in the NS-EN ISO 9972:2015 standard (SINTEF, 2014).

Table 2.1: Air change rate requirements.

Requirement	**n50 [h^{-1}]**	**Applies to**
TEK17 Minimum requirement	≤ 1.5	All buildings
TEK17 Energy-saving measures	≤ 0.6	Residential buildings
NS 3700 Passive house standard	≤ 0.6	Residential buildings
NS 3701 Passive house standard	≤ 0.6	Non-residential buildings

2.4 Airtightness in practice

Timber frame construction is a prevalent form of erecting buildings in Norway, either through load-bearing timber frame walls and roofs, or as non-load-bearing exterior walls in buildings relying on load-bearing constructions made from concrete or steel. In either case, airtightness is often provided through two separate, physical barriers placed in the exterior walls and roofs which constitute the building envelope.

An air barrier is normally situated on the exterior of the timber framing and insulation, preventing cold outdoor air from entering the layers of insulation and thus reducing its insulating properties. This layer must be sufficiently airtight to prevent air from penetrating it, but at the same time allow for vapour diffusion so that moisture can dry out. Along with the exterior wall cladding, these diffusion open, yet airtight barriers serve the purpose of preventing rain from entering the wall. The cladding provides weather protection as a rain-tight exterior layer, creating a ventilated and drained cavity between the air barrier and the cladding. Air barriers can be comprised of a range of different materials, usually in the form of boards or membranes.

A vapour barrier is normally installed on the interior side of an internal wall structure with the intent of preventing humid indoor air from entering the thermal insulation where it might condensate as a result of lower temperatures inside the exterior wall construction. Vapour barriers typically consist of polymer sheets, such as polyethylene (PE) foils and are highly vapour resistant, unlike the exterior air barrier (Blom and Uvsløkk, 2012).

Vapour diffusion resistance of barrier products can be quantified through *Sd values*. The Sd value of a barrier corresponds to the thickness of an air layer required to achieve the equivalent vapour resistance. Vapour barriers must have a relatively high Sd value to prevent moisture from infiltrating the wall structure, while air barriers typically have a lower Sd, allowing any moisture inside the structure to escape. This principle is illustrated

in Figure 2.2. SINTEF recommends an Sd < 0.5 m for air barriers, and Sd > 10 m for vapour barriers. These limit values are in turn used by SINTEF to define products as air or vapour barriers. PE foils used as vapour barriers today typically have a thickness of 0.15 mm, achieving Sd values of around 70 m. For comparison, Table 2.2 presents an overview of some building materials along with their typical Sd values.

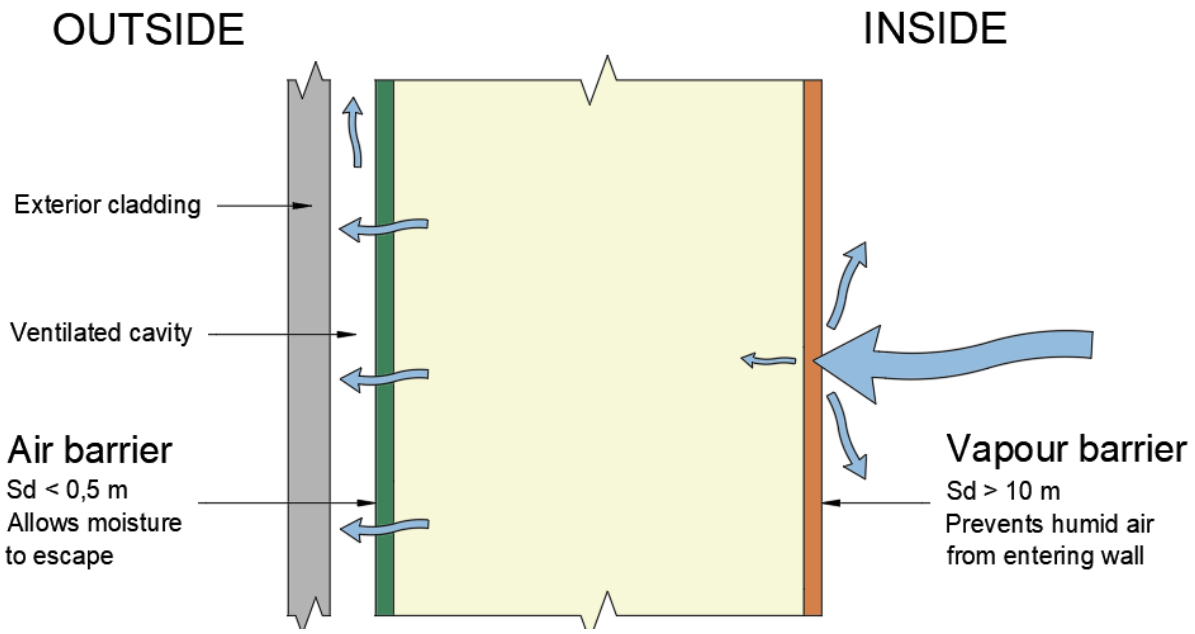

Figure 2.2: Diffusion in exterior wall construction with recommended Sd values according to Geving et al. (2020).

Table 2.2: Typical Sd values for building materials (Geving, 2010).

Material	**Sd [m]**
Diffusion open air barrier	0
Gypsum board, 10 mm	0.08
OSB board, 13 mm	0.4 - 0.6
Plywood, 13 mm	0.6 - 3.3
PVC roofing membrane	20 - 30
PE foil, 0.15 mm	70

The Sd value of a vapour barrier may be lower than 10 m, provided the air barrier it is used in combination with is sufficiently open to diffusion. Geving (2010) recommends the following relation between the Sd values when choosing materials for the air and vapour barriers:

$$\frac{Sd_{vapour\ barrier}}{Sd_{air\ barrier}} > 10 \tag{5}$$

The performance and durability of barrier products on their own are often well documented. Potential issues with airtightness are more likely to arise in joints and connections between the barriers and adjacent components, as well as in penetrations in the barriers. Critical details occur for instance where exterior walls connect to windows, roofs and foundations. Figure 2.3 highlights some of the details of a building envelope in which air leakages typically occur. The Figure outlines in red, an imaginary, continuous airtight layer. In the walls and roof, this line corresponds to the vapour barrier. In the window, the imaginary line continues through the frame and glass pane, while the concrete floor ensures airtightness towards the foundations. Sealing these critical points is essential to achieve continuity of the barriers, thus ensuring the overall airtightness of the building. There are several options for sealing joints and connections, such as clamping, sealants and adhesive tapes.

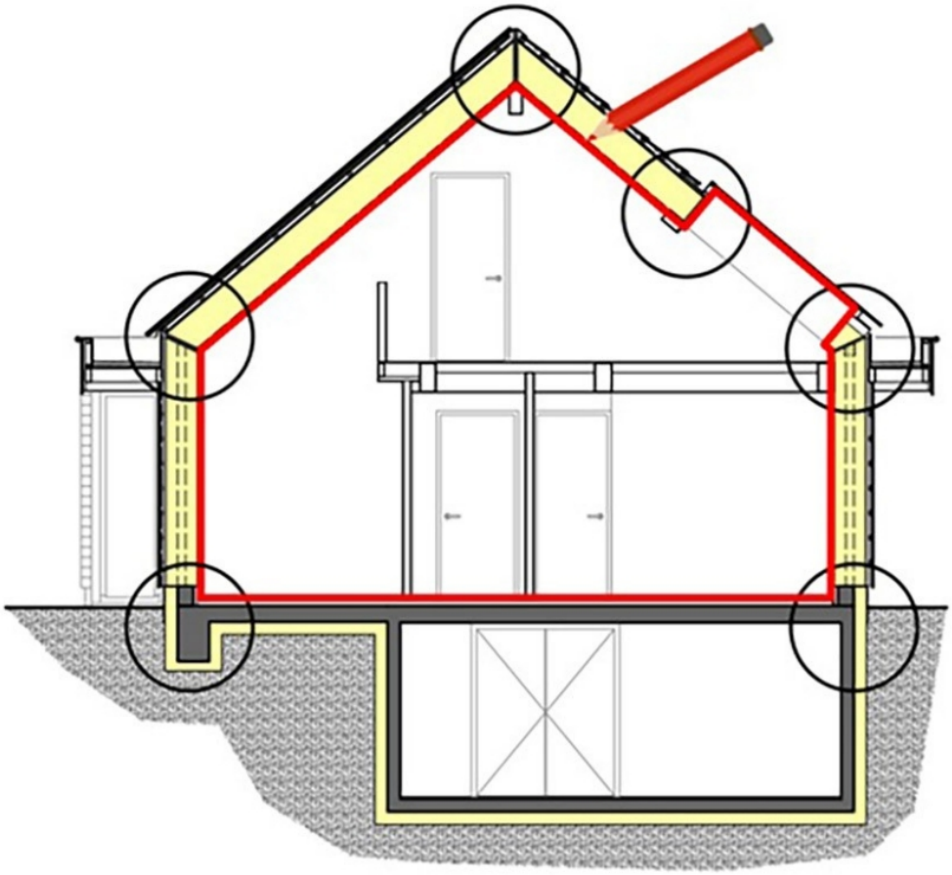

Figure 2.3: Critical details concerning air leakages in a building envelope (Griffon, 2023).

Joints between the separate sheets of a barrier membrane itself are also critical, along with penetrations in the building envelope. Penetrations in the barriers may be intentional, as for plumbing and electrical works, or accidental, resulting from ruptures occurring during construction or in the operational phase (Blom and Uvsløkk, 2012).

2.5 Airtightness reference values

The air permeability of a material or building component is commonly expressed as air leakage rate per area. TEK17 poses requirements to the overall airtightness of buildings through the maximum allowed n50, but does not go into detail regarding the air permeability of building envelopes on a component level, such as exterior walls or roofs.

In the SINTEF guidelines for Technical Approval of air barrier systems, an air permeability of 0.50 m^3/m^2h at a 50 Pa pressure difference is considered sufficient to ensure that an assembled barrier system on its own meets the the n50 requirement in TEK17 (SINTEF, 2017). For reference, Table 2.3 presents the air permeability of a selection of air barrier materials, according to Byggforsk (2003). The table separates between the air permeability of the material by itself, and the material when installed in an exterior wall or roof, including normal proportioning of joints. The difference between the two scenarios indicates the impact of joints on the overall airtightness.

Table 2.3: Air permeability of air barrier materials (Byggforsk, 2003).

Material	**Air permeability [m^3/m^2hPa]**	
	Material without joints	Material including joints
Gypsum plate	< 0.001	0.007 - 0.030
Fibreboard	< 0.001	0.010 - 0.050
Polyethylene fiber cloth	0.002 - 0.020	0.021 - 0.025
Waxed cardboard	0.003 - 0.008	0.008 - 0.014

The air permeability of joints within a barrier system can be estimated by subtracting the permeability of the barrier material itself from that of the assembled system, resulting in the joint permeability expressed as leakage rate per wall or roof area. Alternatively, the permeability of joints may be expressed as leakage rate per joint length.

The joint permeability required to meet a certain air change rate will depend on the total length of the joints, but some general estimates have been made based on Belgian residential buildings of average construction (Van den Bossche et al., 2012, p. 41). In a study on cavity brick walls, Van den Bossche et al. (2012) suggest that an air permeability in wall-window interfaces lower than 0.33 m^3/mh at 50 Pa is sufficient for the building to meet the passive house requirements for airtightness. Furthermore, according to Van Linden and Van den Bossche (2017), a joint between facade panels requires an air permeability lower than 0.048 m^3/mh at 50 Pa to meet the passive house requirement. An air permeability lower than 0.238 m^3/mh is considered to provide "good" airtightness in the same situation (p. 7).

2.6 Adhesive tapes

In recent years, adhesive tapes have become a favoured way of air-sealing buildings. Adhesive tape products have shown satisfactory results when applied for sealing joints, connections and penetrations (Blom and Uvsløkk, 2012). Tapes can be used both as the primary way of sealing and as reinforcement of clamped joints, helping to provide continuity in the

barrier layers. Figure 2.4 illustrates the practical application of adhesive tape on a vapour barrier membrane in the walls and ceiling of a timber frame house. Here, the tape is used to seal joints in the membrane itself and to seal connections between the membrane and timber framing.

Figure 2.4: Adhesive tape used to join sheets of vapour barrier membrane, and to connect the membrane to the timber frame (Bygghjelp, 2019).

An adhesive tape consists of a backing material coated with an adhesive. The backing material and adhesive type will vary depending on the tape's intended use. The surface to which a tape is applied is referred to as a substrate. Different types of adhesive tapes are developed for adhesion to different substrates, with varying airtightness and vapour resistance according to their intended use (Skogstad et al., 2010).

Adhesive tapes can be used to join boards and sheets of membrane together and to connect these to other building components, such as floors and ceilings (Boberach, 2022). Rigid boards can be joined by a simple connection, while joining two sheets of membrane requires the sheets to overlap (DIN 4108-7:2011-01, 2011). This principle is illustrated in Figure 2.5. The Figure shows a vertical cross-section of an exterior wall, where rigid gypsum boards constitute the air barrier, and a PE foil makes up the vapour barrier.

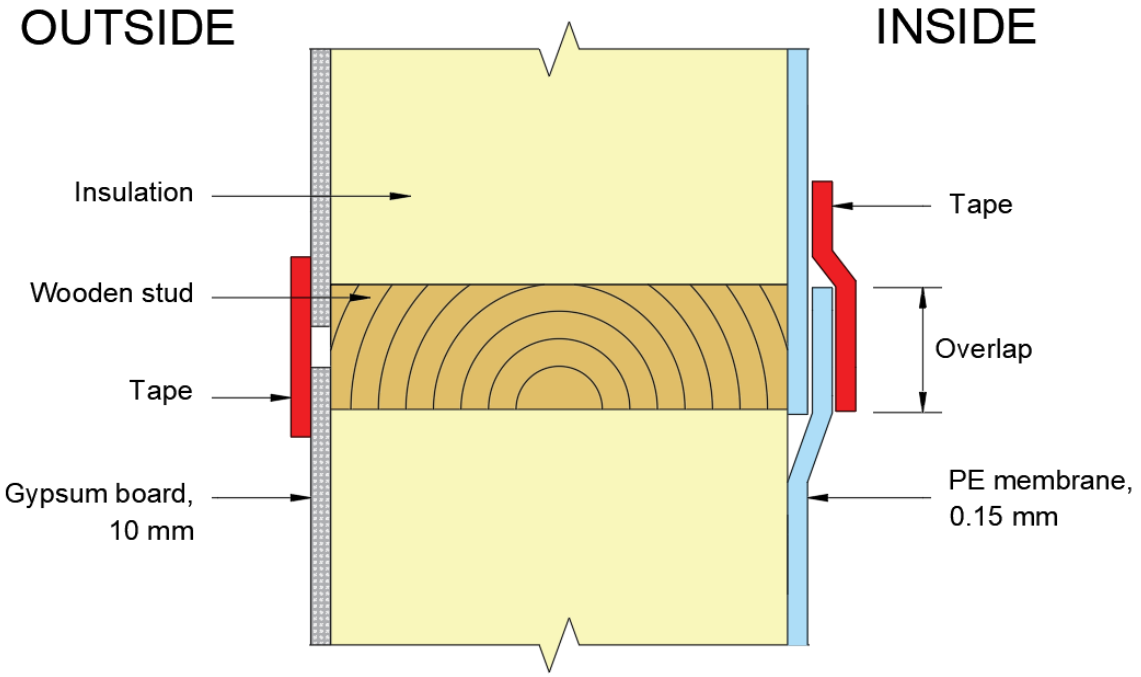

Figure 2.5: Cross-section of an exterior wall showing a simple tape connection of boards (left) and overlapping membranes with single-sided tape (right).

In order for the use of tape to be successful, it is important that the product's performance and durability are properly assessed and documented. The airtightness of a joint or opening sealed by tape is affected by several different parameters, such as temperature, relative humidity, dust and moisture content of materials, as well exposure to UV light and chemical compounds. These conditions may affect the degradation rate by causing dimensional change, material fatigue or oxidation. Factors can also combine in ways leading to synergistic effects, accelerating the deterioration of the tape's airtightness even further (Ylmén, Hansén and Romild, 2012). It is therefore important that tapes are tested in realistic and relevant conditions, to examine how the products react to different climate conditions, including frost, moisture, heat and sun exposure. Research also suggests that installation conditions can have a major impact on the airtightness of tape joints (Antonsson, 2017).

2.7 State of the art

The durability of a product is often assessed by comparing material properties in their initial condition to properties of aged material. As adhesive tapes constitute a relatively new way of air-sealing buildings, knowledge is limited regarding the long-term durability of the solutions (SINTEF, 2019). A range of test methods has been developed in different research communities in order to evaluate the airtightness and durability of adhesive tapes. Some methods measure the airtightness of joints directly, while others are based on measuring the adhesive properties of the tapes.

Leprince et al. (2017) describe two conflicting constraints for developing good evaluation methods; test samples must be large and realistic enough to be relevant and representative, yet simple enough to be reproducible. Large-scale tests may do a better job in simulating realistic conditions but entail greater uncertainty related to the quality of implementation, leading to issues with reproducibility. Large-scale tests are in general also more expensive to conduct (Leprince et al., 2017, p. 10). Small-scale tests are likely to be more reproducible but may fail to account for relevant effects from ageing related to dimensional stability. For instance, research indicates that short test samples of adhesives react differently to ageing compared to long ones (Leprince et al., 2017, p. 11).

In the subsequent sections, different evaluation methods for adhesive tapes are presented. These include standard methods used in product development and certification, as well as experimental methods addressing both airtightness and adhesive properties. The different evaluation methods are later compared in Section 2.8.

2.7.1 Accelerated ageing

To avoid waiting several years in order to test the properties of aged material, methods have been developed to accelerate the ageing process of test samples. Accelerated ageing, i.e. artificial ageing consists of exposing test samples to artificial conditions in order to simulate the long-term effects of ageing on material properties (Fufa et al., 2017, p. 3).

One way of achieving this is by exposing the samples to elevated temperatures to accelerate the speed of chemical reactions causing materials to deteriorate faster. An alternative approach is mechanical ageing through inducing different loads to simulate fatigue resulting from wind pressure or dimensional change. Exposure to high relative humidity can also cause materials to deteriorate faster (Ylmén et al., 2012). Furthermore, artificial UV-radiation can be used to simulate the effects of exposure to sunlight (Fufa et al., 2017)

The properties of a tape joint are affected by a wide range of factors during its ageing, including synergistic effects accelerating the deterioration of its function (Ylmén et al., 2012). Thus it is necessary to combine different mechanisms to obtain relevant ageing effects. Moreover, the ageing effects on a component separately do not necessarily correlate to the effects observed on an assembled system, as materials in combination often influence each other (Leprince et al., 2017, p. 7-8).

Artificial ageing through temperature elevation enables the use of the time-temperature superposition principle, for instance in the form of Arrhenius' Law. This equation, originating from physical chemistry, describes the relation between chemical reaction rates and absolute temperature, making it possible to translate the duration of artificial ageing to natural ageing duration. This only applies, however, when addressing one material at a time (Leprince et al., 2017, p. 6). In reality, the ageing processes of building components are affected by several factors, including moisture, mechanical stress and reactions between chemical compounds. Hence, when it comes to assembled systems, it is difficult to develop a single standard protocol in which a given artificial ageing process would be equivalent to any number of years of natural ageing (Leprince et al., 2017, p. 11).

2.7.2 SINTEF Technical Approval

Adhesive tapes used for air-sealing building envelopes can receive Technical Approval from the Norwegian Institute of applied research (SINTEF). Technical Approval is intended to verify that a given product or system is suitable for use under Norwegian climate conditions and that it meets the technical requirements of the Norwegian building code (TEK). The evaluation includes a durability assessment to ensure that the product functions properly during its technical lifetime (SINTEF, 2022).

Approving a product involves assessment through various laboratory tests. The scope of the assessment depends on whether the Technical Approval addresses a single product separately, or a system consisting of several different products. For separate tape approval, the durability of a product is currently evaluated based on its adhesive and mechanical properties, using the following standardized methods (SINTEF, 2020):

- **Tensile strength and elongation** according to NS-EN 12311-2.
- **Peel resistance of joints** according to NS-EN 12316-2.
- **Shear strength of joints** according to NS-EN 12317-2.

Tensile strength is tested by stretching the tape lengthwise at a constant separating speed of (100 ± 10) mm/min until failure. The applied force and elongation are continuously recorded, resulting in a stress-strain curve from which the Young's modulus is determined as the gradient between 1% and 2% strain. Failure mode and maximum tensile strength are recorded during the test (Standard Norge, 2013*b*).

Peel resistance is defined as the force required to separate a tape from a flexible substrate by tearing it perpendicular to the substrate. Assessment of peel resistance is conducted through a T-peel test as illustrated in Figure 2.6. Separation occurs at a constant speed of (100 ± 10) mm/min until failure. The applied force is recorded continuously during the test along with the failure mode (Standard Norge, 2013*c*).

The shear strength of joints is tested by dragging the tape parallel to the substrate at a constant speed of (100 ± 10) mm/min until it tears or is detached from the substrate. The test is conducted on five rectangular specimens with a width of (50 ± 1) mm. Prior to testing, the samples should be conditioned at (23 ± 2)°C with RH between 30% and 70% for 20 hours. The shear strength is defined as the greatest force recorded during the test expressed in Newton per 50 mm of tape width (Standard Norge, 2010).

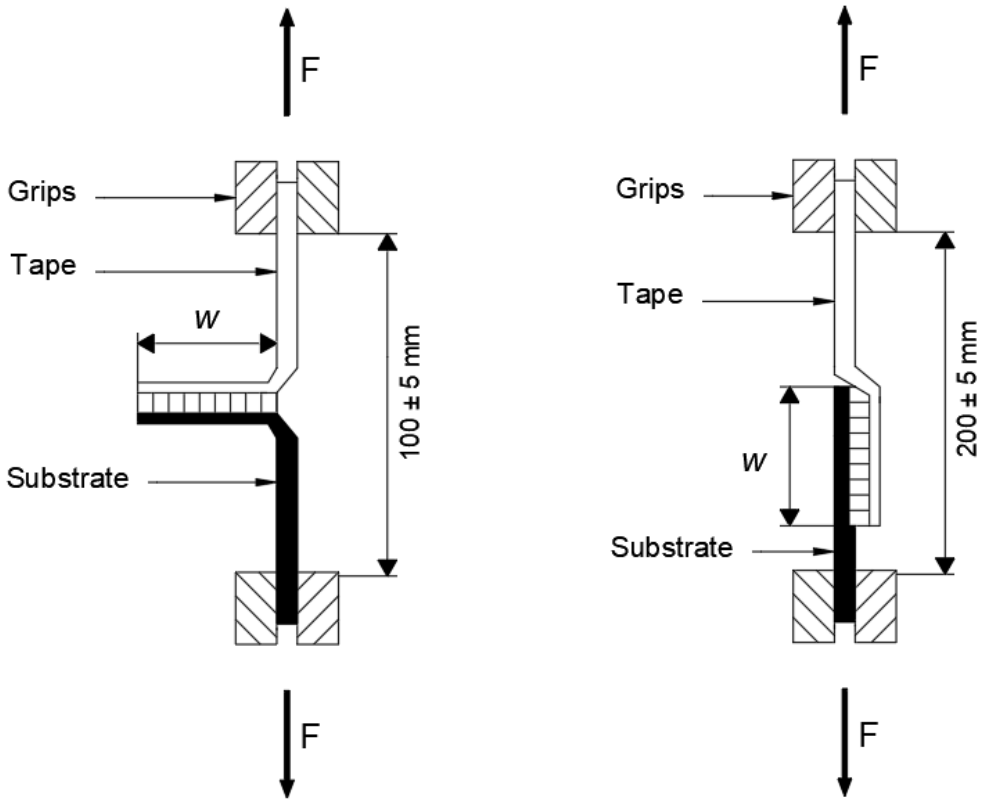

Figure 2.6: Principles of measuring T-peel resistance (left) and shear strength (right) according to Standard Norge (2013*c*, 2010).

Adhesive tapes can be certified for application in air or vapour barrier systems, after which they are often referred to as air barrier tapes or vapour barrier tapes. The SINTEF guidelines demand *satisfactory adhesion* to certain substrates depending on the tape's intended area of application. Table 2.4 shows the standard substrates used during SINTEF Technical Approval when performing the tests described in NS-EN 12316-2 and NS-EN 12317-2. A single tape product can be approved for use in both air and vapour barriers, provided it passes both sets of requirements. In this case, the product is typically referred to as a universal tape.

Tapes approved for use in roof underlays are in addition required to be tested for water tightness when adhered to the same substrates as the air barrier tapes from Table 2.4. Manufacturers can also request SINTEF to perform adhesive tests on other substrates, such as concrete, gypsum board or asphalt fibreboard (SINTEF, 2020).

Table 2.4: Substrates used for durability evaluation during Technical Approval (SINTEF, 2020).

Tape application	**Test substrates**
Air barrier	Painted wood, untreated wood, galvanized and stainless steel, painted and anodized aluminium and air barrier membrane
Vapour barrier	Painted wood, untreated wood and PE foil.

Product durability is evaluated by comparing test results from before and after accelerated laboratory ageing of the samples. Table 2.5 shows the procedures used for accelerated ageing in the context of SINTEF Technical Approval. In order for durability to be deemed satisfactory, the test results must remain within the boundaries of acceptable change after the ageing process compared to the initial tests. Maximum acceptable change is evaluated based on the requirement to the product in its initial condition. Typically, the durability is regarded as sufficient if the reduction in tensile strength, shear strength and peel resistance is less than 50% between initial and artificially aged material (SINTEF, 2020).

Table 2.5: Artificial ageing process used in SINTEF Technical Approval (SINTEF, 2020).

Tape application	**Ageing procedure**
Air barrier	14 days in the climate simulator NT BUILD 495, followed by 168 days in a heat chamber at 70°C according to NS-EN 1296.
Vapour barrier	48 hours of UV/heat ageing according to NS-EN 1297 (without water praying) followed by 12 weeks (84 days) of ageing in a heat chamber at 70°C according to NS-EN 1296.

Unlike a separate tape, an air barrier system is required to have its airtightness tested according to NS-EN 12114:2000 to receive Technical Approval. If the system utilizes an adhesive tape for sealing, separate Approval is required for the tape itself (SINTEF, 2017). Airtightness is measured with a blower test setup as illustrated in Figure 2.7. Test specimens should be produced in a way that is representative of how the system would be installed in a real situation (Standard Norge, 2000).

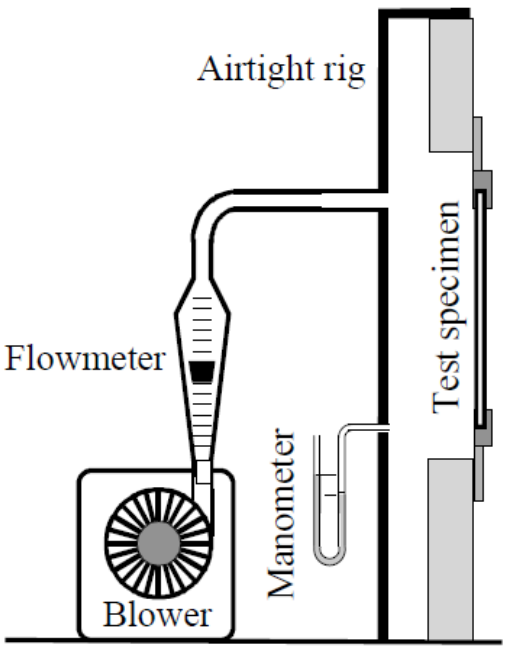

Figure 2.7: Setup for evaluating airtightness of building components (Standard Norge, 2000).

Tests should be conducted in a laboratory with an ambient climate of 18-22°C, 100 000 to 102 000 Pa atmospheric pressure and 25 to 50% relative humidity. A specimen is pressurized up to 50 Pa while measuring the supplied airflow, which in turn corresponds to the air leakage rate, n50. The SINTEF guidelines for Technical Approval of air barrier systems and roofing underlays describe two different minimum requirements, which can be used to classify systems based on their performance in standardized tests. Classifications and requirements are shown in Table 2.6 (SINTEF, 2017, p. 8).

Table 2.6: Airtightness classification of air barrier systems according to SINTEF (2017).

Classification	**n50 [m^3/m^2h]**	**Description**
1	< 0.50	Air barrier system is considered sufficiently airtight to satisfy the n50 requirements of TEK17 and the passive house standard before the vapour barrier is installed.
2	< 2.50	Air barrier system is considered sufficiently airtight to avoid cooling from wind, but not to meet the airtightness requirement prior to installing the vapour barrier.

Evaluating airtightness as part of the Technical Approval of vapour barrier systems is only necessary if the barrier material consists of something other than PE foil (SINTEF, 2020). In this case, the air leakage rate of the system shall not exceed 0.1 m^3/m^2h at 50 Pa (SINTEF, 2017).

2.7.3 Sletnes and Frank

As part of the TightEN project, Sletnes and Frank (2020) have systematized and analyzed existing peel and shear measurement data to better understand the importance of different parameters. The study is based on data collected by SINTEF over a span of 10 years through product certification and research. During this year period, SINTEF performed peel and shear resistance measurements, according to NS-EN 12316-2 and 12317-2 respectively, on more than 30 different tapes and nine different substrates. Measurements were conducted using the following substrate materials: air barrier, Vapour barrier, Painted wood, Untreated wood, Steel, Concrete, Glass, Gypsum board, and OSB.

The test samples had been subject to one of three different ageing programs. One ageing program utilized the climate simulator NT BUILD 495, exposing the test specimens to four different climate conditions; ultraviolet (UV) and infrared radiation, water spray, freezing (-20°C) and ambient laboratory conditions, changing from one condition to another once every hour. This was followed by ageing in a heat chamber for 12, 22 or 24 weeks at 70°C. A second ageing program involved 2 days of exposure to UV light followed by 12 weeks in the heat chamber (70°C). The third program consisted exclusively of 24 weeks in the heat chamber (Sletnes and Frank, 2020, p. 2).

The study found that the measured peel resistance was more sensitive to ageing compared to shear strength. However, peel resistance prior to ageing was a poor predictor of peel resistance after ageing. Yet, the results showed a clear correlation between shear strength before and after ageing, as shear strength appeared to change little in many of the samples. Both peel and shear resistance varied considerably more between different tapes compared to between different substrates, both before and after ageing (Sletnes and Frank, 2020, p. 8).

2.7.4 Experimental methods

Fufa et al. (2017) describe a lack of reliable test procedures for tapes used in building application and express the need for new methods to evaluate the durability of product performance. Efforts to develop new test procedures for adhesive tapes have resulted in a range of methods, using different layouts, scales and substrate materials. Some studies combine airtightness evaluation with the measuring of mechanical tape properties such as peel and shear resistance. This section presents a summary of some previous studies featuring experimental evaluation methods, describing test procedures and observations.

Antonsson (2017)

The Swedish research institute RISE has developed a method for evaluating the airtightness of a full-scale wall assembly. The method utilizes a rig made up of a 3x3 meter steel frame into which a timber frame wall is to be constructed. A concrete sole is cast into the bottom of the steel frame to simulate a slab foundation. The wall assembly includes timber framing, insulation, an interior, diffusion-tight vapour barrier, and an exterior air barrier open to diffusion, as well as plastic pipes penetrating the wall. An example can be seen in Figure 2.8.

During testing, the steel frame is connected to a pressure chamber for static and dynamic pressurization. The wall is exposed to both positive and negative pressure differences of 50, 75, 100, 125 and 150 Pa, with the air leakage rate being simultaneously measured at each pressure step. The frame and wall can later be fitted into a climate chamber for accelerated ageing through elevated temperatures. Mechanical ageing by dynamic pressurization of the wall assemblies also constitutes a part of the accelerated ageing process. Airtightness durability is assessed by comparing measured air leakage rates before and after the ageing process (Antonsson, 2017).

The method was used to study how airtightness is affected by varying assembly conditions. Three different wall systems were assembled using different tapes and barrier products. Each of the three systems was assembled under three different climatic conditions:

- **"Ideal conditions"** corresponding to an indoors laboratory environment, at 22°C.
- **Cold and humid environment** in a climate chamber at 5°C and 90-95% RH.
- **Dusty environment** created by blowing sawdust, crushed concrete and gypsum on membranes prior to assembly.

Figure 2.8: Full-scale wall assembly showing vapour barrier (Antonsson, 2017).

The cold and humid, and dusty environments were meant to mimic realistic conditions on a construction site, to see how the resulting airtightness and durability compare to systems assembled under more favourable conditions in a laboratory.

All wall assemblies were tested before and after six weeks of ageing at 60°C and 50% RH. The results showed that the systems assembled under ideal conditions had low air permeability rates both before and after ageing. All three systems assembled under ideal conditions had leakage rates (n50) lower than 0.1 l/m^2s (0.360 m^3/m^2h) before ageing. After ageing they all maintained n50 leakage rates lower than 0.3 l/m^2s (1.080 m^3/m^2h), which is sufficient to meet the requirements of the FEBY12 passive house standard (Antonsson, 2017, p. 22).

Systems installed under cold and humid conditions showed a comparatively greater reduction in airtightness after ageing. One of the systems was also considerably less airtight prior to ageing when compared to assembly under ideal conditions. Systems assembled in the dusty environment were more airtight prior to ageing compared to those installed in humid conditions. However, they became significantly less airtight after the ageing process, where one of the systems saw the leakage rate increase by 720%. Table 2.7 sums up the highest leakage rates recorded at 50 Pa in the study for each assembly condition (Antonsson, 2017).

Table 2.7: Largest n50 recorded among systems before and after ageing (Antonsson, 2017)

Assembly conditions	**Before ageing [m^3/m^2h]**	**After ageing [m^3/m^2h]**
Ideal conditions	0.259	1.130
Cold and humid environment	1.631	5.699
Dusty environment	0.349	1.940

For the systems assembled under ideal conditions, the leakages could in most cases be traced back to pipe penetrations and screws. After detecting and improving one single leakage point around a pipe penetrating one of the test samples, the air leakage rate was reduced by 50% for the wall assembly as a whole (Antonsson, 2017, p. 42).

Møller and Rasmussen (2020)

Møller and Rasmussen (2020) utilize a test rig intended to imitate a ceiling section to evaluate the airtightness of vapour barrier systems sealed with tape. The test rig consists of a wooden frame with two oblique boards simulating rafters. The test samples involve PE foils taped to the inside of the wooden frame with a pipe penetration in its centre, sealed with an adhesive collar. A fan is used to pressurize the test rig from below. An illustration of the setup is provided in Figure 2.9.

Figure 2.9: Test rig and sample simulating a roof section by Møller and Rasmussen (2020).

Møller and Rasmussen (2020) performed measurements of peel and shear resistance for the same tapes used in the airtightness evaluation. Peel and shear resistance were tested according to EN 12316-2 and EN 12317-2 respectively. The peel test was conducted using both concrete and vapour barriers as substrates. The study evaluated nine different vapour barrier systems, Peel and shear tests were performed on five individual specimens from each system. One specimen of each system was installed for evaluating airtightness. Each specimen was tested through three separate measurement series. The airtightness was measured at positive and negative pressure differences of 10, 22, 34, 46, 58, 70 and 82 Pa. Linear regression was later used to determine the air leakage rate n50. Peel, shear and airtightness samples were exposed to the same accelerated ageing process, consisting of 84 days at 70°C and 90% RH, followed by 84 days in a ventilated oven at 70°C.

After ageing, eight of the nine systems showed an increase in peel resistance greater than 20%. In the shear tests, four of the systems showed an increase, while four showed a marginal decrease. Only one system displayed a substantial reduction of around 30%. As for the airtightness, n50 was measured to lay around 1 - 4 m^3/h for all systems prior to ageing. After ageing, the leakage rates increased by 200-300% for most of the systems, with n50 typically measured around 11 - 12 m^3/h.

The authors describe the airtightness measurements as reproducible, as each specimen was tested at least three times with little variation between results (Møller and Rasmussen, 2020, p. 7). In their conclusion, they raise the question of whether the standardized methods of peel and shear resistance are relevant, as they produced results contradicting the results from airtightness tests.

Van Linden and Van den Bossche (2017)

In a study from Ghent University in Belgium, Van Linden and Van den Bossche (2017) uses a test rig with sample dimension 1232x1232 mm to measure the airtightness of tape applied to solid boards of concrete, OSB and fibreboard. The test method involves installing 16 boards measuring 295x295 mm into the rig with 18 mm gaps in-between as shown in Figure 2.10. Adhesive tape is later applied over the gaps, as can be seen in the photo to the right in Figure 2.10. The test samples were pressurized in eight steps; 50, 100, 150, 200, 250, 300, 450 and 600 Pa. Measurements were later curve fitted using the aforementioned power law described in Equation 3. The resulting curve was used to estimate the leakage rate at a reference pressure difference of 50 Pa, n50.

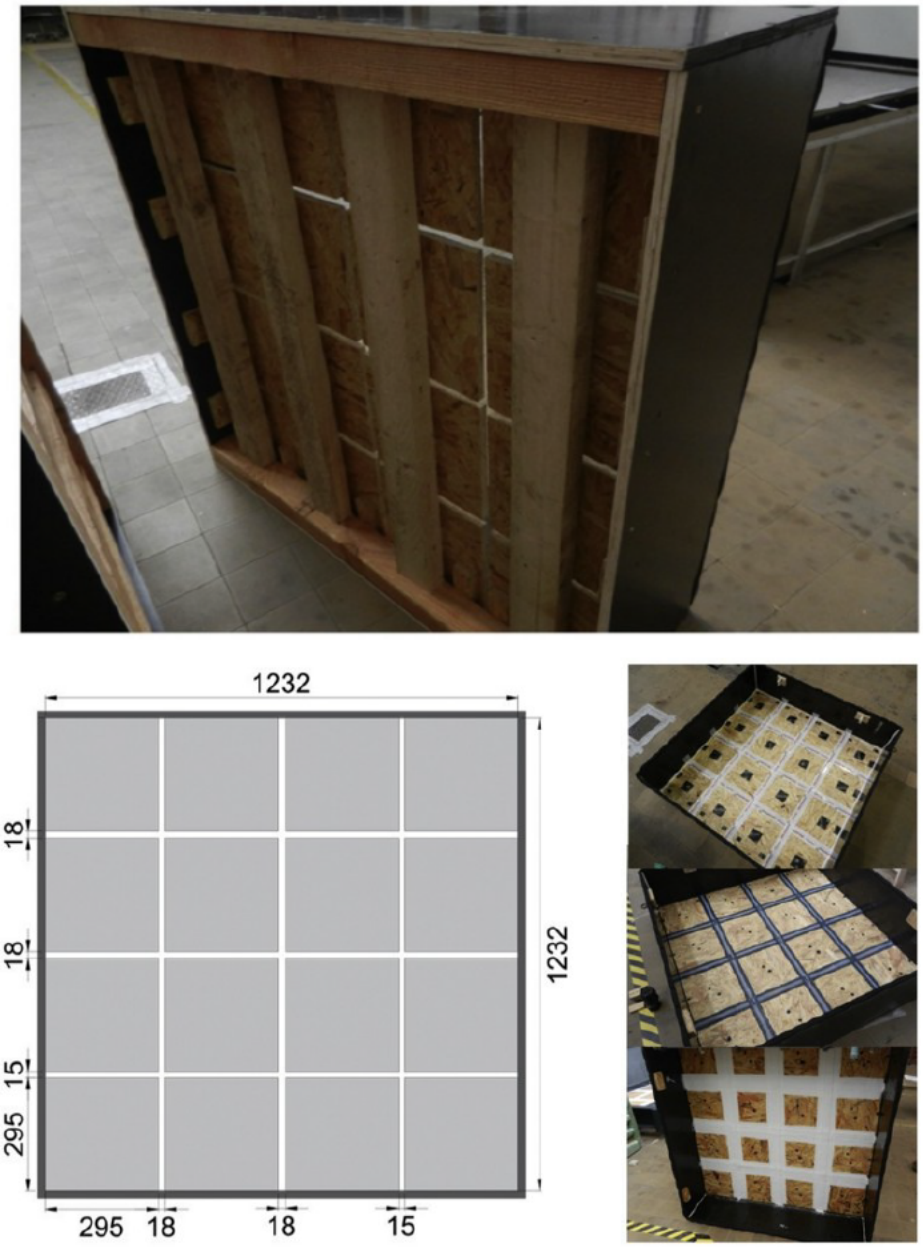

Figure 2.10: Test rig and samples used by Van Linden and Van den Bossche (2017).

Ageing of the test samples included wetting prior to a 24-hour drying period. This was followed by mechanical ageing where the samples were pressurized at 1000 Pa through 200 pulsations. Lastly, the wetting and drying procedure was repeated once more.

Results from the study showed that the airtightness of the tapes varied considerably depending on the substrate. Tape applied to OSB or fibreboard had an air permeability of 0.02 - 0.05 m^3/mh, while the same tapes were typically 10 times more airtight when concrete constituted the substrate. The artificial ageing procedure affected permeability rates comparatively little, as only one out of ten samples saw a significant increase, constituting approximately 30%. Among the fibreboard samples, one sample saw permeability decrease by around 30 %. In contrast, another sample incorporating the same substrate failed during the ageing procedure (Van Linden and Van den Bossche, 2017, p. 7).

Ylmén et al. (2012)

Ylmén et al. (2012) have conducted a study evaluating the airtightness of barrier systems using a test rig consisting of walls, floor and ceiling in a realistic scale. A 2.4-meter tall timber frame construction is built on top of a 2.2x2.2 meter cast concrete foundation. Three of the walls are outfitted with a window, while the fourth includes a door. Figure 2.11 illustrates the test rig. The timber framework makes it possible to install insulation, piping and air and vapour barriers. A blower door system is mounted to the door frame to pressurize the test rig. Air leakage rates are measured at five pressure steps of both positive and negative pressure differences before fitting the measurements to a curve. This curve is then used to estimate n50 at reference conditions.

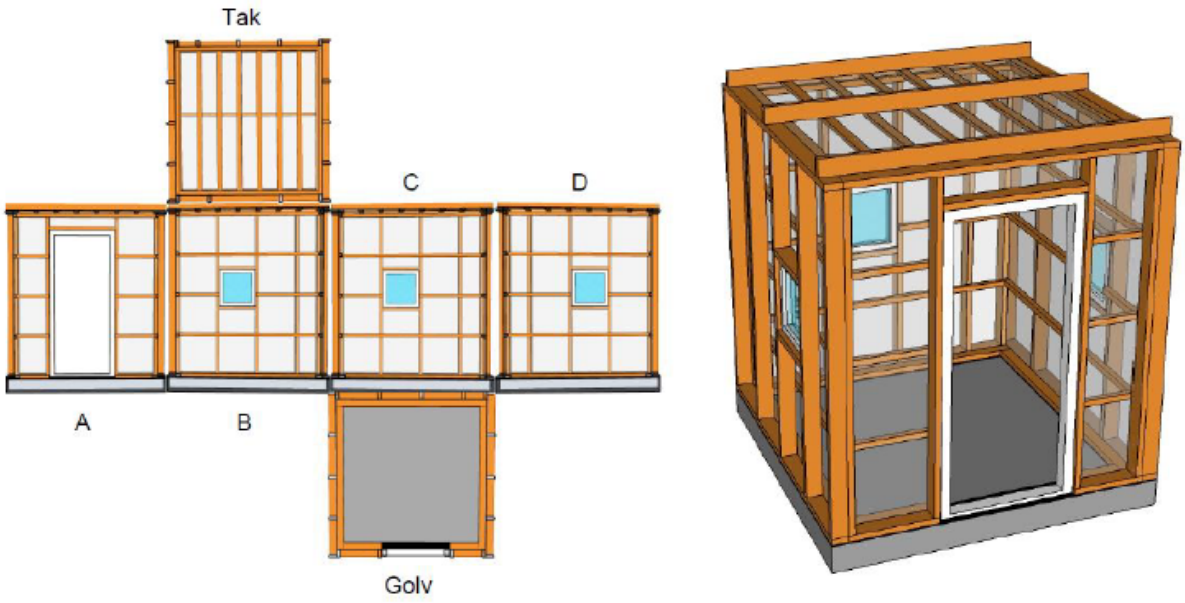

Figure 2.11: Full-scale test rig used by Ylmén et al. (2012).

During the study, multiple barrier systems and sealing products were combined in a test sample, including several different tapes and sealants along with wood strips. The rig was exposed to accelerated ageing through 12 months at 80°C and 50% RH, under the assumption that a 10°C temperature elevation would lead to a doubling in reaction speeds. Assuming 20°C constitutes natural conditions, the accelerated ageing process would then be equivalent to well over 50 years of natural ageing. To simulate winter conditions, the relative humidity was lowered to 30% for one week every month during this process.

Parallel to the airtightness evaluation, standardized peel and shear resistance measurements were performed on the same sealing products as those installed in the rig. The peel and shear samples were left inside the test rig during the ageing process so that they were exposed to the same conditions. While the air leakage rate of the test rig increased by 100% after artificial ageing, the adhesive tapes showed a 10 to 20 % increase in shear resistance after the ageing process. A thermal camera was used to locate leakages in the rig after ageing, whereof many could be traced to air pockets between the tape and substrate (Ylmén et al., 2012).

2.8 Comparison of methods

The experimental methods take different approaches to evaluate tape durability. Most apparent is the difference in how the standardized methods mainly rely on quantifying adhesive properties, while the experimental methods assess airtightness. The methods differ in several ways but also share common features. Table 2.8 provides an overview comparing some of their aspects. This section will further compare the results and observations made when applying the different methods.

Table 2.8: Experimental methods for durability assessment of adhesive tapes.

Method	**Antonsson**	**Møller and Rasmussen**	**Van Linden and Van den Bossche**	**Ylmén et al.**
Dimensions	3 x 3 m	0.5 x 0.5 m	1.2 x 1.2 m	2.2 x 2.2 x 2.4 m
Airtightness	Yes	Yes	Yes	Yes
Peel resistance	No	Yes	No	Yes
Shear strength	No	Yes	No	Yes
Substrates	Air/vapour barrier	Vapour barrier	Concrete/OSB/ fibreboard	Air/vapour barrier
Ageing process	Heat, RH	Heat, RH	Dynamic pressurization	Heat, RH
Load	60°C, 50%	70°C, 90%	1000 Pa	80°C, 50%
Duration	6 weeks	84 + 84 days	200 Pulses	12 months

The methods developed by Antonsson (2017) and Ylmén et al. (2012) simulate building components with realistic dimensions, making the tests and ageing processes highly representative. However, full-scale testing can be costly and time-consuming. Issues with reproducibility have also led to questions of whether the full-scale methods are assessing the quality of implementation rather than product properties (Leprince et al., 2017, p. 10).

The studies conducted by Antonsson (2017) and Ylmén et al. (2012) only involved testing one single specimen of each configuration, making it difficult to conclude on the reproducibility of the two methods. Møller and Rasmussen (2020) and Van Linden and Van den Bossche (2017) were able to test more samples, making it easier to evaluate the reproducibility of their methods. Reduction of scale may, on the other hand, cause the results to be less representative (Leprince et al., 2017, p. 11).

Ylmén et al. (2012) and Møller and Rasmussen (2020) came to the conclusion that there is no clear correlation between airtightness and mechanical properties, such as peel and shear resistance. Despite their differing test scales, both studies found that peel and shear resistance tends to improve after accelerated ageing while the airtightness deteriorates. Still, some of the observations may appear counter-intuitive when compared with other research: While Van Linden and Van den Bossche (2017) found that the airtightness of

taped joints depended on the substrate, Sletnes and Frank (2020) found that peel and shear resistance varied more between different tapes than between different substrates.

Out of the studies, Van Linden and Van den Bossche (2017) are the only ones addressing airtightness using concrete as a substrate. While several of the studies reviewed by Sletnes and Frank (2020) included concrete as a substrate for peel and shear resistance measurement, concrete is not included as a standard substrate in the current SINTEF guidelines for Technical Approval of adhesive tapes.

The two full-scale methods and Møller and Rasmussen (2020) include adhesive tape joints linking two or more different materials, for instance, wood and PE foil, or wood and concrete. Different materials undergo different dimensional changes in response to varying temperature and moisture content, which might lead to skewed deformation and tension in the tape. This can in turn affect adhesive properties or airtightness (Ylmén et al., 2012, p. 9). Studying this phenomenon in isolation would be relevant to better understand how the airtightness of tape joints evolves in the long term.

3 Materials and methods

As part of this master's thesis, an experimental method has been developed to evaluate the air permeability and durability of joints sealed with adhesive tapes. The method in development is presented in Section 3.1. The procedure used to collect and analyze data is inspired by NS-EN 12114:2000 (Standard Norge, 2000).

The reproducibility, repeatability and accuracy of the method are assessed through a measurement program described in Section 3.2. The program involves measuring the air permeability of specimens from six different material samples. Each test sample consists of a given combination of one adhesive tape and a substrate. Test samples and specimens are described in Section 3.2.2. Specimens are tested before and after artificial ageing to assess whether the test setup is suitable for evaluating the durability of adhesive tapes. The ageing procedures are described in Section 3.4.

Parallel to the air permeability evaluation, the same material samples are tested for peel resistance in accordance with the national standard NS-EN 12316-2:2013 (Standard Norge, 2013*c*). The peel resistance measurements are conducted on non-aged and artificially aged test specimens, exposed to the same ageing procedure as the corresponding air permeability specimens. The method used to measure peel resistance is described in Section 3.3.

The purpose of performing standardized peel resistance measurements of the material samples is to examine how the durability evaluation from the method in development compares to a currently well-established test method, i.e. NS-EN 12316-2:2013. Results from the two methods are compared to observe whether there is a correlation between the air permeability and adhesive properties of the materials.

3.1 Air permeability test method

The experiments are conducted using a test rig in the laboratories of SINTEF Community in Trondheim. A schematic drawing of the setup is shown in Figure 3.1. The setup includes a Test Stand made from welded-together steel plates unto which a test specimen is installed, thus creating an enclosed volume. The Test Stand is more thoroughly described in Section 3.1.1.

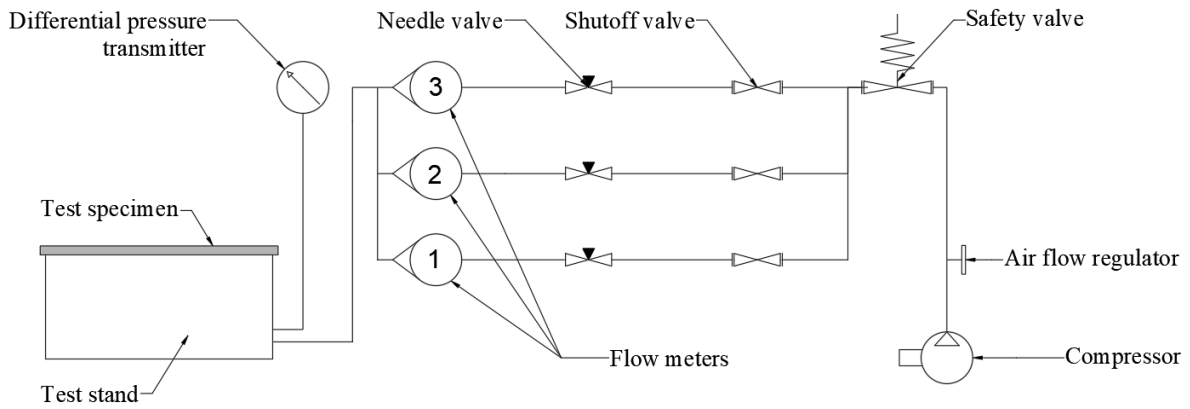

Figure 3.1: Schematic drawing of the test setup.

The Test Stand is pressurized by supplying compressed air through a custom-made pressurization rig, shown in Figure 3.2, creating a positive static pressure difference Δp between the inside of the Test Stand and the laboratory environment. The test specimens are consequentially exposed to the same pressure difference Δp, which is measured with a resolution of 0.1 Pa using an FCO432 differential pressure transmitter (DPT). The DPT is connected to the Test Stand through a rubber tube, and measures the pressure difference between the Test Stand and the ambient environment with an accuracy of $<$0.25% on each reading (Furness Controls, 2023).

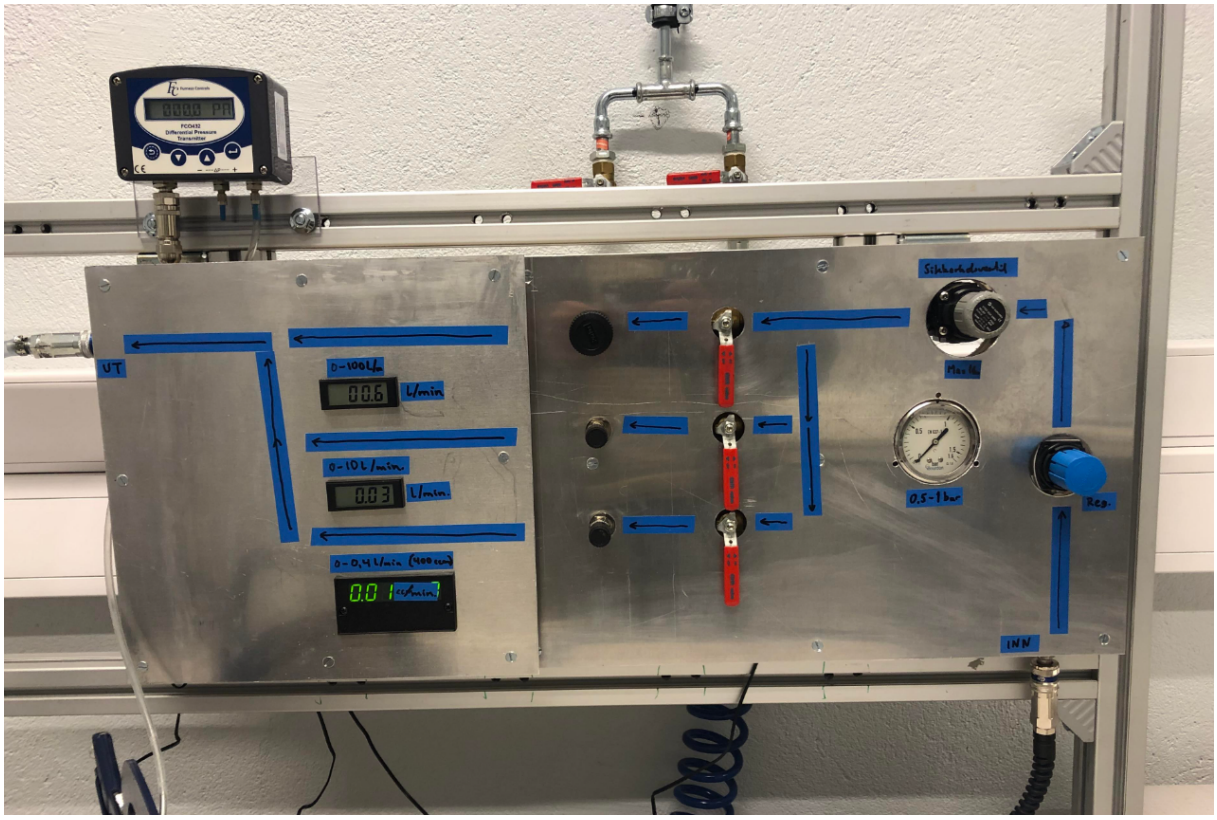

Figure 3.2: Close-up photo of the pressurization rig.

Three Flow Meters, as shown enumerated in Figure 3.1, are used to monitor the airflow rate $\dot{V}$ supplied to the Test Stand. Each Flow Meter is connected to its own separate air conduit which can be opened or closed off using shutoff valves. Between each shutoff valve and Flow Meter is a needle valve which enables finer adjustment of the airflow.

Flow Meter 1 uses an electronic manometer to provide the volumetric airflow based on pressure differences in the air conduit. The manometer handles pressures up to 2 bar. A safety valve starts releasing air if the pressure in the rig exceeds 1 bar. Flow Meters 2 and 3 are thermal mass Flow Meters, giving the flow rate based on temperature differences in the air conduit. If air continuously flows through the thermal Flow Meters over a long time, temperature elevation may lead to offset and fluctuations in the readings. To prevent this, it is important to close the shutoff valves between measurement series to let the instrument cool down.

Flow Meters 1 and 2 can measure flow rates with a resolution of 0.01 ml/min and 0.01 l/min within the ranges of 0 - 0.4 and 0 - 10 l/min respectively. Flow Meter 3 measures the airflow rate with a resolution of 0.1 l/min within the range of 0 - 100 l/min. Only one Flow Meter is used to take measurements at a time, while the other two remain shut off from the air supply. Since Flow Meter 1 provides readings with the highest resolution, it is used until the pressurization of a specimen requires flow rates greater than 0.4 l/min. At this point, the air supply to Flow Meter 1 is shut off and Flow Meter 2 takes over. Likewise, Flow Meter 3 takes over when the required flow rate surpasses 10 l/min.

The pressure levels and corresponding flow rates are in turn used to determine the air leakage rate through the specimen through linear regression. The measurement and calculation procedures used to obtain the test results are described further in Sections 3.1.3 - 3.1.5.

On 18.01.2023, the residual leakage rate of the pressurization rig was measured at 0.1 ml/min (0.000006 m^3/h) at a pressure difference of 100 Pa. This value does not take into account system leakage from the Test Stand.

3.1.1 Test Stand

The Test Stand consists of a box welded together from three steel plates, 2mm thick, leaving one side open for mounting test samples. The box is outfitted with 50 mm flanges pointing outwards from said opening. The flanges act as support for the test samples and allow for the fastening of clamps. The Test Stand is designed with dimensions allowing test samples to fit inside the heat chamber used for artificial ageing at SINTEF Community. A sketch of the box with dimensions is provided in Figure 3.3.

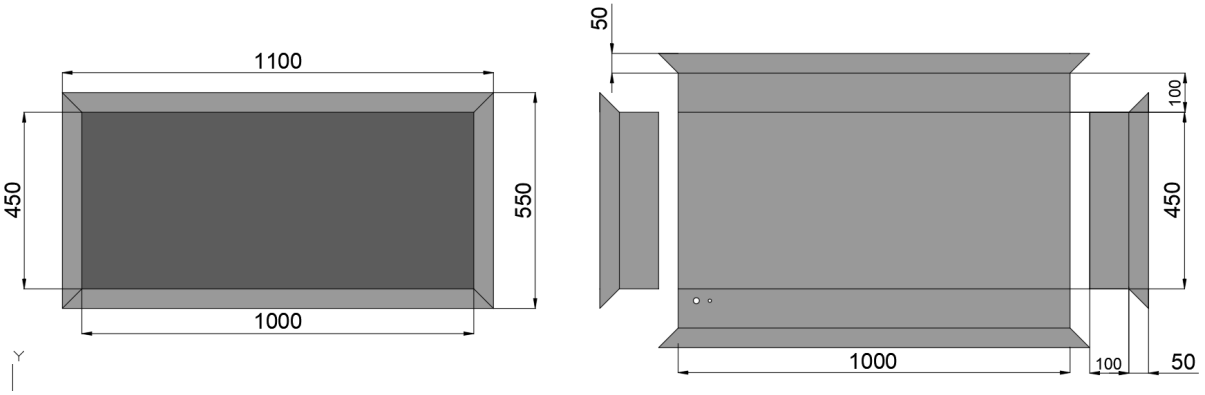

Figure 3.3: Dimensions of the Test Stand in mm as seen from above (left) and the steel plates prior to being welded together (right).

Hollow sections of steel (50x25mm) are welded together to form a frame corresponding to the shape and size of the flanges. This frame is to be put on top of the test samples to distribute the compression forces from clamps when fastening the test samples. A continuous rubber gasket, of equal shape and size as the flanges, is laid directly on top of the flanges to provide an airtight seal between the Test Stand and samples. The 50 mm wide gasket is made of 5 mm thick EPDM rubber with a shore hardness of 60.

Figure 3.4 shows a stylized cross-section of the assembled Test Stand with a test sample installed in it. A close-up illustration of the sealing principle is shown in Figure 3.5. The effective sample area is defined by the inner circumference of the rubber gasket and was measured to be 0.46 m^2.

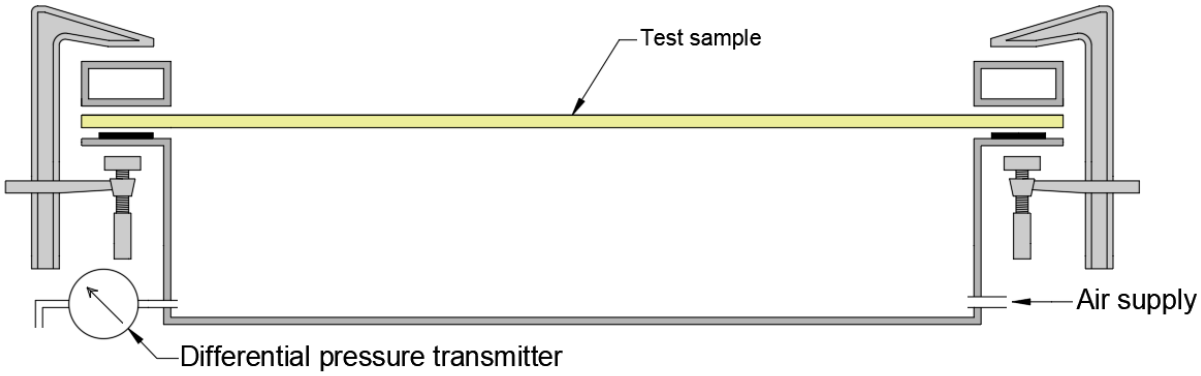

Figure 3.4: Stylized cross-section of the Test Stand with a test sample installed.

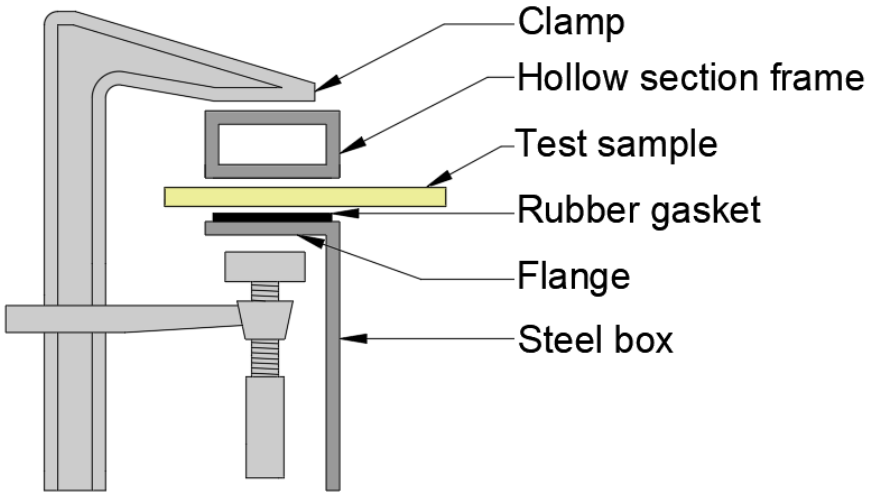

Figure 3.5: Cross-section showing the principle of sealing samples to the Test Stand.

Pressurized air is used to generate a positive pressure difference between the inside of the Test Stand and the laboratory environment. In order to simulate the effects of a negative pressure difference on a given specimen, the specimen can be turned upside down as shown in Figure 3.6. While conducting the experiments, leakage rates at positive pressure differences are measured by testing specimens with the tape facing upwards. Testing specimens with the tape facing downwards simulates measuring the leakage rate at negative pressure differences.

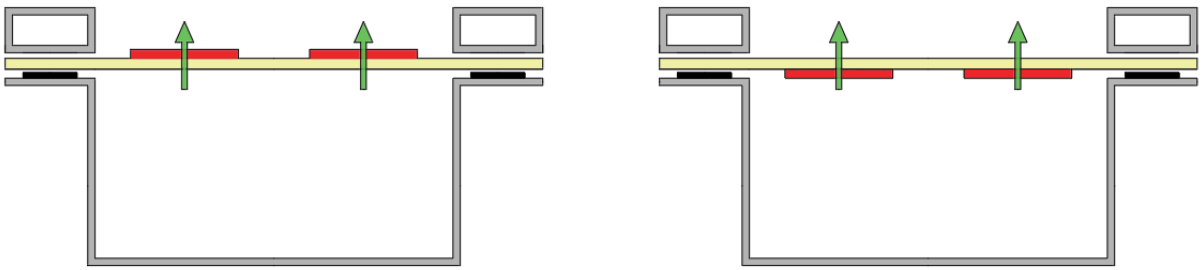

Figure 3.6: Tape joint exposed to positive pressure difference (left) and simulated negative pressure difference (right).

The steel box is penetrated by two openings. One is dedicated to connecting the air supply fitting, and the other is for attaching a silicone tube with an outer diameter of 6 mm, which connects to the differential pressure transmitter. An air supply hose is connected to the Test Stand through a quick-connect coupling with a 1/4-inch thread size. The connection to the pressure transmitter tube is sealed off with wax to reduce potential leakages. Both connections are shown in Figure 3.7.

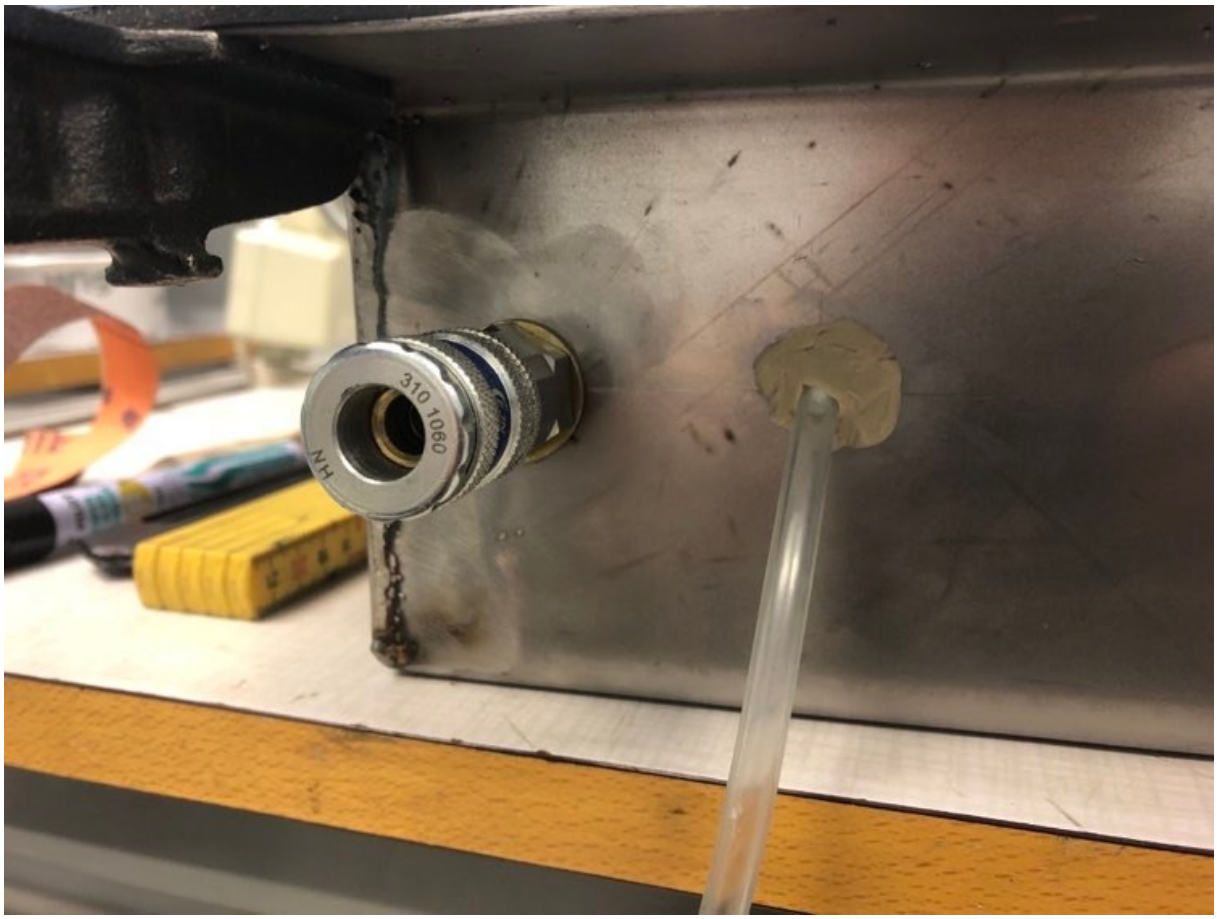

Figure 3.7: Connections for air supply (left) and differential pressure transmitter (right).

3.1.2 Preparation of specimen

A test specimen is prepared by cutting the substrate material into rectangular pieces of approximately 1200x650 mm. With these dimensions, the substrate sheet extends past the steel frame, allowing for adjusting the specimen when installing it to the Test Stand.

The joints are created by inducing four 900 mm long cuts in the substrate with a wallpaper knife, before covering them with lengths of tape as shown in Figure 3.8. The tape shall extend at least 30 mm past the cut in the longitudinal direction. The distance between each cut is 100 mm. After applying the tape, a rubber roller is rolled over the joints with applied force to remove potential air pockets between the tape and substrate.

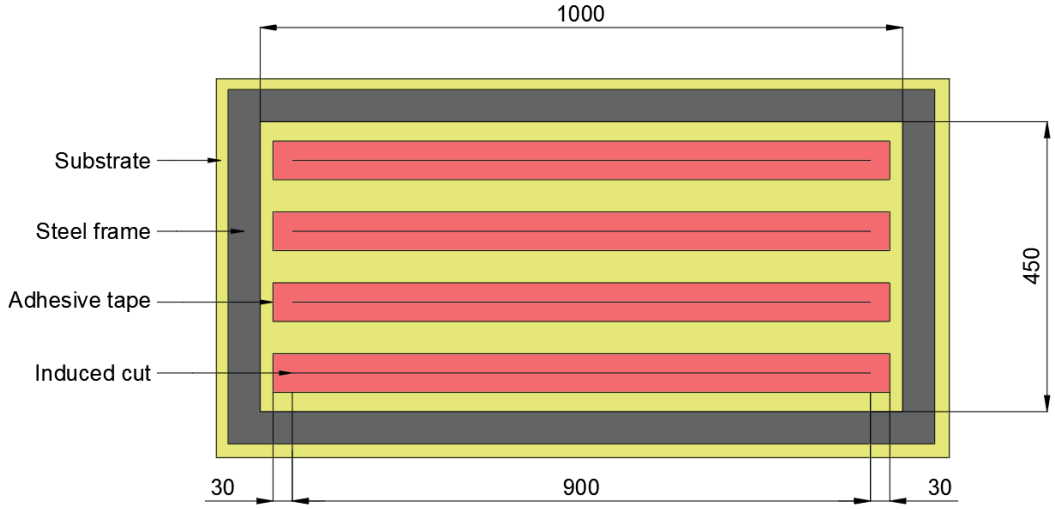

Figure 3.8: Layout of test specimen with dimensions in mm.

3.1.3 Data collection

Data collection is conducted in accordance with the test procedure described in NS-EN 12114:2000 for specimens fitted in a non-airtight test rig. The measuring begins with pressurizing the Test Stand with compressed air through the pressurization rig, creating a positive pressure on its inside. The airflow is regulated manually until the pressure difference rests at one of several predetermined levels. Pressure steps are determined according to Annex A of NS-EN 12114:2000. 100 Pa is used as the maximum pressure difference Δp_{max}, while 10 Pa is used as the lowest pressure Δp_{min}. The number of pressure steps N are chosen to be 7. The pressure steps Δp_i are determined by Equation 6, giving intervals between steps on a logarithmic scale (Standard Norge, 2000).

$$\Delta p_i = 10^{i\frac{log(\Delta p_{max})-log(\Delta p_{min})}{N}+log(\Delta p_{min})} \tag{6}$$

The formula gives the following seven pressure steps: 10, 15, 22, 32, 46, 68, 100 Pa. Figure 3.9 illustrates how the pressure varies during a measurement series. Three pressure pulses of 110 Pa are applied for three seconds each, before proceeding to the pressure steps. The pressure pulses should be 10% greater than Δp_{max}, in accordance with NS-EN 12114:2000.

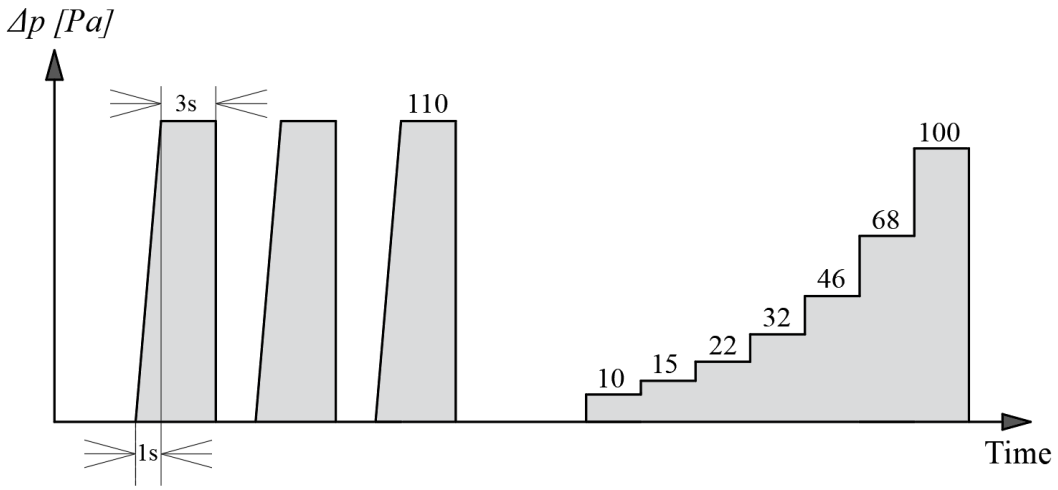

Figure 3.9: Pressure difference as a function of time during a measurement series.

In order to obtain the leakage rate at a given pressure step, the system must be in a steady state, where the pressure difference remains static at the given airflow rate. A steady state implies that the supplied airflow to the Test Stand is equal to the total leakage $\dot{V}_{tot}$ through the sample and Test Stand as shown in Equation 7.

$$\dot{V}_{tot} = \dot{V}_{sample} + \dot{V}_{system} \tag{7}$$

The leakage through the sample can further be divided into joint and substrate leakage as shown in Equation 8. If the substrate is considered airtight, the substrate leakage is neglected. Figure 3.10 illustrates the different types of leakages.

$$\dot{V}_{tot} = \dot{V}_{joint} + \dot{V}_{substrate} + \dot{V}_{system} \tag{8}$$

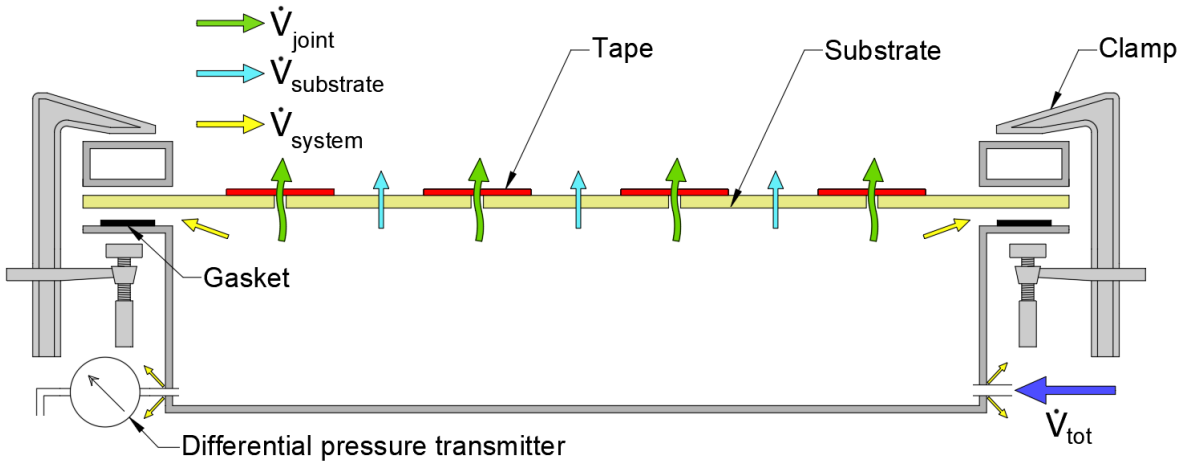

Figure 3.10: Stylized cross-section of the Test Stand showing air supply and leakage types.

The volumetric airflow going into the Test Stand can be regulated and monitored continuously. When the pressure stabilizes at one of the predetermined steps, the airflow rate and corresponding pressure level are recorded. The system is considered to be in a steady state if the ratio between the airflow and pressure difference remains stable for 30 seconds.

Prior to testing the samples themselves, reference measurements are conducted to evaluate the system leakage for each installation $\dot{V}_{system}$. The system leakage account for the sum of leakages going through the Test Stand itself, as well as the connection between the sample and the Test Stand. Reference measurements are taken by installing a sheet of PE membrane covering the samples as shown in Figure 3.11. The Test Stand is then pressurized to the predefined steps while recording the corresponding air leakage rates. Assuming the PE foil is airtight, the reference measurements are considered to be equal to the system leakage rate $\dot{V}_{system}$. After taking the reference measurements, the PE foil is cut open, exposing the test sample itself. The same measurement procedure is repeated, with the measured airflow now resulting in the total air leakage rate $\dot{V}_{tot}$, constituting the sum of leakages through the sample and the system.

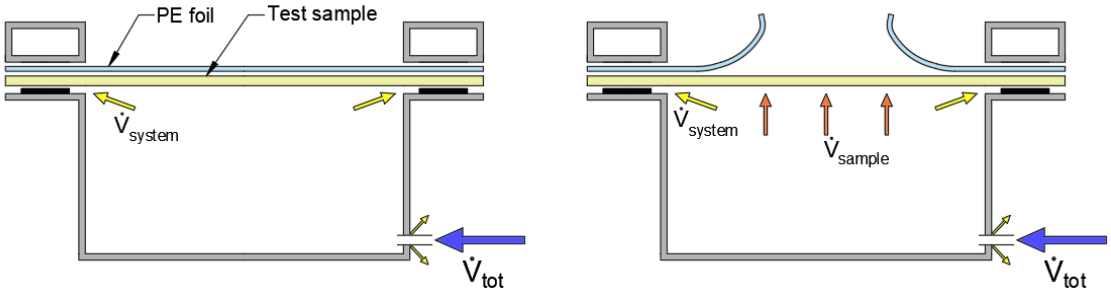

Figure 3.11: Measurement of system leakage rate (left) and total leakage rate (right).

Every test specimen is tested as described, through two measurement series of each leakage type. If the difference between the two measured values is larger than 10% of the smallest value, a third measurement series is conducted. During the measurement procedure, two consecutive reference measurement series are completed on each specimen before the PE foil is cut open, followed by two measurement series of the total leakage rate. The specimen remains fastened in the Test Stand through the entirety of this procedure.

3.1.4 Correction for reference conditions

In addition to recording the airflow rates, several properties related to the laboratory conditions are measured in order for the results to be comparable to similar experiments conducted under different climatic conditions.

The additional measurements include the following:

- Air temperature T.
- Absolute air pressure in laboratory p.
- Relative humidity of laboratory air ϕ.

SINTEF continuously monitors the atmospheric pressure in the laboratory with a resolution of 0.01 kPa. Temperature and relative humidity are measured with a handheld humidity and temperature indicator, HMI 41/45.

NS-EN 12114:2000 states that correction for reference conditions is necessary if the laboratory fails to meet one of the following conditions (Standard Norge, 2000):

- 18 to 22°C air temperature.
- 100 000 to 102 000 Pa atmospheric pressure.
- 25 to 50% relative humidity.

If these conditions are not met, the airflow rates are to be corrected as follows:

$$\dot{V}_0 = \dot{V}\sqrt{\frac{\rho}{\rho_0}} \tag{9}$$

$\dot{V}_0$ is the corrected airflow rate at reference conditions.
$\dot{V}$ is the measured airflow rate at laboratory conditions.
ρ_0 is the density of the air at reference conditions: $\rho_0 = 1.1988$ kg/m^3.
ρ is the density of the air at laboratory conditions, calculated in Equation 10.

$$\rho = \frac{p_a - 0.378802 p_w}{287.055 T} \tag{10}$$

T is the absolute temperature [K].
p_a is the atmospheric pressure [Pa].
p_w is the water vapour pressure [Pa] calculated using Equation 11.

$$p_w = 610.5 \cdot \phi \cdot exp\left(\frac{21.875 \cdot (T - 273.15)}{T - 7.65}\right) \tag{11}$$

ϕ is the relative humidity of the air.

3.1.5 Data processing

The recorded air leakage rate $\dot{V}_{tot}$ includes extraneous leakages going through the substrate and the Test Stand itself that need to be subtracted in order to obtain the air leakages going through the tape joints.

Leakage through the test sample, $\dot{V}_{sample}$, is calculated by subtracting the system leakage from the total leakage rate:

$$\dot{V}_{sample} = \dot{V}_{tot} - \dot{V}_{system} \tag{12}$$

Subtracting the substrate leakage results in the leakage through the joints:

$$\dot{V}_{joint} = \dot{V}_{sample} - \dot{V}_{substrate} \tag{13}$$

The substrate leakage of a given sample is evaluated by implementing the previously described measurement procedure on an intact piece of the associated substrate, free from cuts and tape joints. The intact substrate is tested before and after artificial ageing, parallel to the sample with tape joints. PE foil is considered to be practically airtight, hence $\dot{V}_{substrate}$ is neglected when evaluating the joint leakage of samples where these materials constitute the substrate.

A regression model described in NS-EN 12114:2000 is used to find the correlation between the pressure difference and leakage rate for each test sample. The aim is to express the relation between the pressure and leakage rate as a power law as seen in Equation 14 (Standard Norge, 2000).

$$\dot{V}(\Delta p) \rightarrow \dot{V} = C(\Delta p)^n \tag{14}$$

The data sets containing the reference measurements $\dot{V}_{system}$, substrate leakage $\dot{V}_{substrate}$ and the total leakage rate $\dot{V}_{tot}$ are treated separately, resulting in three different regressions. Table 3.1 outlines the process resulting in the three regressions for any given specimen.

Table 3.1: Overview of data collection and processing for a specimen.

Leakage type	**Measuring**	$\rightarrow$	**Correction**	$\rightarrow$	**Average**	$\rightarrow$	**Regression**
Total	$2 \cdot \dot{V}_{tot,i}$	$\rightarrow$	$2 \cdot \dot{V}_{0,tot,i}$	$\rightarrow$	$\bar{\dot{V}}_{0,tot}$	$\rightarrow$	$C_{tot}(\Delta p)^{n_{tot}}$
System	$2 \cdot \dot{V}_{sys,i}$	$\rightarrow$	$2 \cdot \dot{V}_{0,sys,i}$	$\rightarrow$	$\bar{\dot{V}}_{0,sys}$	$\rightarrow$	$C_{sys}(\Delta p)^{n_{sys}}$
Substrate	$2 \cdot \dot{V}_{sub,i}$	$\rightarrow$	$2 \cdot \dot{V}_{0,sub,i}$	$\rightarrow$	$\bar{\dot{V}}_{0,sub}$	$\rightarrow$	$C_{sub}(\Delta p)^{n_{sub}}$

Pressurization of a specimen may lead to deformations affecting its air permeability between measurements. For this reason, the three leakage types are evaluated through two separate, subsequent measurement series each, to ensure leakage rates do not fluctuate

between series. The substrate leakage is measured on a separate specimen, consisting of an intact piece of substrate. Measured airflow rates, shall be corrected for reference conditions according to Equation 9 if needed. For each leakage type, at every pressure step, the averages of the two corrected measurement series are calculated, resulting in the data sets $\bar{\dot{V}}_{0,tot}$, $\bar{\dot{V}}_{0,sys}$ and $\bar{\dot{V}}_{0,sub}$, which are used as input for the regression analyses.

The flow coefficient C and exponent n is found through linear regression. In order to do this, the exponential equation must first be transformed:

$$ln(\dot{V}) = ln(C) + n \cdot ln(\Delta p) \tag{15}$$

The logarithmic expressions are replaced with y, a and x for a simplified equation:

$$y = a + n \cdot x \tag{16}$$

where:

$$y = ln(\dot{V}), \quad a = ln(C) \text{ and } \quad x = ln(\Delta p)$$

Linear regression is then used to determine the coefficients a and n, beginning with finding the averages:

$$\bar{x} = \frac{1}{N}\sum_{i=1}^{N} x_i \tag{17}$$

$$\bar{y} = \frac{1}{N}\sum_{i=1}^{N} y_i \tag{18}$$

N is the number of pressure steps.

This is followed by estimating the variances:

$$s_x^2 = \frac{1}{N-1}\sum_{i=1}^{N}(x_i - \bar{x})^2 \tag{19}$$

$$s_y^2 = \frac{1}{N-1}\sum_{i=1}^{N}(y_i - \bar{y})^2 \tag{20}$$

$$s_{xy} = \frac{1}{N-1}\sum_{i=1}^{N}(x_i - \bar{x})(y_i - \bar{y}) \tag{21}$$

The closest estimates for a and n are then calculated according to Equation 22 and 23 respectively (Standard Norge, 2000).

$$a = \bar{y} - n\bar{x} \tag{22}$$

$$n = \frac{s_{xy}}{s_x^2} \tag{23}$$

The flow coefficient is then determined as follows:

$$C = e^a \tag{24}$$

The three regressions conducted for a given specimen result in three functions expressing its total leakage rate, the system and the substrate leakage respectively. The estimated mean leakage rate through the tape joint, $\dot{V}_{joint}$, is obtained by subtracting the system and substrate leakage from the total leakage rate:

$$\dot{V}_{joint}(\Delta p) = C_{tot}(\Delta p)^{n_{tot}} - C_{sys}(\Delta p)^{n_{sys}} - C_{sub}(\Delta p)^{n_{sub}} \tag{25}$$

The mean leakage rate through the joint is divided by the length of the joint, l, to express the air permeability of the tape joint q_{joint}:

$$q_{joint}(\Delta p) = \frac{\dot{V}_{joint}(\Delta p)}{l}[m^3/mh] \tag{26}$$

The results from the regression analysis used to estimate the air permeability of the joints at a 50 Pa pressure difference, q_{50}.

3.1.6 Error analysis

The uncertainty related to the results from the regression analysis is evaluated using a method described in Annex B.2 in NS-EN 12114:2000. The method is used to establish a 95% confidence interval for both coefficients. The evaluation begins with estimating the variances of the coefficients (Standard Norge, 2000):

$$s_n = \frac{1}{s_x}\left(\frac{s_y^2 - n s_{xy}}{N-2}\right)^{\frac{1}{2}} \tag{27}$$

$$s_a = s_n\sqrt{\frac{\sum_{i=1}^{N} x_i^2}{N}} \tag{28}$$

The 95% confidence interval of y is calculated based on the standard deviation of the estimated mean, $\bar{y}$, from the regression, which is calculated using Equation 29 (ISO, 2014, p. 14).

$$s_{\bar{y}} = s_n \cdot \left(\frac{N-1}{N} s_x^2 + (x - \bar{x})^2 \right)^{\frac{1}{2}} \tag{29}$$

To establish a confidence interval for each coefficient, NS-EN 12114:2000 uses the significance limits of a two-sided Student t-distribution, $T(P, \nu)$, where P is the probability and ν represents the degrees of freedom, equal to $N - 2$. Here, P is set to 0.95, in order to achieve a 95% confidence interval. N is the number of pressure steps used during the measurement procedure. Previously, in Section 3.1.3, N was chosen to be 7.

The confidence levels of the n, a and y can thus be expressed as:

$$I_n = s_n \cdot T(P, N-2) = s_n \cdot T(0.95, 5) \tag{30}$$

$$I_a = s_a \cdot T(P, N-2) = s_a \cdot T(0.95, 5) \tag{31}$$

$$I_y = s_y \cdot T(P, N-2) = s_n \cdot T(0.95, 5) \tag{32}$$

Values for I_n, I_a and I_y are calculated using the confidence limits of a two-sided Student t-distribution, which are presented in Table 3.2. Consequentially, there is a probability P of 0.95 that the coefficient n lies within the interval $[n - I_n, n + I_n]$, and likewise for a and y.

Table 3.2: Two-sided confidence limits of a Student t-distribution (Standard Norge, 2000).

	T(*P*, *N*-2) for probability *P* =					
N-2	0,8	0,9	0,95	0,99	0,995	0,999
1	3,078	6,3138	12,706	63,657	127,32	636,619
2	1,886	2,9200	4,3027	9,9248	14,089	31,598
3	1,638	2,3534	3,1825	5,8409	7,4533	12,924
4	1,533	2,1318	2,7764	4,6041	5,5976	8,610
5	1,476	2,0150	2,5706	4,0321	4,7733	6,869
6	1,440	1,9432	2,4469	3,7074	4,3168	5,959
7	1,415	1,8946	2,3646	3,4995	4,0293	5,408
8	1,397	1,8595	2,3060	3,3554	3,8325	5,041
9	1,383	1,8331	2,2622	3,2498	3,6897	4,781
10	1,372	1,8125	2,2281	3,1693	3,5814	4,5787
NOTE: From Kiem & Lentner (ed.): Documenta Geigy, Scientific Tables. Geigy, Basle, 1970.						

3.2 Measurement program

This Section describes a measurement program used to assess the aptness of the previously described test method. The measurement program is planned out with the intention of assessing the reproducibility, accuracy and repeatability of the test method.

3.2.1 Test Stand leakage evaluation

Installing test specimens to the Test Stand involves fastening and tightening them with clamps to provide an airtight seal between the steel box and the test sample. The air permeability of the sealing itself, along with the connections to the differential pressure transmitter and air supply, may vary between each installation, depending on the placement and tightening of clamps. Air leakages originating from the seals and connections in the Test Stand constitute the system leakage, $\dot{V}_{system}$.

The system leakage constitutes a systematic uncertainty when evaluating the air permeability of the test samples. A series of tests have thus been performed in an effort to evaluate the magnitude and variations of the system leakages. Results from these tests are used to assess whether the system leakages vary along with the installation technique, and in turn how the system leakage can be minimized.

The Test Stand leakage evaluation is performed by installing a sheet of PE foil over the Test Stand's opening, before pressurizing the Test Stand until a steady pressure difference of 100 Pa is achieved. The airflow rate going into the Test Stand is simultaneously recorded under the assumption that the PE foil is airtight. The recorded flow rate is consequently assumed to be equal to the system leakage. This test procedure is repeated, varying the number of clamps to assess how this affects the system leakage rate. The test starts out using 8 clamps, as shown in Figure 3.12, before the test is repeated using 12 clamps.

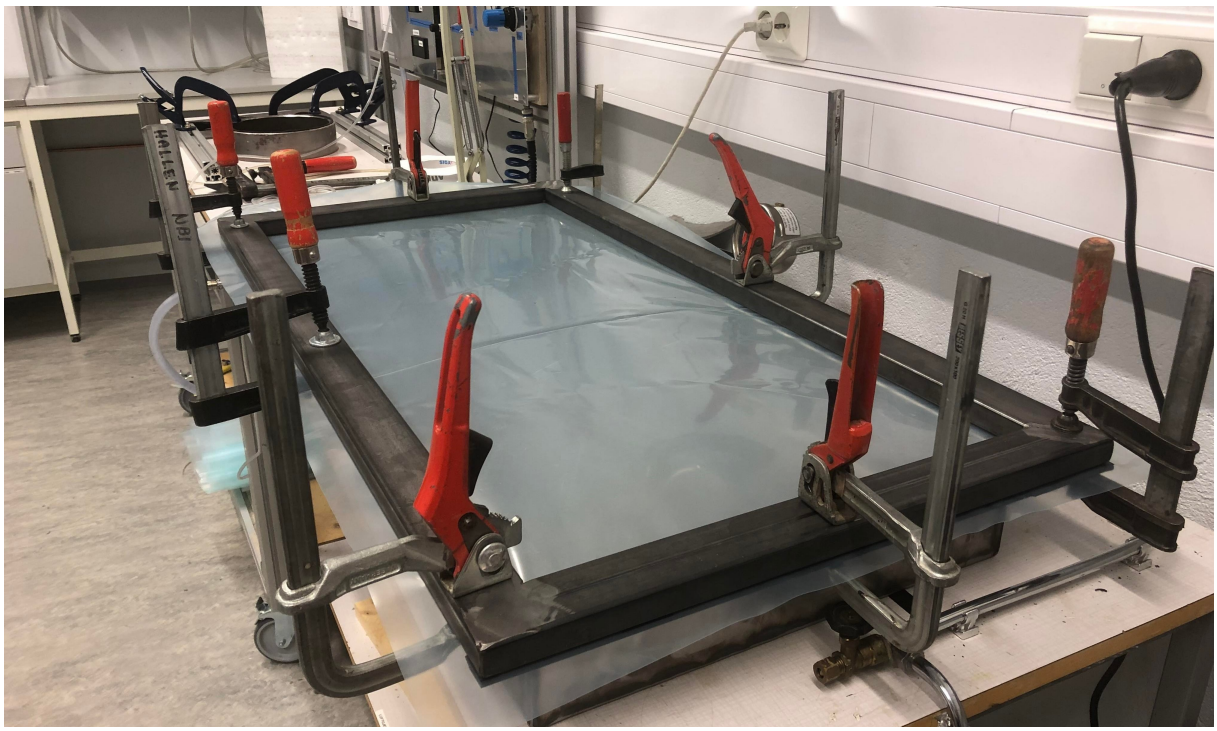

Figure 3.12: Test Stand leakage evaluation setup using 8 clamps.

Leak detection tests are conducted to detect and locate potential leakages in the Test Stand. These tests are performed by spraying soapy water on expected leakage points in the Test Stand before pressurizing it. These points include the welding joints and the connections to the air supply and differential pressure transmitter. Any leakages will then become visible as soap bubbles appear on the outside of the stand.

3.2.2 Material samples

The method in development is used to evaluate the air permeability of six different material samples, made by combining different adhesive tapes and substrate products. Several material combinations are included in the experiments to examine whether the method is suitable for making a general, quantitative assessment of product permeability and durability, or if the quality of workmanship in each individual specimen is the determining factor for the measurement results.

The material samples used in these experiments consist of combinations of three commercially available tape products and two different substrates, as shown in Table 3.3 and 3.4. The tapes chosen for the samples include a universal tape (T1) for use in both air and vapour barriers, an air barrier tape (T2) and a duct tape (T3). Both T1 and T2 have received Technical Approval from SINTEF for their respective areas of use.

The duct tape, T3, is developed for sealing applications in HVAC systems (heating, ventilating, air conditioning) and has not received any Technical Approval from SINTEF for use in either air or vapour barrier systems.

Table 3.3: Adhesive tapes used in material samples.

Tape	**Description**
T1	Universal tape with an acrylic adhesive with flexible backing.
T2	Air barrier tape with a modified acrylic adhesive and rigid backing.
T3	Duct tape with a rubber adhesive and a PE-coated cloth backing.

Different substrates are chosen to observe how the air permeability of the tapes varies depending on the surface it is adhered to. Some substrates, such as PE foil are practically airtight, making it easier to measure an isolated joint leakage rate. For substrates that are comparatively air permeable, it may be necessary to measure and subtract the leakage going through the substrate itself before obtaining the joint leakage.

Both air barrier material and PE membrane constitute standard substrates in the context of SINTEF Technical Approval, and are among the end-use substrates with which adhesive tapes are typically used. Because of this, they were considered to be the most relevant test substrates, along with wood and concrete. Wood and concrete are, however, not included in the study due to limited time and resources.

Table 3.4: Substrates used in material samples.

Substrate	Description
PEF	Vapour barrier, 0.20 mm PE foil.
ROM	Roofing membrane consisting of PU film covered with PP felt.

Table 3.5 provides an overview of the material samples created by combining the aforementioned tapes and substrates. The overview includes NT-ROM, consisting of the roofing membrane without any cuts or tape, which is used to estimate the substrate leakage rate of the ROM samples. This does not apply to the PE membrane since it is assumed in advance to be airtight enough for the substrate leakage to be neglected.

Table 3.5: Combinations constituting material samples.

	PEF	ROM
T1	T1-PEF	T1-ROM
T2	T2-PEF	T2-ROM
T3	T3-PEF	T3-ROM
No Tape	-	NT-ROM

3.2.3 Parallel specimens

The reproducibility of the method is assessed by assembling and testing several identical specimens of all material samples. The parallel specimens are installed and tested under identical conditions to assess the uncertainty related to the implementation of each individual specimen. Conducting tests on several parallel specimens also provides more data to be analyzed, which allows for drawing more confident general conclusions related to the air permeability of different material samples. Table 3.6 provides an overview of the specimens from each of the material samples. Appendix A includes a more detailed overview of the relation between material samples, specimens and measurement series.

Table 3.6: Overview of material samples and respective specimens.

Material sample	Test specimens
T1-PEF	T1-PEF-A, T1-PEF-B, T1-PEF-C, T1-PEF-D
T2-PEF	T2-PEF-A, T2-PEF-B, T2-PEF-C
T3-PEF	T3-PEF-A, T3-PEF-B, T3-PEF-C
T1-ROM	T1-ROM-A, T1-ROM-B
T2-ROM	T2-ROM-A, T2-ROM-B
T3-ROM	T3-ROM-A, T3-ROM-B
NT-ROM	NT-ROM-A, NT-ROM-B

3.2.4 Repeatability evaluation

Repeatability is evaluated by testing three of the specimens from Table 3.6 through three separate measurement series, where the specimen is removed and reattached to the Test Stand between each series. Every installation and test is performed in the same manner, to examine how the measured air permeability of a given specimen varies depending on the installation. As the specimen ideally should have the same air permeability in each measurement series, this repeatability evaluation is meant to give an indication of whether the test method is accurate and reliable. Table 3.7 provides an overview of the specimens and measurement series used to evaluate the repeatability of the test method.

Table 3.7: Specimens and measurement series used for repeatability evaluation.

Test specimen	Measurement series
T1-PEF-A	T1-PEF-A1, -A2, -A3
T1-PEF-D	T1-PEF-D1, -D2, -D3
T2-PEF-C	T2-PEF-C1, -C2, -C3

3.2.5 Comparison to peel resistance

Peel resistance tests are performed parallel to the air permeability tests, using the same material samples. The measurement program involves preparing and testing a total of 10 individual peel specimens from every material sample, with five of the specimens tested in a non-aged condition, and the remaining five tested after artificial ageing. Section 3.3 describes the peel resistance test procedure.

The purpose of the parallel peel resistance tests is to compare how air permeability and peel resistance change as a result of artificial ageing, to see whether there exists a correlation between the results from the two methods. Peel specimens are exposed to the same artificial ageing procedures as their corresponding air permeability specimens, as described in Section 3.4, in an effort to make the results comparable.

3.3 Peel resistance test

Peel resistance is measured in accordance with the Norwegian national standard NS-EN 12316-2:2013. The measurements are performed in the laboratories of SINTEF Community, in line with their accredited test procedure. The procedure is described through Sections 3.3.1 and 3.3.2

3.3.1 Apparatus and test procedure

The tests utilize a Zwick/Roell Z010 Material Tensile Testing Machine which was last calibrated on 07.12.2022. The machine is outfitted with two metal grips for fastening test specimens which can provide tensile forces up to 10 kN. Figure 3.13 shows a photo of the testing machine.

During the test, the substrate and tape are fastened to the lower and upper grip respectively, as seen in Figure 3.14. The upper grip pulls upwards, which results in the tape gradually being peeled off the substrate. The grip moves at a constant speed of 100 mm/min while the peeling force is continually measured and logged by a load cell. The test continues until the joint fails.

Figure 3.13: Zwick/Roell Z010 Material Tensile Testing Machine.

Figure 3.14: Peel resistance specimen in the testing machine.

When a test is completed, the failure mode is recorded as one of the following:

- A: Peeling of joint - failure of adhesive.
- B: Break outside of joint - failure of substrate or tape backing material.
- C: Delamination of sheet - separation of material layers parallel to the joint.

The maximal peel resistance of the specimen is recorded, while a computer automatically calculates its average peel resistance in accordance with NS-EN 12316-2:2013.

3.3.2 Preparation of specimen

Peel resistance specimens are prepared according to EN 13416. Preparation begins with cutting out 100x200 mm pieces of substrate material with a machine press. A 50 mm wide piece of adhesive tape is applied to the substrate so that the length of the joint is 100 mm as shown in Figure 3.15. If the adhesive tape is wider than 50 mm, it is cut into 50x300 mm strips with a machine press prior to applying it to the substrate. In the end, the contact surface between the substrate and tape should measure approximately 50x100 mm. Figure 3.16 provides a photograph of a ready-prepared specimen. Non-aged test specimens are conditioned at (23 ± 2)°C and 48% RH for 24 hours after assembly before testing.

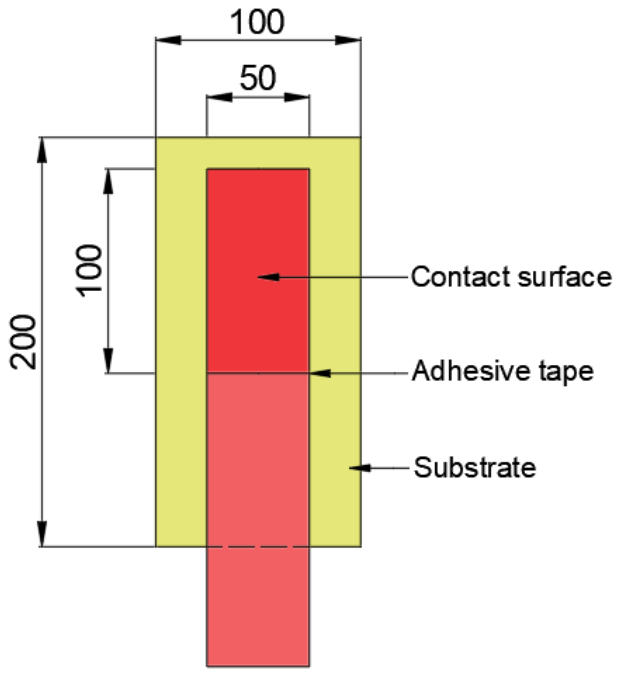

Figure 3.15: Layout of peel resistance specimen with dimensions in mm.

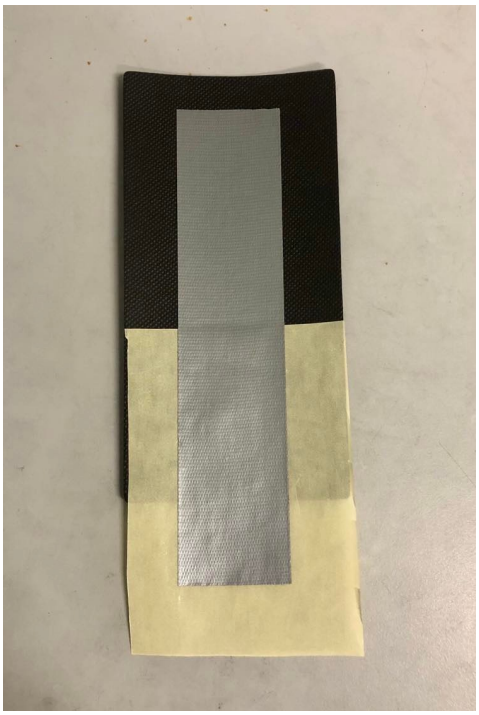

Figure 3.16: Photograph of a peel resistance specimen.

3.4 Ageing procedures

As in the context of Technical Approval, the test samples are exposed to different procedures for accelerated ageing, depending on the products' area of use. In this study, the ageing procedure varies depending on the substrate material. The material samples where PEF constitutes the substrate are aged artificially in a manner inspired by the SINTEF Technical Approval guidelines for vapour barriers. Samples using the ROM substrate are aged in a manner more similar to the guidelines for the Technical Approval of air barriers (SINTEF, 2022).

3.4.1 Heat chamber - PEF samples

The material samples which include PEF as substrate are artificially aged in a ventilated heat chamber at $70°C$, similar to the process used for durability evaluation during Technical Approval of vapour barrier tapes. The heat chamber warms up the ambient laboratory air, resulting in a relatively low humidity inside the chamber.

Air permeability specimens hang vertically inside the heat chamber, each weighed down by a 23x48 mm wooden plank fastened to the lower end of the substrate sheet, as shown in Figure 3.17 The specimens are weighed down to keep them in a vertical position and prevent the different specimens from interfering with each other during the ageing procedure. The peel resistance specimens are laid horizontally on shelves inside another identical heat chamber, as shown in Figure 3.18. All specimens remain in the heat chamber for six weeks.

Figure 3.17: Air permeability specimens in the heat chamber.

Figure 3.18: Peel resistance specimens in the heat chamber.

3.4.2 Climate simulator - ROM samples

The ROM samples undergo accelerated ageing using the NT BUILD 495 method, which involves exposure to cycles of UV light, heat, water, and frost to replicate various climatic stresses (NORDTEST, 2000). Since air barriers and roof underlays are situated on the outer side of the building envelope, they are susceptible to various climatic strains such as rain and fluctuating temperatures. Furthermore, exposure to sunlight can occur during the construction phase. For this reason, NT BUILD 495 is used for ageing the ROM samples as opposed to heat ageing alone.

NT BUILD 495 involves mounting test specimens in a vertical position inside a climate simulator carousel. The climate simulator exposes the samples to cycles of:

- A: UV light and heat radiation perpendicular to specimen, at $63 \pm 5°C$.
- B: Wetting with a spray, at a rate of $15 \pm 2\ l/(m^2h)$.
- C: Frost, at $-20 \pm 5°C$
- D: Ambient laboratory climate, at $23 \pm 5°C$.

The carousel alternates between climate conditions by rotating once every hour in the order A-B-C-D, as illustrated in Figure 3.19. This cycle is repeated continuously for the duration of the ageing procedure before the specimens are extracted and tested.

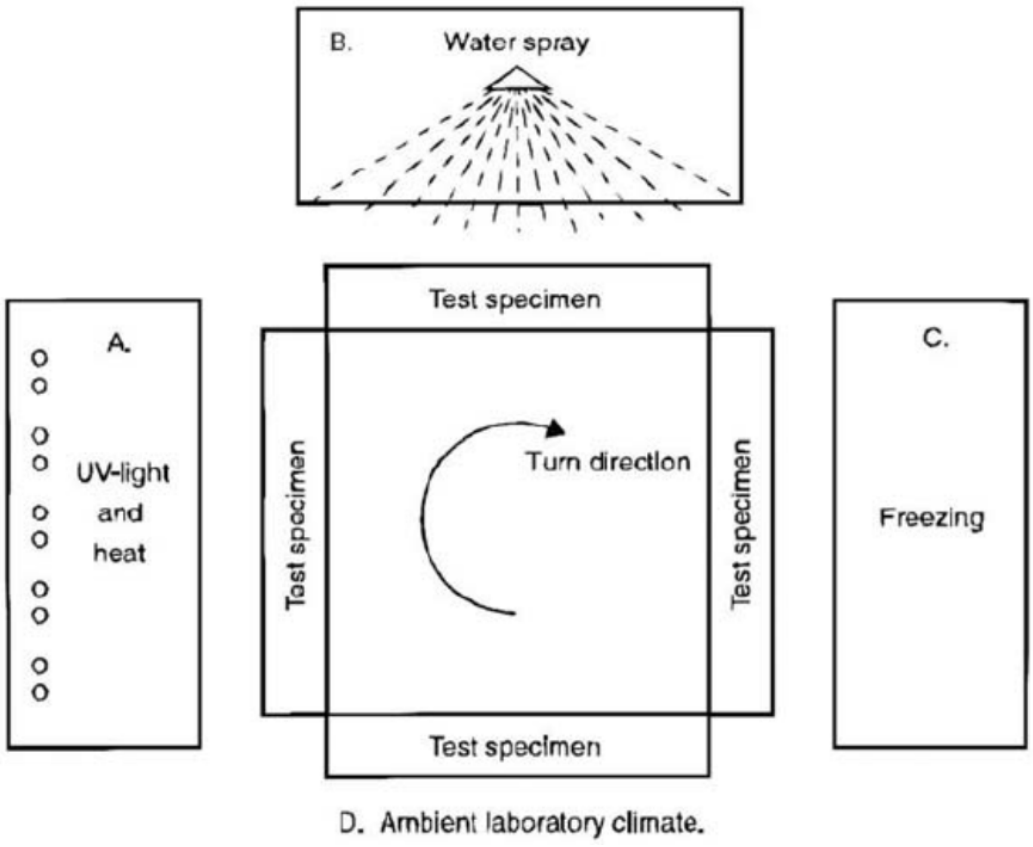

Figure 3.19: Climate simulator setup according to NT BUILD 495 (NORDTEST, 2000).

In the context of SINTEF Technical Approval, NT BUILD 495 is included in the standard procedures for artificial ageing during the durability evaluation of air barrier tapes. However, Technical Approval of air barrier tapes involves exposing the materials to additional heat ageing for 12/24 weeks after two weeks in the climate simulator (SINTEF, 2020).

For the purpose of the thesis, the specimens remain in the climate simulator for six weeks. Due to time constraints, the ageing procedure does not involve additional heat ageing. A disclaimer from the developer of the method specifies that: "Accelerated ageing test in a laboratory always carries the risk that the material might undergo degradation by other mechanisms than those which will take place by natural ageing" (NORDTEST, 2000). Consequently, it is not possible to directly translate the time spent in the climate simulator into any given number of years of natural ageing.

Air permeability specimens are mounted in the carousel, by stapling the top end of the substrate to wooden beams as shown in Figure 3.20. The specimens are weighed down using 23x48 mm planks to keep them in a vertical position. Parallel specimens are placed one above the other. Halfway through the ageing procedure, the parallel specimens switch positions with each other. This is done in an effort to counteract the effects of potential differences in climatic exposure between the lower and upper sections of the carousel. The peel resistance specimens are stapled to a 1200x600 mm wooden board, which is in turn fastened to a wooden beam in the carousel, as shown in Figure 3.21.

Figure 3.20: Air permeability specimens in the climate carousel.

Figure 3.21: Peel resistance specimens in the upper half of the carousel.

4 Results

The following sections present results from the measurement program used to evaluate the suitability of the test method in development. Section 4.1 addresses the airtightness of the Test Stand itself, while Section 4.2 presents results from measurements involving different material samples. Results from parallel peel resistance measurements are featured in Section 4.3 as a basis for comparing the method in development to currently established evaluation methods. Appendix B provides an overview of the results from the measurement program, while the raw measurement data from the air permeability tests are featured in Appendix C.

4.1 Test Stand leakage

The Test Stand leakage evaluation procedure described in Section 3.2.1 was performed on two different dates; 24.03.2023 and 12.04.2023. On both occasions, the test procedure was performed through two separate measurement series. The first two measurement series were performed prior to testing any material sample, and thus constituted the first utilization of the Test Stand. The two subsequent measurement series were performed three weeks later. During these three weeks, the Test Stand had already been used to measure air permeability rates of non-aged material samples through 15 separate measurement series.

Figure 4.1 illustrates results from the Test Stand leakage evaluation, showing the leakage rate at a 50 Pa pressure difference, $\dot{V}_{50}$, estimated from linear regression. The illustration shows the estimated leakage rates when using 8 and 12 clamps respectively. The date corresponding to each measurement series is annotated in the figure.

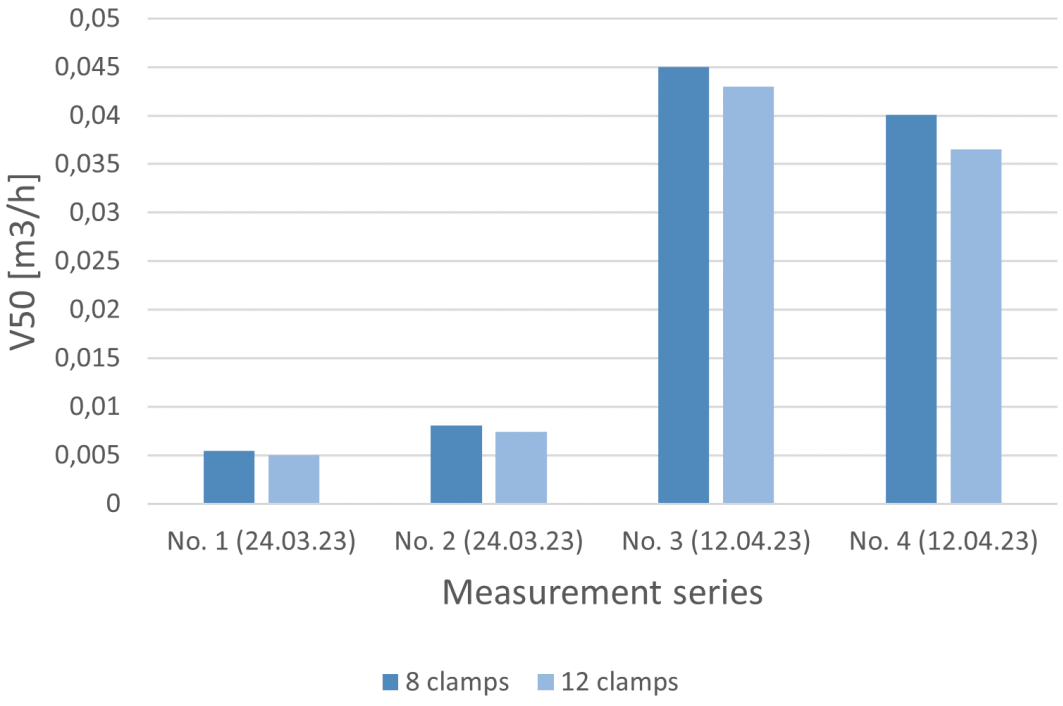

Figure 4.1: System leakage rates $\dot{V}_{50}$ resulting from Test Stand leakage evaluation.

Estimated leakage rates varied substantially between each measurement series, ranging from 0.00503 to 0.04500 m^3/h. The number of clamps used to seal the specimens seems to affect the airtightness of the Test Stand, but this effect is small compared to the variations observed between the individual measurement series. In the tests conducted on 12.04.2023, the measured leakage rates were significantly higher, having increased on average by a factor of 6.6 compared to the prior measurements. For comparison, increasing the number of clamps from 8 to 12 only led to a 7% reduction in the leakage rate on average. The lowest leakage rate measured at 100 Pa in any of the measurement series was 0.00912 m^3/h, which is 1500 times larger than the lowest recorded system leakage of the pressurization rig itself, not including the Test Stand, which was 0.000006 m^3/h (0.1 ml/min) at 100 Pa. On account of this, it is assumed that the system leakage rate mainly can be traced back to the Test Stand and its connections, rather than the pressurization rig.

Leak detection tests using soapy water were performed on two separate occasions; 24.03.2023 and 12.04.2023. None of the tests revealed any air leakages around the tube connections, welding joints or rubber gasket.

4.2 Air permeability tests

Air permeability evaluation of material samples was performed in accordance with the previously described measurement program, using 12 clamps for sealing the specimens during tests. Due to time constraints, air permeability measurements were conducted exclusively on specimens with a positive pressure difference as described in Figure 3.6. Hence, the following results do not include measurements where a simulated negative pressure difference was used.

When measuring the permeability of ROM samples, one of the substrate leakage specimens, NT-ROM-A, was discovered to be more permeable than other ROM specimens containing joints. For instance, the least permeable ROM specimen, T2-ROM-B, had a permeability rate of 0.0649 m^3/m^2h, while the substrate leakage of NT-ROM-A was equivalent to 0.0923 m^3/m^2h. Because of this, it was decided not to subtract the substrate leakage rate from any of the ROM measurements when estimating joint permeability rates.

4.2.1 Durability of material samples

Specimens were tested according to the same measurement procedure before and after artificial ageing to determine the durability of joint permeability. All artificially aged specimens were conditioned in the laboratory at (23 ± 2)°C and 48% RH for more than 48 hours prior to performing the tests.

Figure 4.2 shows the results from the durability evaluation expressed as average air permeability at 50 Pa, q_{50} before and after ageing. Error bars express the standard deviations across the material samples. The calculated average values and standard deviations do not take into account specimens which deviated significantly from the other parallel specimens, including T1-PEF-A, T1-PEF-D and T2-PEF-C. These disregarded specimens are addressed later, as part of the reproducibility evaluation in Section 4.2.2. The dashed line in the chart corresponds to the passive house threshold of 0.048 m^3/mh, as described by Van Linden and Van den Bossche (2017).

Prior to ageing, permeability rates ranged from 0.0004 to 0.0223 m^3/mh, while after ageing, rates were in the range 0.0121 - 1.1047 m^3/mh, not accounting for failed specimens. Converted to leakage rate per effective area, these ranges correspond to 0.0031 - 0.1745 and 0.0947 - 8.6454 m^3/m^2h, respectively. For comparison, permeability rates lower than 0.50 m^3/m^2h are considered sufficient to meet the n50 requirements of TEK17 and NS3700 according to the guidelines for Technical Approval of air barrier systems SINTEF (2017).

All parallel specimens of sample T3-PEF and T3-ROM failed after artificial ageing, as illustrated by the hatched bars in Figure 4.2. For illustrative purposes, the lengths of these bars are not representative of the actual permeability of the failed specimens. Failed specimens are addressed in Section 4.2.5.

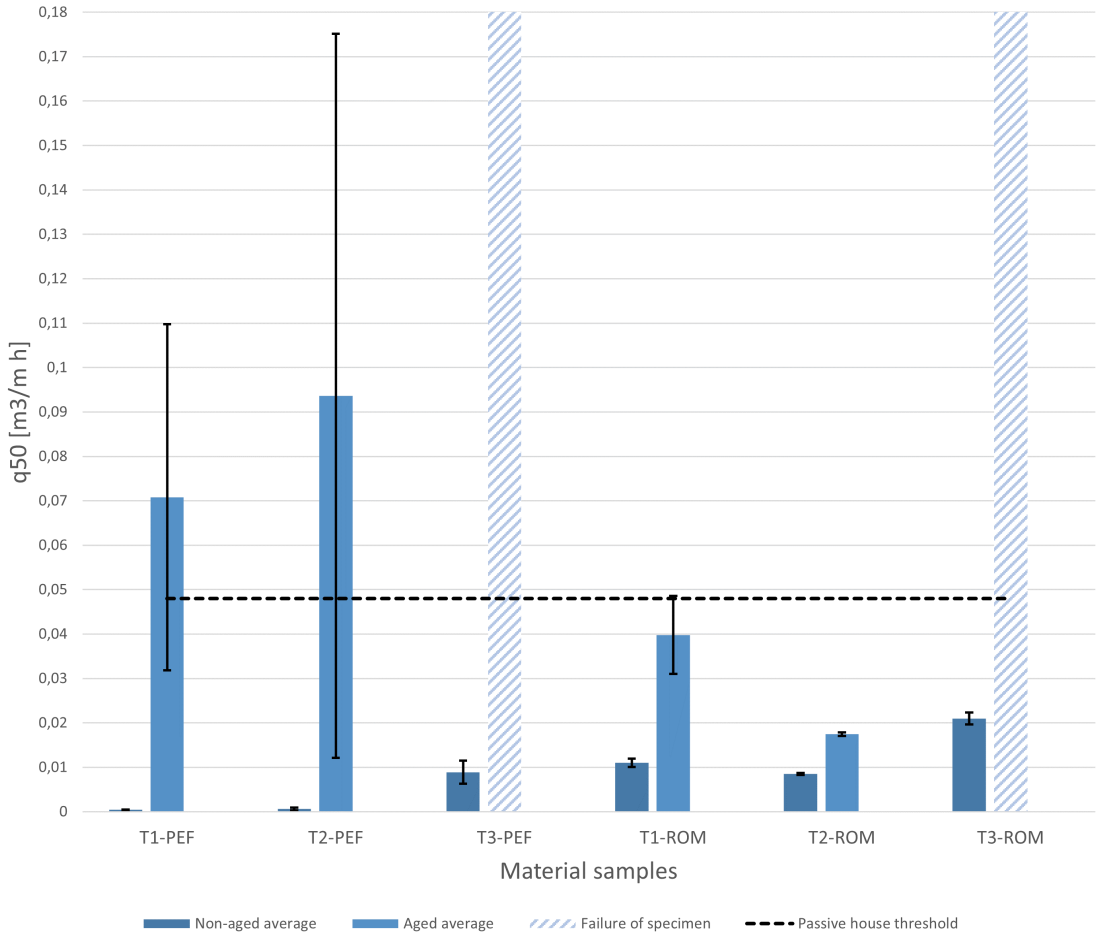

Figure 4.2: Average air permeability and standard deviations of material samples before and after artificial ageing.

All of the material samples become more air permeable after the artificial ageing process. However, the increase is more significant among the PEF samples. While the PEF samples are comparatively less permeable before ageing, they eventually surpass the permeability rates of the ROM samples when tested after the ageing process. All material samples are within the passive house threshold prior to ageing, but only T1-ROM and T2-ROM remain airtight enough to stay below this threshold in artificially aged condition. Table 4.1 shows the relative change in air permeability among the material samples, not including the failed T3-PEF and T3-ROM.

Table 4.1: Relative change in air permeability after artificial ageing.

PEF samples	Relative change	ROM samples	Relative change
T1-PEF	+ 15 200 %	T1-ROM	+ 260 %
T2-PEF	+ 14 800 %	T2-ROM	+ 100 %

Figure 4.3 and 4.4 shows average air permeability rates along with standard deviations in non-aged and aged specimens separately to provide better visibility. Figure 4.4 includes a horizontal line corresponding to the aforementioned passive house threshold. The height of bars representing failed specimens does not correspond to the actual permeability.

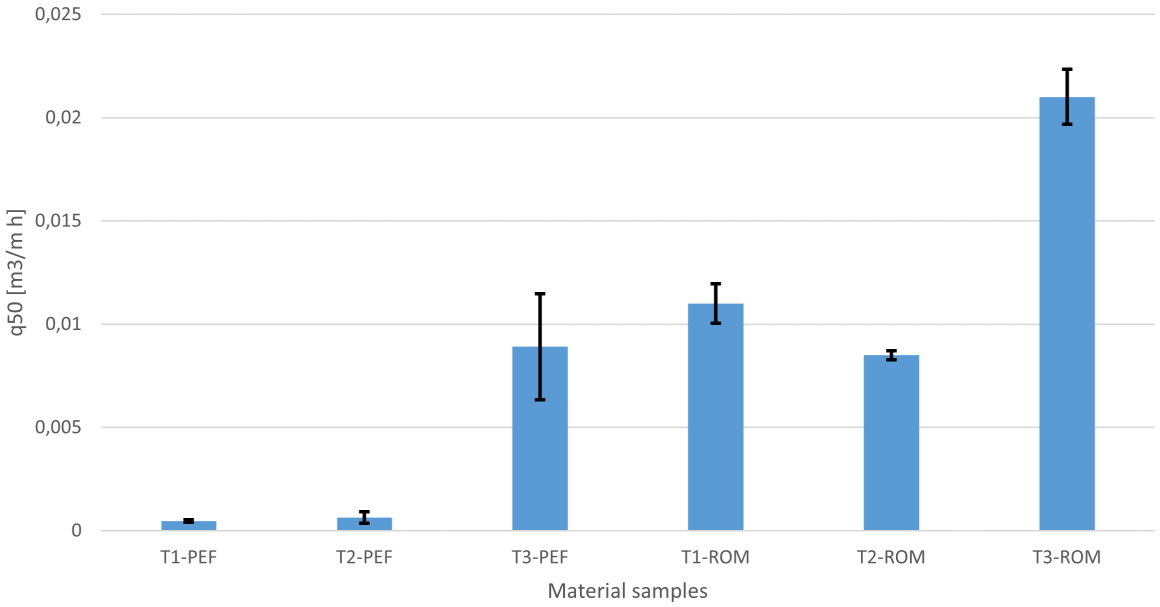

Figure 4.3: Non-aged average air permeability and standard deviations of material samples.

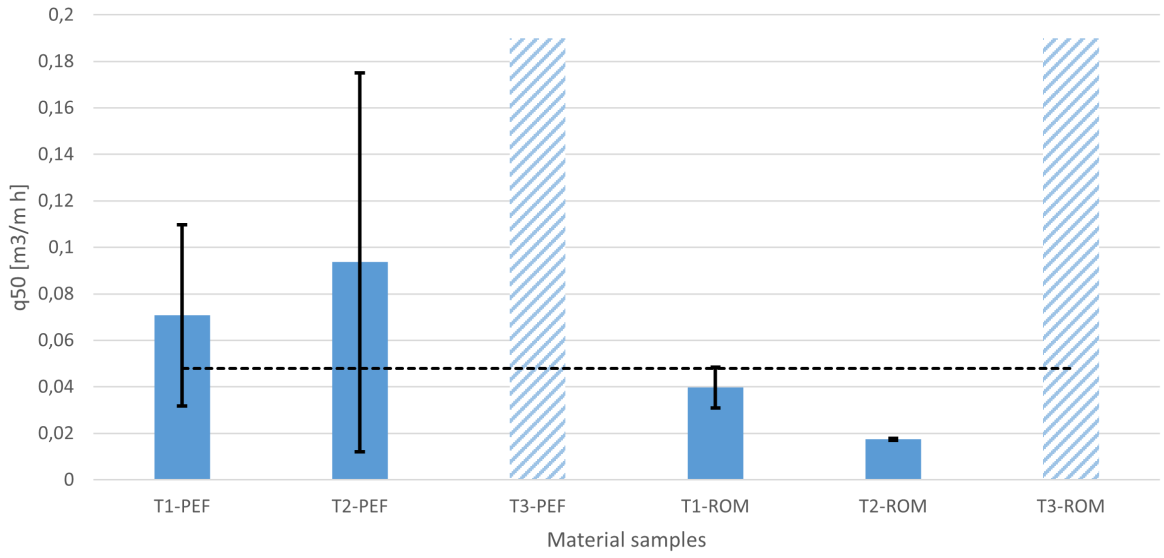

Figure 4.4: Aged average air permeability and standard deviations of material samples.

4.2.2 Reproducibility

Figure 4.5 shows the estimated mean joint permeability q_{50} of test specimens prior to ageing. Specimens tested through several measurement series as part of the repeatability evaluation are represented by the average permeability rate from the three measurement series. T3-PEF-A is excluded from the chart for visual purposes, as its air permeability was considerably higher than the other specimens, with q_{50} estimated to 0.1098 m^3/mh. Apart from T3-PEF-A, all specimens have joint permeability rates lower than the passive house threshold of 0.048 m^3/mh described by Van Linden and Van den Bossche (2017).

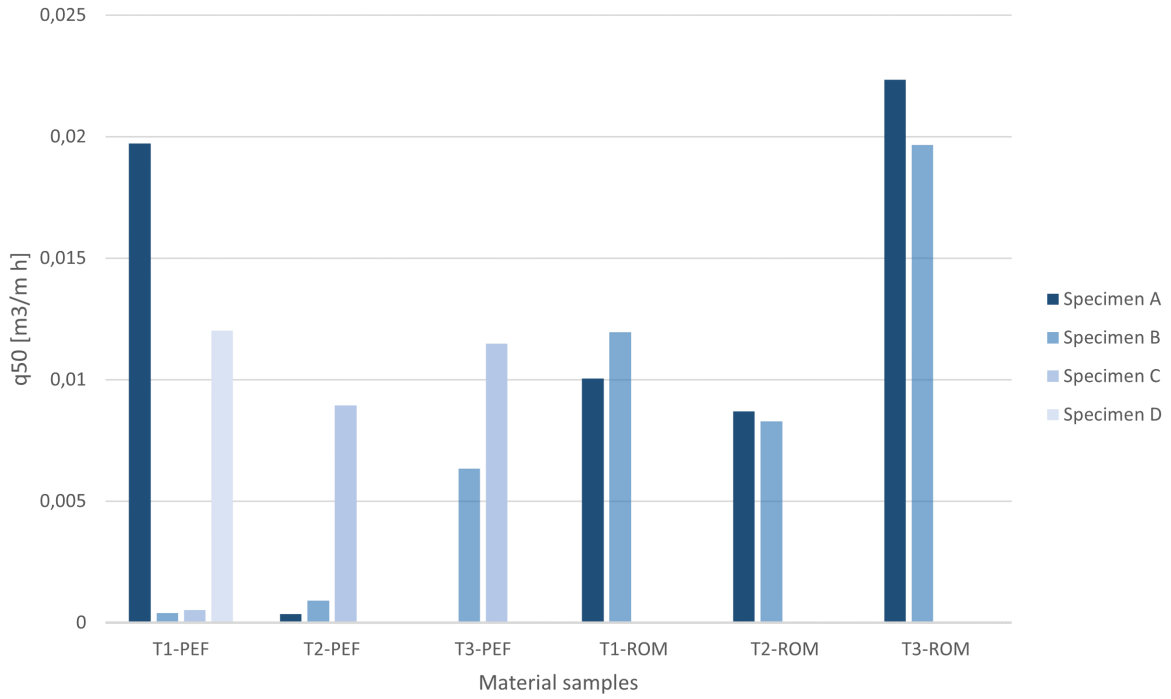

Figure 4.5: Estimated joint permeability rate of non-aged specimens at 50 Pa.

Air permeability varies substantially among the PEF samples and between individual parallel specimens, perhaps most clearly in the case of sample T1-PEF, where the air permeability rates of the specimens range from 0.00041 to 0.01971 m^3/mh. The ROM samples are on average less air permeable, but the measurement results remain more consistent between parallel specimens.

Figure 4.6 shows the estimated air permeability rates of specimens after six weeks of artificial ageing. T3-PEF and T3-ROM are not included, as they failed during the ageing process. Specimens T1-PEF-D, T2-PEF-C were not exposed to artificial ageing due to time constraints. In the chart, a dashed horizontal line marks the passive house threshold, while a solid line indicates the upper limit for what is considered "good airtightness" at 0.238 m^3/mh according to Van Linden and Van den Bossche (2017).

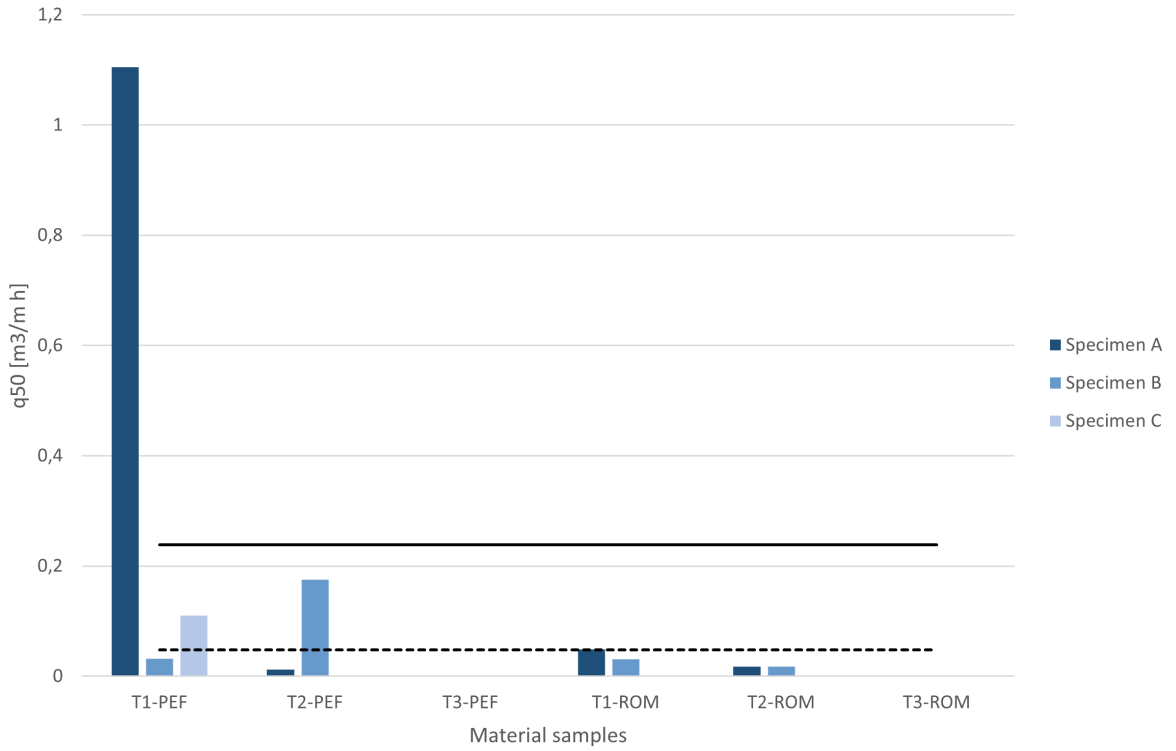

Figure 4.6: Estimated joint permeability rate of aged specimens at 50 Pa.

Apart from T1-PEF-A and the failed T3-PEF and T3-ROM specimens, other specimens retain "good" airtightness after ageing. Similar to the non-aged measurements, the permeability rates of the PEF samples vary significantly between parallel specimens, while ROM samples provide more consistent results. When comparing individual parallel specimens, those which were relatively permeable initially likewise became increasingly more permeable after ageing.

4.2.3 Accuracy

The magnitude of system leakage rates $\dot{V}_{50}$ estimated from reference measurements varied between approximately 0.005 and 0.070 m^3/h. Estimated joint leakage rates lay in the range 0.001 - 0.300 m^3/h.

In specimens with relatively high air permeability ($q_{50} < 0.005 m^3/mh$), the measured system leakage and total leakage rates were in most cases easily distinguishable, for instance, when evaluating T1-PEF-A1 in non-aged condition. Figure 4.7 provides an illustration of the measurement results from T1-PEF-A1, showing measurements corrected for reference conditions and the resulting regression curves.

In the chart, system leakage represents the reference measurement results $\dot{V}_{sys}$, while the total leakage rate $\dot{V}_{tot}$ includes both specimen and system leakage. Unbroken lines constitute the estimated mean values from the regression analysis. Dotted lines indicate 95% confidence intervals. The vertical distance between the unbroken lines is equivalent to the estimated mean joint leakage rate $\dot{V}_{joint}$.

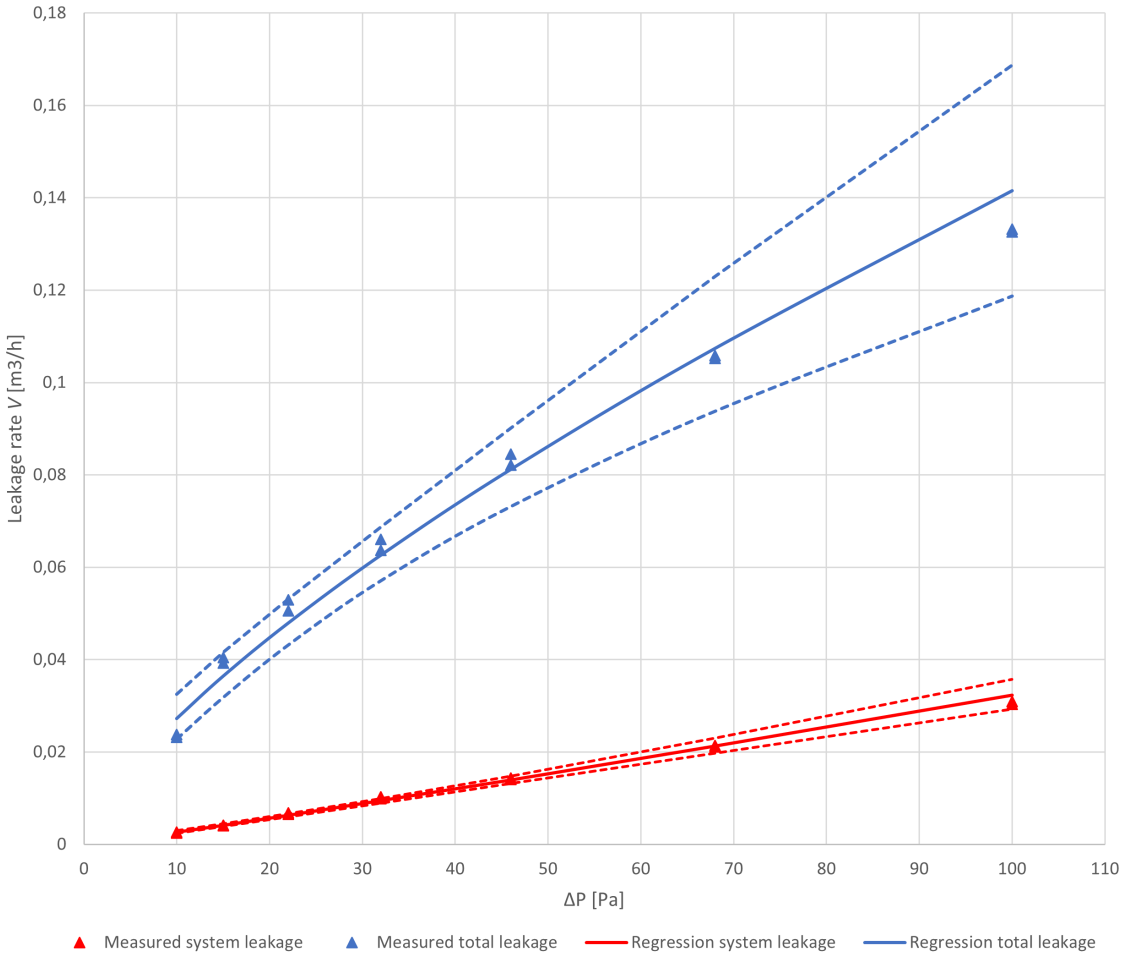

Figure 4.7: Measurement series T1-PEF-A1 with regression curves.

In some of the less permeable specimens, the difference between system leakage and total leakage was not as apparent as in Figure 4.7. Several specimens were estimated to be significantly less permeable than the Test Stand itself, i.e. $\dot{V}_{joint} \ll \dot{V}_{sys}$. For instance, T1-PEF-C, when evaluated in non-aged condition, was estimated to be among the least permeable specimens when evaluating joint leakage. However, the reference measurements of the specimen yielded a comparatively large system leakage rate, resulting in a small difference between the measured total leakage and system leakage rate. This is illustrated in Figure 4.8, which shows corrected measurement results along with regression curves.

In T1-PEF-C, the difference between the system and total leakage was small, yet measurable when using Flow Meter 1. However, the measurements are thought to have become more uncertain when using Flow Meters 2 and 3, as these readings had lower resolutions and were prone to fluctuations. Flow Meter 1 was used for measurements when airflow rates were lower than 400 ml/min (0.024 m^3/h). At higher flow rates, the measured system and total leakage occasionally overlapped, as seen in Figure 4.8 at 100 Pa. Although the mean total leakage consistently remains higher than the system leakage, their confidence intervals overlap.

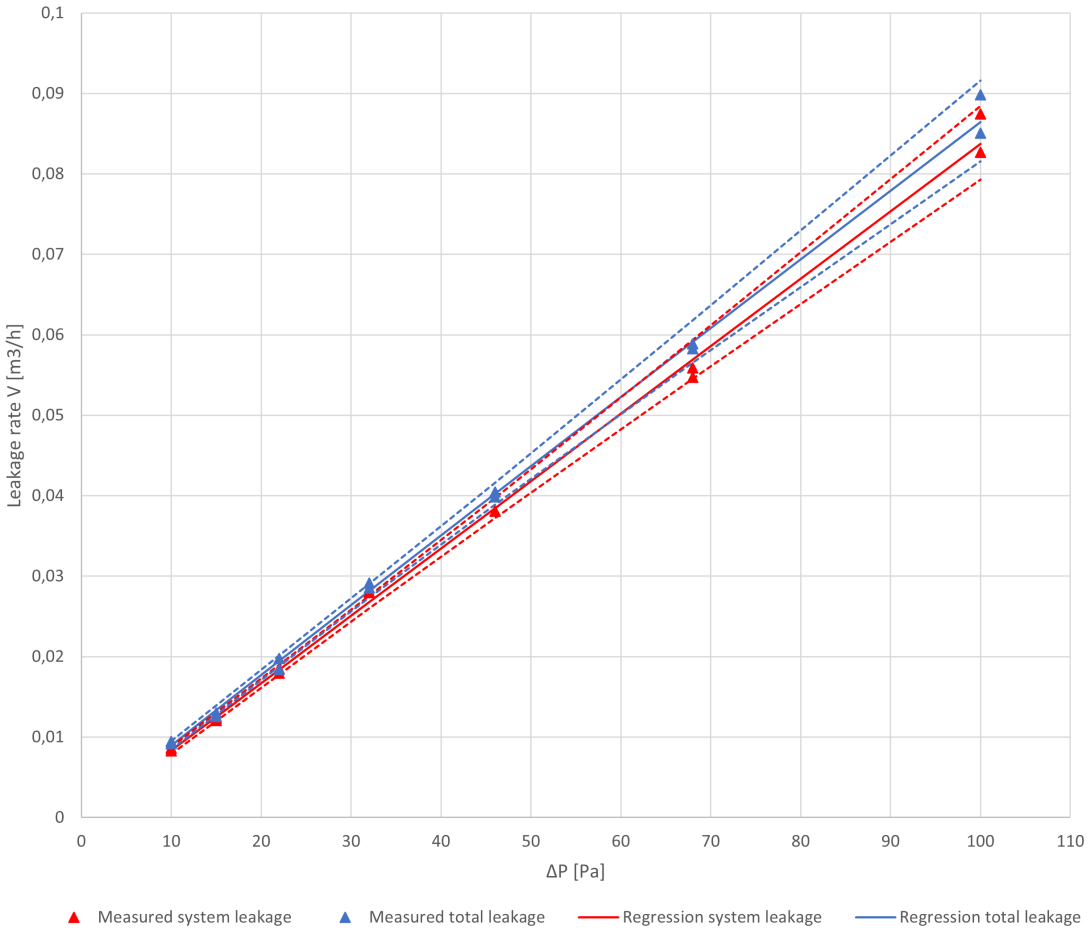

Figure 4.8: Measurement series T1-PEF-C with regression curves.

4.2.4 Repeatability

The repeatability evaluation featured air permeability measurements of three specimens, each tested through three separate measurement series in non-aged condition. Figure 4.9 shows the estimated mean joint permeability q_{50} obtained through regression of each measurement series.

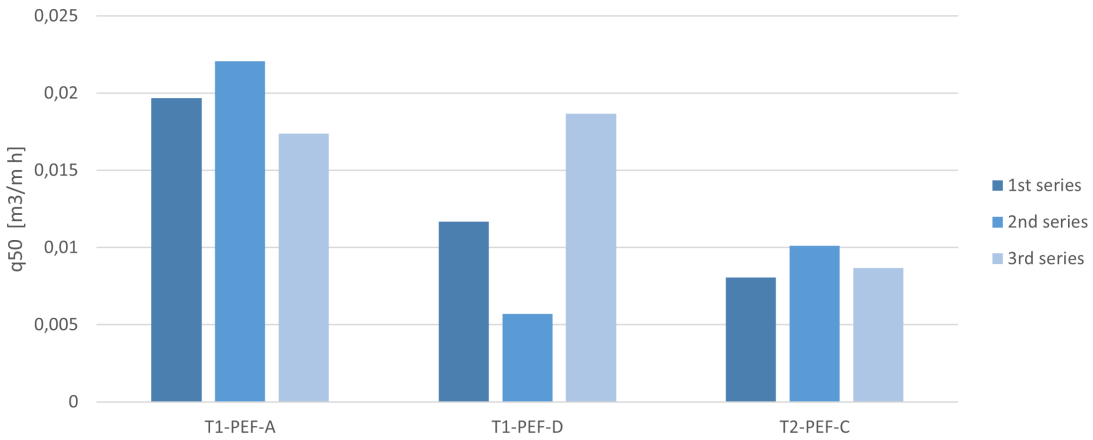

Figure 4.9: Repeatability evaluation results showing joint permeability rates at 50 Pa.

The air permeability of T1-PEF-D varied substantially between each measurement series, with a standard deviation of 0.00529 m^3/mh, making up 44% of the specimen mean. The standard deviations of T1-PEF-A and T2-PEF-C are 0.00192 and 0.00087 m^3/mh respectively, which constitute approximately 10 % of the mean value for both specimens. The average standard deviation is 0.00269 m^3/mh when accounting for all three specimens.

Figures 4.10 - 4.12 show the regression curves from the measurement series performed on T1-PEF-A, T1-PEF-D and T2-PEF-C as part of the repeatability evaluation. The curves represent the estimated mean joint permeability for each measurement series, as a function of the pressure difference ΔP.

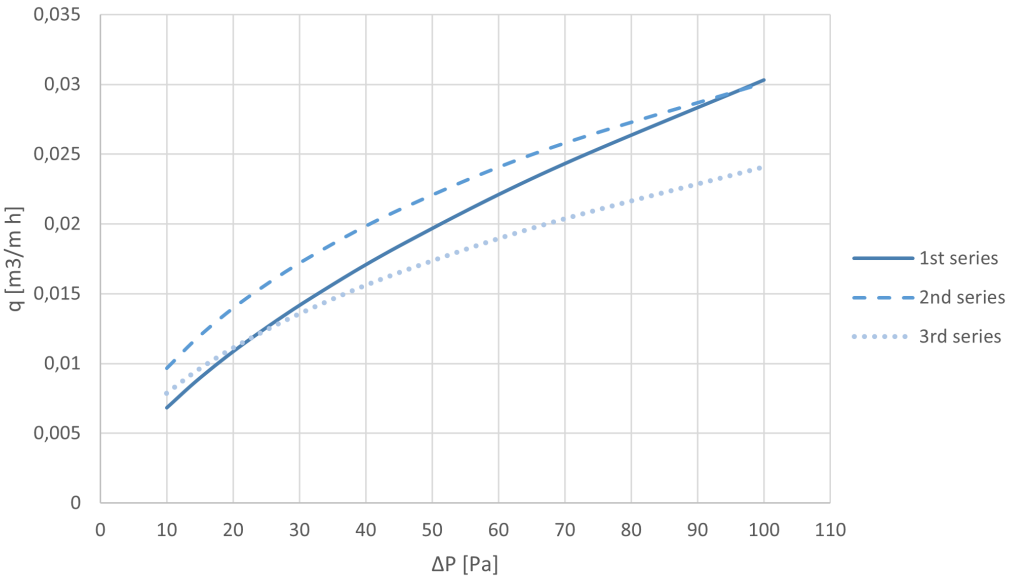

Figure 4.10: T1-PEF-A joint leakage regression curves.

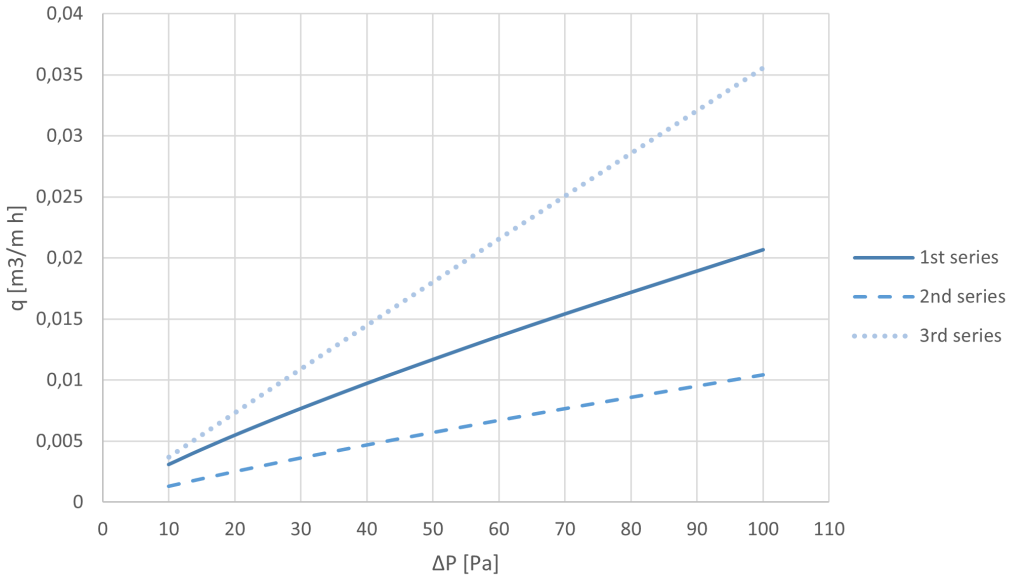

Figure 4.11: T1-PEF-D joint leakage regression curves.

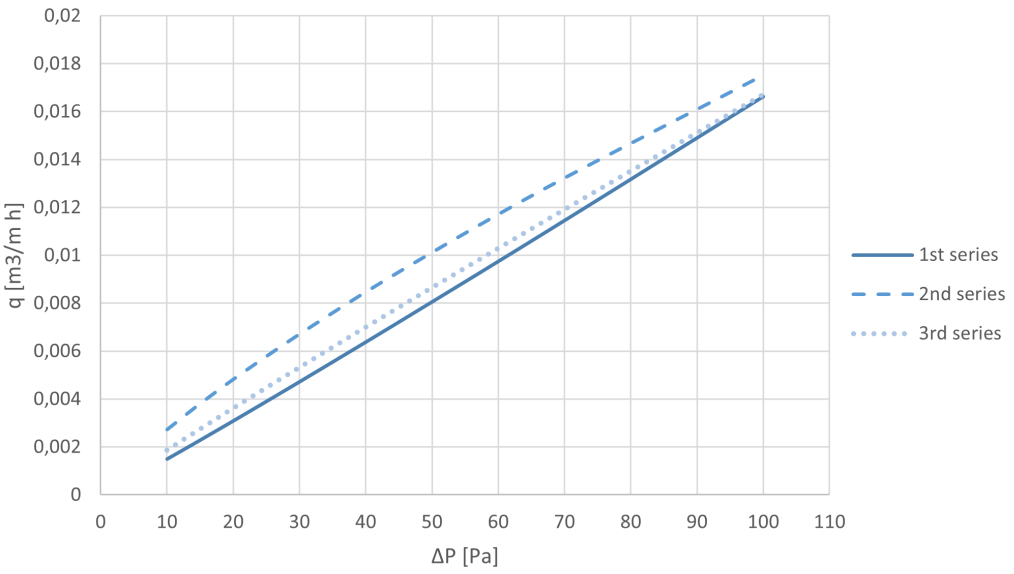

Figure 4.12: T2-PEF-C joint leakage regression curves.

While the regression results from T1-PEF-A and T2-PEF-C are relatively consistent, with minor offsets, the regression curves of T1-PEF-D clearly diverge. The specimens do not appear to become more permeable after each successive series, as the estimated permeability rates seemingly vary randomly between the three series.

4.2.5 Visual inspection of specimens

Specimens were visually inspected before and after performing the ageing procedures. This section presents observations of imperfections in specimens which may have impacted air permeability measurement results.

T1-PEF

Among the T1-PEF specimens, two out of four had significantly larger leakage rates when measured in aged condition. The high air permeability rates are believed to be a result of sub-optimal execution in the preparation of specimens when applying the tape to the substrate. Figure 4.13 shows one of the air canals between the PE foil and tape in T1-PEF-A. After ageing in the heat chamber, the frequency and size of air canals increased across all parallel specimens. Several bulges formed in the PE foil, in which the tape was no longer adhering to the substrate, as can be seen in Figure 4.14

T2-PEF

T2-PEF-C had a relatively large leakage rate compared to its other parallel specimens. The reason is believed to be an air canal discovered in one of the tape joints, as shown in Figure 4.15. No such defects were discovered among the other parallel specimens. T2-PEF-C was not exposed to artificial ageing due to time constraints. However, Figure 4.16 shows an air canal formed in T2-PEF-B during the heat ageing procedure.

T3-PEF

In non-aged condition the air permeability of T3-PEF-A was estimated to be 0.1098 m^3/mh, nearly 10 times larger than that of the second most permeable parallel specimen. Due to this discrepancy, measurement results from T3-PEF-A were not taken into account when estimating the average permeability rate and standard deviation of the T3-PEF material sample as a whole. The specimen had one visible air canal beneath the tape as seen in Figure 4.17. After the heat ageing, larger air canals appeared in all T3-PEF specimens. Figure 4.18 shows air canals in T3-PEF-A after the ageing procedure.

Figure 4.13: T1-PEF-A, non-aged condition.

Figure 4.14: T1-PEF-A, aged condition.

Figure 4.15: T2-PEF-C, non-aged condition.

Figure 4.16: T2-PEF-B, aged condition.

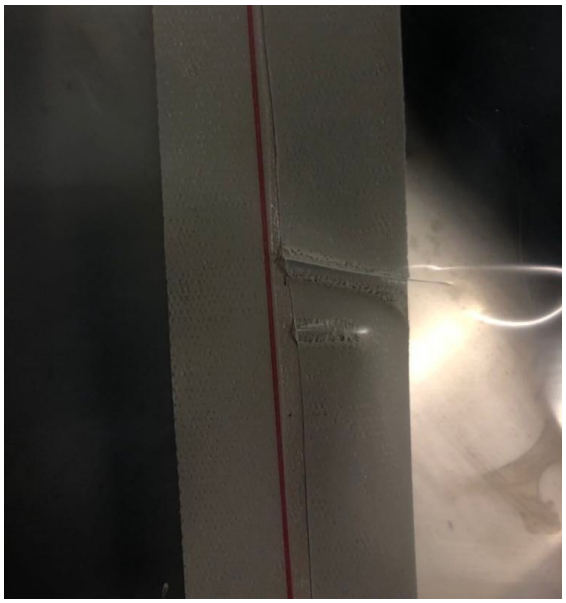

Figure 4.17: T3-PEF-A, non-aged condition.

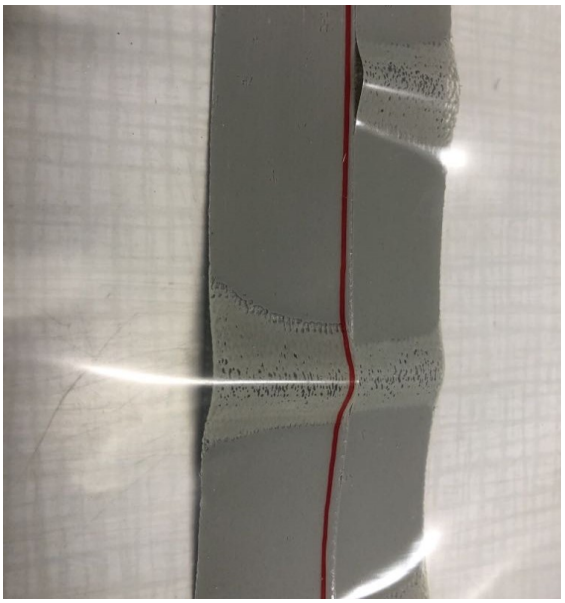

Figure 4.18: T3-PEF-A, aged condition.

T1-ROM and T2-ROM

Specimens from the T1-ROM and T2-ROM samples were prepared without notable imperfections. After completing the ageing procedure, specimens remained intact without significant deformations. Nevertheless, a minor wrinkle was observed in the roofing membrane in T1-ROM-A. In intersections between this wrinkle and the joints, the tape appears to have lost contact with the substrate, as seen in Figure 4.19.

Figure 4.19: T1-ROM-A, aged condition.

T3-ROM

Both specimens of the T3-ROM sample were dismounted from the climate simulator after only 12 days, due to significant deterioration observed during a visual inspection. The tape had been separated from the substrate in several places along the joints, with the adhesive still attached, partly to the substrate and partly to the tape backing material. Figure 4.20 and 4.21, show this phenomenon displayed in T3-ROM-A, from the front and back side of the specimen respectively. Both specimens were tested in an effort to determine their leakage rates, but the test rig could not provide sufficient airflow to elevate the pressure inside the Test Stand. On account of this, both T3-ROM specimens were deemed as failed tests after artificial ageing.

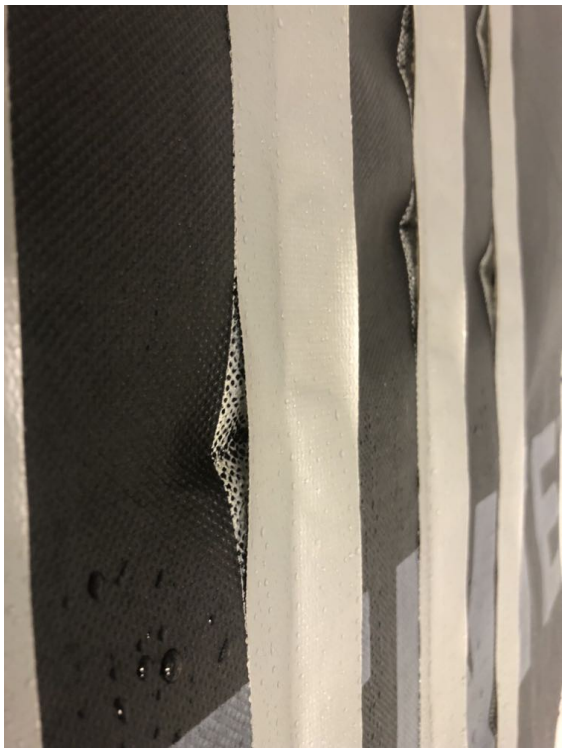

Figure 4.20: T3-ROM-A, aged front.

Figure 4.21: T3-ROM-A, aged back side.

4.3 Peel resistance measurement

Peel resistance measurements were performed on non-aged specimens and specimens exposed to artificial ageing for six weeks. Results from the tests are expressed as the average peel resistance across five parallel specimens from each material sample, calculated according to NS-EN 12316-2:2013. Results are presented in Figure 4.22, with error bars representing standard deviations.

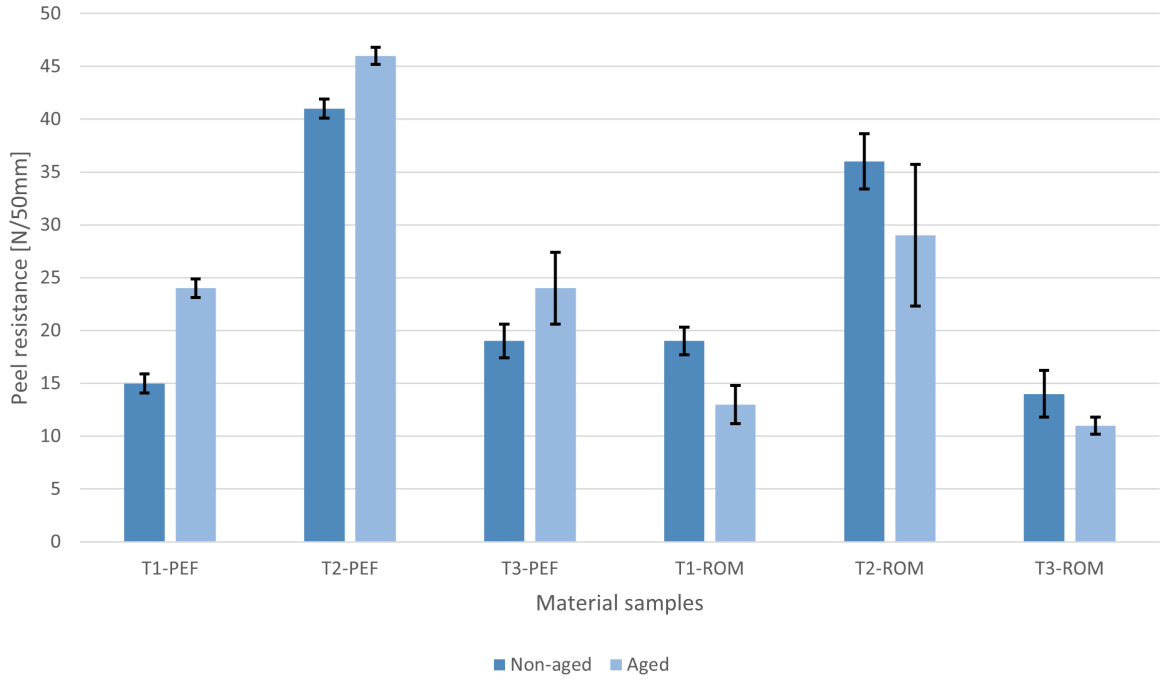

Figure 4.22: Mean peel resistance and standard deviations of material samples.

Average peel resistance measured among the non-aged specimens ranged from 15 to 41 $N/50mm$ for the PEF samples, and from 14 to 36 $N/50mm$ among the ROM samples. On both substrates, T2 displayed a peel resistance approximately two times greater than that of T1 and T3.

Following the heat ageing procedures, the PEF samples exhibited a moderate increase in peel resistance, while all ROM samples experienced a decrease in peel resistance after undergoing ageing in the climate simulator. The relative change in peel resistance among the material samples is shown in Table 4.2.

Table 4.2: Relative change in peel resistance after artificial ageing.

PEF samples	**Relative change**	**ROM samples**	**Relative change**
T1-PEF	+ 60 %	T1-ROM	- 32 %
T2-PEF	+ 12 %	T2-ROM	- 19 %
T3-PEF	+ 26 %	T3-ROM	- 21 %

Table 4.3 shows the most prevalent failure mode of each material sample. All non-aged specimens failed due to adhesive failure, i.e. mode A. Among the artificially aged specimens, failure mode A was still predominant, although the T2-PEF specimens failed due to delamination, i.e. mode C.

Table 4.3: Peel failure mode of material samples.

Material sample	**Non-aged specimens**	**Aged specimens**
T1-PEF	A	A
T2-PEF	A	C
T3-PEF	A	A
T1-ROM	A	A
T2-ROM	A	A
T3-ROM	A	A

All specimens except for T3-PEF and T3-ROM made it through the ageing procedure without visible deformations. The T3-PEF specimens displayed bulging in the contact surface as shown in Figure 4.23. The tape was still adhering to the substrate, without any visible air canals. The T3-ROM specimens did not bulge in the same manner. However, the adhesive tended to fail around the edges of the contact surface, causing the tape to lose contact with the substrate as seen in Figure 4.24

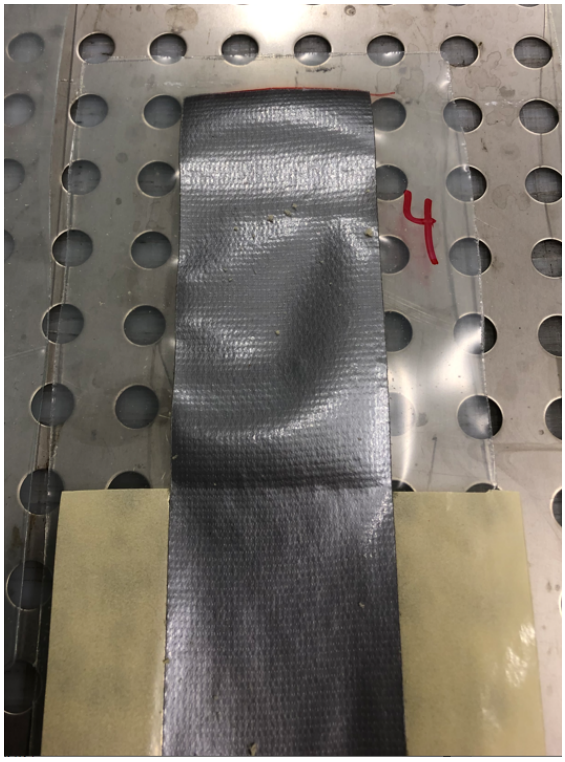

Figure 4.23: T3-PEF peel specimen, aged.

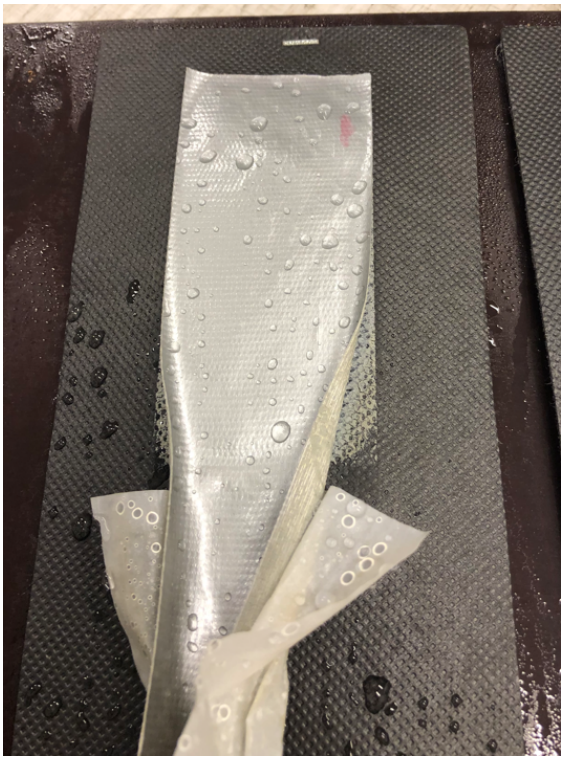

Figure 4.24: T3-ROM peel specimen, aged.

Table 4.4 presents the relative change in air permeability and peel resistance after artificial ageing compiled together. With regard to airtightness, all material samples and specimens were degraded. In terms of peel resistance, only the ROM samples showed signs of degradation, while, in contrast, peel resistance increased moderately among the PEF samples.

Table 4.4: Relative change in air permeability and peel resistance after artificial ageing.

Material sample	**Relative change**	
	Air permeability	Peel resistance
T1-PEF	+ 15 200 %	+ 60 %
T2-PEF	+ 14 800 %	+ 12 %
T3-PEF	Failed	+ 26 %
T1-ROM	+ 260 %	- 32 %
T2-ROM	+ 100 %	- 19 %
T3-ROM	Failed	- 21 %

5 Discussion

The discussion chapter aims to assess the ability of the test method in development, to make reproducible, accurate and repeatable measurements in the context of durability evaluation of adhesive tapes. The assessment relies on the interpretation of results and observations obtained from the measurement program, while also taking into account the insights gained from the literature review. This includes comparing the method to other test methods previously described, before discussing how the method potentially can be implemented as part of a product development or certification process. Limitations associated with the test method and measurement program are subsequently addressed.

5.1 Measurement results

The measured system leakage rates were too large for the Test Stand to be considered an airtight test rig according to NS-EN 12114, in which the system leakage must make up less than 5% of the smallest recorded leakage rate of a test specimen. In Test Stand leakage evaluations performed before and after a three-week period, in which the Test Stand had been actively used, a significant rise in system leakage rates was observed, amounting to approximately 800% at 50 Pa pressure difference. The number of clamps used to seal specimens to the Test Stand had a comparatively small impact on the system leakage rate, as increasing the number from 8 to 12 only reduced leakage rates by 7% on average. Despite performing soapy water leak detection tests both before and after the three-week period, no leakages were identified. It can not be ruled out that the perceived increase in system leakage rates over time is the result of the deterioration of one or several of the Test Stand components. One hypothesis is that compression forces from the clamps have caused hardening and/or permanent deformations in the rubber gasket over time, gradually making the frame-sealing mechanism less effective. Besides this, uneven distribution of compressive forces, due to varying placement and tightening of clamps, may explain the fluctuating system leakage rates between measurement series.

Utilization of the method in development to measure permeability rates of the material samples resulted in significantly varying estimates, both between different materials and among parallel specimens of the same material sample. Nevertheless, upon excluding the most deviating specimens from the analysis, the average q_{50} rates of the material samples were distinguishable from one another, with comparatively small standard deviations. This implies that the method, to some extent, able to quantitatively assess permeability in specimens and differentiate between material samples, given that the specimens are prepared uniformly. However, since a large share of the leakages of the ROM samples is believed to originate from substrate leakage, expressing these permeability rates in terms of leakage per joint length is considered problematic. When the substrate accounts for the majority of specimen leakage rate and joint leakage remains comparatively small, accurately isolating the joint leakage rate becomes impractical. As a result, the permeability estimates among the ROM specimens do not necessarily represent the inherent characteristics of the tape joints themselves. Joint permeability rates estimated among the PEF samples are considered to better represent the airtightness of the joints separately, due to the low permeability of the PE foil.

The substantial disparity in air permeability observed among parallel specimens of the PEF samples suggests that the test method is highly responsive to the implementation quality of individual specimens, which presents a challenge to the reproducibility of the method. Discrepancies observed between parallel specimens using the same tape and substrate were most apparent among the PEF samples, both in non-aged and aged condition. This is likely a consequence of the flexibility of the substrate complicating specimen preparation, leading to more frequent occurrence of bulges and air canals. ROM samples showed lower relative standard deviations among parallel specimens, suggesting a higher level of reproducibility due to the substrate being comparatively rigid.

In the repeatability evaluation, the measurements conducted on two out of three specimens remained relatively consistent. However, significant variations in leakage rates were observed across the three measurement series performed on specimen T1-PEF-D. These variations can potentially be attributed to the narrowing of air canals between the tape and substrate, as the specimen undergoes stretching during its installation to the Test Stand. As a consequence, variations in substrate tension between the different test series may have led to fluctuating permeability rates.

Several of the test specimens were practically airtight compared to the Test Stand itself, such as T2-PEF-A and T2-PEF-B in non-aged condition. This made it difficult to measure the specimen permeability, separate from the system leakage. Consequently, it was difficult to accurately determine what share of the measured total leakage rate went through the specimen as opposed to leaking through the Test Stand. Therefore, the estimated joint permeability rates are considered uncertain in specimens where the system and total leakage rates are in close proximity to each other. This uncertainty is believed to be exacerbated in measurements performed with Flow Meters 2 and 3, as these are regarded as less accurate compared to Flow Meter 1, due to lower display resolution and fluctuating readings.

Despite the relatively large variations in airtightness among the specimens, all but one had permeability rates below the passive house threshold values described by Van Linden and Van den Bossche. Moreover, the specimen which failed to remain below this threshold was deemed to have been inadequately implemented, as a result of sub-optimal workmanship. Based on this, the air permeability test appears adequate for verifying that permeability rates of successfully implemented specimens remain below a predetermined threshold value of similar magnitude, despite the reproducibility and accuracy limitations associated with the method.

While all specimens displayed increased permeability rates after artificial ageing, the increase was significantly larger in specimens exposed to ageing in the heat chamber. This difference could indicate an asymmetry in the effects of the two ageing procedures, where strains from the climate simulator might be mild, and the heat ageing comparatively intense. It is, however, difficult to determine how the impact of the artificial ageing procedures compares to the natural ageing of the products.

Peel resistance was affected differently by the ageing procedures compared to air permeability. For instance, the three PEF samples aged in the heat chamber exhibited increased peel resistance while the airtightness of joints composed of the same materials degraded. The most apparent discrepancy was observed during the durability evaluations of T3-PEF,

in which all specimens failed the permeability tests, while the peel resistance, on average, increased by 26% after ageing. A similar trend was observed in T1-PEF and T2-PEF, although the specimens did not fail. *Based on these observations, it can be established that there is not necessarily a correlation between the airtightness and peel resistance of joints sealed with adhesive tapes.* The increase in permeability rates after ageing is believed to be a result of air canals forming in the joints as the tape and substrate undergo differential dimensional change due to fluctuations in temperature and moisture content. While these air canals may have a large impact on permeability rates, they are believed to not necessarily affect peel resistance significantly, since they make up a comparatively small portion of the total contact surface between tape and substrate.

In terms of airtightness durability, T3 exhibited the poorest performance among the tapes on both substrates as all its associated specimens failed during the artificial ageing procedure. Since T3 is a tape not developed or certified for permanent application in air or vapour barrier systems, the failure of the T3-PEF and T3-ROM specimens can be regarded as an indication that the method in development is able to detect unsuitable tapes. In contrast, the peel resistance measurements alone did not provide sufficient grounds to conclude that T3 was unsuitable.

As none of the material samples displayed a peel resistance reduction larger than 50% after ageing, all tapes have sufficient adhesion to the substrates to meet the durability requirements outlined in the SINTEF Technical Approval guidelines for air and vapour barrier tapes. It is, however, important to acknowledge that the ageing procedures employed in this study deviated to some extent from those specified in the SINTEF guidelines. Furthermore, the guidelines require testing of peel resistance to more substrate materials.

5.2 Comparison of evaluation methods

The method in development can be considered a medium-scale test method as it constitutes a compromise, in terms of specimen size and complexity, between the standardized peel, shear and tensile tests, and the full-scale methods presented in the literature review.

The permeability test method is considered less reliable in quantifying properties inherent to various product combinations compared to the peel resistance test, NS-EN 12316-2, as the permeability estimates appear to depend heavily on the implementation quality of individual specimens. Nevertheless, by measuring air permeability directly, the method in development does not rely on a supposed correlation between airtightness, and mechanical or adhesive properties. As the main purpose of adhesive tape in this context is to provide airtightness, the concept of measuring air permeability directly is considered a potentially more valid approach to product evaluation.

The method in development is less complex compared to the full-scale methods utilized by Antonsson and Ylmén et al., as it only assesses individual barriers without considering components such as windows, timber framing or pipe penetrations. The reduction of scale and complexity is regarded as beneficial for time and cost efficiency in performing tests, and potentially also with regard to reproducibility. Still, this scale reduction and simplification of specimens may cause relevant ageing mechanisms and factors to be disregarded, rendering the test less representative of realistic conditions.

5.3 Limitations

Due to the relatively low number of parallel specimens, the results obtained from the air permeability and durability evaluation of the material samples are considered uncertain. The preparation of the specimens themselves is perceived as a significant source of uncertainty in the method in general, as the leakage rates seem to rely strongly on the quality of individual specimens. Specimens involving thin or flexible substrates, such as PE foil, are deemed particularly problematic with regard to reproducibility, as pockets of air can easily form between tape and substrate during preparation.

The accuracy of the permeability measurements is negatively impacted by relatively large and fluctuating system leakage rates which were observed across the various measurement series. As several specimens were less permeable than the Test Stand itself, it was difficult to determine a specimen leakage rate apart from the system leakage. Due to fluctuating readings and low measurement resolution, the results obtained using Flow Meters 2 and 3 are in particular considered uncertain. In addition, substrate leakage constitutes a source of error when estimating joint permeability. Since it proved impractical to simply subtract the estimated substrate leakage to obtain the joint leakage rate, it is difficult to determine what share of the measured leakage can be attributed to the tape joint itself. This issue was particularly evident in material samples where the substrate exhibited a notably lower level of airtightness compared to the joint.

The heat ageing procedure performed on the PEF samples is considered problematic with regard to representing relevant conditions. Elevating the temperature to $70°C$ caused deformations in the PE foil, likely due to differential thermal expansion between the tape and substrate, leading to the formation of air canals in T1-PEF and T3-PEF. While exposure to elevated temperatures is intended to accelerate deterioration through chemical reactions, the differential thermal expansion occurring at 70°C effectively resulted in mechanical strain on the samples, which would likely not occur at lower temperatures, typical to the inside of an exterior wall.

Additionally, weighing down the test specimens may have induced mechanical tensions in the materials which differ from what would be observed in situ, for instance in a vapour barrier mounted in a wall. These tensions may have altered the way the tapes and materials contract or expand in relation to each other at elevated temperatures, thereby potentially making the artificial ageing conditions deviate further from natural conditions. Moreover, it is believed that the increased temperature resulted in greater flexibility of the polyethylene membrane, which in turn facilitated the mechanical deformation induced by applying weight to the specimens. This likely contributed to the occurrence and propagation of air canals during ageing, as was observed in several of the PEF specimens.

The ageing procedure performed on the PEF peel resistance specimens deviates from the SINTEF Technical Approval guidelines for vapour barrier tapes, as it did not include exposure to UV radiation for 48 hours prior to heat ageing. In addition, the duration of the heat ageing procedure was only half of the 12 weeks used during durability evaluation in Technical Approval. As for the ROM samples, current guidelines for Technical Approval of air barrier tapes demand only two weeks in NT BUILD 495 as opposed to 6. According to the guidelines, air barrier tapes must undergo additional heat ageing for 24 weeks, which was not implemented in this thesis.

The measurement program exclusively involved specimens with joints composed of simple tape joints used to cover cuts in membranes, thus not accounting for overlapping joints. Overlapping joints are believed to potentially exhibit different responses, compared to simple joints, to both climatic strains during artificial ageing and to mechanical strains induced by pressurization during the measurement procedure. Moreover, as specimens were exclusively subjected to a positive differential pressure, the impact of negative pressure differences on permeability rates remains unexplored.

6 Conclusion

Sufficient airtightness in buildings is essential to meet increasingly stringent energy efficiency requirements and to prevent damages and issues arising from moisture transfer. In order to achieve this, it is crucial to seal joints, connections and penetrations in the building envelope, using solutions and products with satisfactory performance in the long term. For this purpose, a test method was developed as part of this thesis, to assess the durability of adhesive tapes based on air permeability.

Based on results from the measurement program, the test method appears capable of measuring permeability rates with sufficient accuracy to distinguish different material combinations from each other, provided test specimens are prepared in a uniform manner. However, permeability rate estimates depended heavily on the implementation quality of individual specimens, making it difficult to determine what share of the leakages could be attributed to inherent product properties as opposed to the quality of workmanship. This impacted reproducibility negatively, in particular across material samples involving flexible substrates.

Due to fluctuating system leakage rates and limitations regarding reproducibility, the permeability test in its current form, is not perceived as adequate for making precise quantitative assessment of airtightness inherent to distinct tape products. Nevertheless, the method is considered accurate enough to determine whether the permeability rates of material samples remain below relevant threshold values.

The degradation of airtightness observed after ageing in the permeability test was not consistent with the durability evaluation based on peel resistance measured according to NS-EN 12311-2. While all material samples experienced a significant increase in air permeability after ageing, the parallel peel resistance measurements provided a significantly more optimistic durability assessment. Nevertheless, the results obtained from the method in development appear to correlate with those obtained from other experimental approaches that assess air permeability.

6.1 Practical implementation

Despite the limitations of the test method presented in this thesis, the general concept is considered a viable approach to durability evaluation of air and vapour barrier tapes in the context of product development and certification. Through further development and improvement, the method in development is considered to have the potential for integration into a wider test program, for instance, in the context of SINTEF Technical Approval of separate tape products. Here, the method could potentially be implemented as a supplementary evaluation to already established methods, such as NS-EN 12311-2, NS-EN 12316-2 and NS-EN 12317-2.

The Test Stand is considered highly configurable, as it allows for the specimen layout to be altered, for instance by utilizing solid boards as substrates and including additional components, such as adhesive pipe collars. This versatility makes it possible to perform permeability tests on the same standard substrates already used in the Technical Ap-

proval of air and vapour barrier tapes. Furthermore, specimens can be inverted, enabling exposure to both positive and negative pressure differences.

While the test method in its current form might not be capable of accurately determining the air permeability and durability of joints, it is believed that an improved version can achieve satisfactory precision in determining specimen leakage rates by incorporating improvements aimed at minimizing system leakage rates. The permeability of a specimen as a whole expressed as leakage per unit area, can then be used for comparison against predefined threshold values. In terms of durability evaluation criteria, it is considered more suitable to establish absolute threshold values for permeability before and after ageing, in contrast to current guidelines for peel and shear resistance evaluation, in which durability is evaluated based on the relative change in material properties after artificial ageing.

6.2 Improvements

While the broader concept of the method in development is considered a suitable option for evaluating air permeability and durability of adhesive tapes, several improvements can be made to the layout of specimens, equipment, and procedures for permeability measurement and artificial ageing. The following measures are suggested to improve the accuracy of the test method, based on the current Test Stand:

- Performing a leak detection test using tracer gas would reveal potential leakage in the Test Stand, enabling targeted measures to reduce system leakage rates, for instance through replacing the rubber gasket, or air sealing the welding joints.
- Replacing screw clamps with lever clamps could improve repeatability by ensuring greater consistency in the manner specimens are sealed to the Test Stand.

Additional improvements can be made to ensure that specimens better represent relevant and realistic conditions:

- The layout of specimens could be altered to feature overlapping joints.
- Altering specimen dimensions and increasing the length of joints might help the method to better account for relevant ageing effects related to dimensional stability.
- As an alternative to weighing specimens down during artificial ageing, specimens could be mounted to a frame in a vertical position to simulate a timber frame wall construction. This way, mechanical strains exerted on the materials would more closely resemble realistic conditions.

6.3 Further research

As part of further research on adhesive tape durability, the following recommendations are proposed:

- Seek confirmation of results by testing more material samples and parallel specimens.
- Examine how assembly conditions affect permeability rates, both initially and after artificial ageing.
- Perform tests on specimens using both positive and negative differential pressure.
- Look further into the relation between artificial and natural ageing, and their impact on air permeability.
- Compare the airtightness and durability of simple connections versus overlapping joints.
- Run parallel permeability tests on products in full-scale to examine how airtightness durability is affected by altering dimensions.
- Include more substrates in permeability tests, such as solid boards of wood, gypsum or concrete.
- Perform tests on tape joints between two different substrate materials, to investigate the effects of skewed deformation on the air permeability.

References

Antonsson, U. (2017), 'Lufttäta klimatskal under verkliga förhållanden'.

Blom, P. and Uvsløkk, S. (2012), 'Bygg tett! Prosjektrapport 98'.

Boberach, C. (2022), 'Development of a Test Procedure for Determining Air Permeability of Adhesive Tapes for Air Barriers in Lightweight Construction'.

Byggforsk (2003), '573.121 Materialer til luft- og damptetting'.

Bygghjelp (2019), 'Dampsperre og tape', https://www.bygghjelpas.no/cof-4/.

Commission, E. (2021), 'Energy performance of buildings directive', https://energy.ec.europa.eu/topics/energy-efficiency/energy-efficient-buildings/energy-performance-buildings-directive_en.

DIN 4108-7:2011-01 (2011), 'Thermal insulation and energy economy in buildings Part 7: Air tightness of buildings – Requirements, recommendations and examples for planning and performance'.

Direktoratet for byggkvalitet (2012), 'Disse kontrollområdene omfattes av obligatorisk uavhengig kontroll', https://dibk.no/saksbehandling-tilsyn-og-kontroll/Hvilke-kontrollomrader-omfattes-av-obligatorisk-uavhengig-kontroll/.

Direktoratet for Byggkvalitet (2017), 'Byggteknisk forskrift TEK17', https://dibk.no/regelverk/byggteknisk-forskrift-tek17/.

European Commission (2020), 'In focus: Energy efficiency in buildings', https://commission.europa.eu/news/focus-energy-efficiency-buildings-2020-02-17_en.

Forskningsrådet (2021), 'Bygger bedre kunnskap for en mer bærekraftig byggebransje', https://www.forskningsradet.no/sok-om-finansiering/hvem-kan-soke-om-finansiering/naringsliv/prosjekter-naringslivet/bygger-bedre-kunnskap-for-en-mer-barekraftig-byggebransje/.

Fufa, S. M. et al. (2017), 'Durability evaluation of adhesive tapes for building applications', *Construction and Building Materials* .

Furness Controls (2023), 'Differential Pressure Transmitter (FCO432)', https://www.furness.com/product/fco432/.

Geving, S. (2010), 'Alternative dampsperrer med uttørkingsmulihet innover?', http://www.bygningsfysikk.no/NorskBygningsfysikkdag2010/08_Geving.pdf.

Geving, S., Bergheim, E. and Gullbrekken, L. (2020), 'Bruk av eldre sperresjikt ved etterisolering', https://sintef.brage.unit.no/sintef-xmlui/bitstream/handle/11250/2647762/Pages%2Bfrom%2BByggeindustrien_03.pdf?sequence=1&isAllowed=y.

Griffon (2023), 'Airtight Construction', https://www.griffon.eu/en/applications/airtight-construction.

ISO (2014), 'ISO 14857:2014 Thermal performance in the built environment — Determination of air permeance of building materials'.

ISO (2015), 'Thermal performance of buildings —Determination of air permeability of buildings — Fan pressurization method'.

Leprince, V. et al. (2017), 'Durability of building airtightness, review and analysis of existing studies', *38th AIVC Conference, Nothingham Uk* .

Møller, E. and Rasmussen, T. (2020), 'Testing Joints of Air and Vapour Barriers, Do We Use Relevant Testing Methods?'.

NORDTEST (2000), 'NT BUILD 495: Building materials and components in the vertical positions: Exposure to accelerated climatic strains'.

SINTEF (2014), '474.624 Luftlekkasjemåling av bygninger. Hensikt og vurdering', https://www.byggforsk.no/dokument/4126/luftlekkasjemaaling_av_bygninger_hensikt_og_vurdering.

SINTEF (2017), 'Guidelines for technical approval for wind barriers and roofing underlays', https://www.sintefcertification.no/file/index/4252.

SINTEF (2019), 'Durable adhesive airtight solutions for energy effective building envelopes', https://www.sintef.no/prosjekter/2019/tighten/.

SINTEF (2020), 'Guidelines for SINTEF Technical Approval for Tapes used in buildings'.

SINTEF (2022), 'SINTEF Technical Approval', https://www.sintefcertification.no/portalpage/index/56.

Skogstad, H. B., Kvalvik, M. and Jelle, B. P. (2010), 'Bruk tape med varig heft', https://www.sintef.no/globalassets/upload/artikkel-10-byggaktuelt.pdf.

Sletnes, M. and Frank, S. (2020), 'Performance and durability of adhesive tapes for building applications. from product documentation to scientific knowledge (and back again)', *XV International Conference on Durability of Building Materials and Components* .

Standard Norge (2000), 'NS-EN 12114 Thermal performance of buildings Air permeability of building components and building elements Laboratory test method'.

Standard Norge (2010), 'NS-EN 12317-2 Flexible sheets for waterproofing Determination of shear resistance of joints Part 2: Plastic and rubber sheets for roof waterproofing'.

Standard Norge (2013*a*), 'NS 3700:2013 Criteria for passive houses and low energy buildings - Residential buildings'.

Standard Norge (2013*b*), 'NS-EN 12311-2 Flexible sheets for waterproofing Determination of tensile properties Part 2: Plastic and rubber sheets for roof waterproofing'.

Standard Norge (2013*c*), 'NS-EN 12316-2 Flexible sheets for waterproofing Determination of peel resistance of joints Part 2: Plastic and rubber sheets for roof waterproofing'.

Thue, J. V. (2016), *Bygningsfysikk*, 1 edn, Fagbokforlaget.

Van den Bossche, N. et al. (2012), 'Airtightness of the window–wall interface in cavity brick walls', *Energy and Buildings* .

Van Linden, S. and Van den Bossche, N. (2017), 'Airtightness of sealed building joints: Comparison of performance before and after artificial ageing', *Building and Environment* .

Ylmén, P., Hansén, M. and Romild, J. (2012), 'Beständighet hos lufttäthetslösningar'.

Appendix

List of Appendices

Appendix A – Material samples and specimens

The table shows the relation between material samples, specimens and measurement series used in the permeability measurement program.

Material samples	**Specimens**	**Measurement series**
T1-PEF	T1-PEF-A	T1-PEF-A1
		T1-PEF-A2
		T1-PEF-A3
	T1-PEF-B	T1-PEF-B
	T1-PEF-C	T1-PEF-C
	T1-PEF-D	T1-PEF-D1
		T1-PEF-D2
		T1-PEF-D3
T2-PEF	T2-PEF-A	T2-PEF-A
	T2-PEF-B	T2-PEF-B
	T2-PEF-C	T2-PEF-C1
		T2-PEF-C2
		T2-PEF-C3
T3-PEF	T3-PEF-A	T3-PEF-A
	T2-PEF-B	T3-PEF-B
	T2-PEF-C	T3-PEF-C
T1-ROM	T1-ROM-A	T1-ROM-A
	T1-ROM-B	T1-ROM-B
T2-ROM	T2-ROM-A	T2-ROM-A
	T2-ROM-B	T2-ROM-B
T3-ROM	T3-ROM-A	T3-ROM-A
	T3-ROM-B	T3-ROM-B
NT-ROM	NT-ROM-A	NT-ROM-A
	NT-ROM-B	NT-ROM-B

Appendix B – Overview of measurement program

Permeability measurements

Specimen	Built	Tested		Ageing			q50, regression [m3/m h]	
		Non-aged	Aged	Started	Finished	Duration	Non-aged	Aged
T1-PEF-A1	27.03.2023	27.03.2023	16.05.2023	31.03.2023	12.05.2023	6 weeks	0,019687	1,104739858
T1-PEF-A2	27.03.2023	27.03.2023					0,022084	
T1-PEF-A3	27.03.2023	27.03.2023					0,017381	
T1-PEF-B	27.03.2023	28.03.2023	16.05.2023	31.03.2023	12.05.2023	6 weeks	0,000407	0,031841541
T1-PEF-C	28.03.2023	28.03.2023	16.05.2023	31.03.2023	12.05.2023	6 weeks	0,000517	0,109784679
T1-PEF-D1	17.04.2023	17.04.2023	-	-	-	-	0,011685	-
T1-PEF-D2	17.04.2023	17.04.2023	-				0,005710	
T1-PEF-D3	17.04.2023	18.04.2023	-				0,018664	
T2-PEF-A	28.03.2023	29.03.2023	16.05.2023	31.03.2023	12.05.2023	6 weeks	0,000348	0,012138628
T2-PEF-B	30.03.2023	30.03.2023	16.05.2023	31.03.2023	12.05.2023	6 weeks	0,000910	0,175118678
T2-PEF-C1	17.04.2023	18.04.2023	-	-	-	-	0,008058	-
T2-PEF-C2	17.04.2023	19.04.2023	-				0,010123	
T2-PEF-C3	17.04.2023	19.04.2023	-				0,008662	
T3-PEF-A	27.03.2023	28.03.2023	16.05.2023	31.03.2023	12.05.2023	6 weeks	0,109821	Failed test
T3-PEF-B	29.03.2023	29.03.2023	16.05.2023	31.03.2023	12.05.2023	6 weeks	0,006344	Failed test
T3-PEF-C	30.03.2023	30.03.2023	16.05.2023	31.03.2023	12.05.2023	6 weeks	0,011477	Failed test
T1-ROM-A	29.03.2023	29.03.2023	16.05.2023	31.03.2023	12.05.2023	6 weeks	0,010051	0,048561305
T1-ROM-B	30.03.2023	30.03.2023	16.05.2023	31.03.2023	12.05.2023	6 weeks	0,011948	0,031011368
T2-ROM-A	29.03.2023	30.03.2023	16.05.2023	31.03.2023	12.05.2023	6 weeks	0,008703	0,017065293
T2-ROM-B	30.03.2023	30.03.2023	16.05.2023	31.03.2023	12.05.2023	6 weeks	0,008282	0,017833013
T3-ROM-A	29.03.2023	30.03.2023	12.04.2023	31.03.2023	12.04.2023	12 days*	0,022336	Failed test
T3-ROM-B	30.03.2023	30.03.2023	12.04.2023	31.03.2023	12.04.2023	12 days*	0,019668	Failed test
NT-ROM-A	29.03.2023	29.03.2023	-	-	-	-	0,011846	-
NT-ROM-B	25.04.2023	25.04.2023	-	-	-	-	0,007698	-

Peel resistance measurements

Sample	Built	Tested		Ageing			Peel resistance [N/50 mm]	
		Non-aged	Aged	Started	Finished	Duration	Mean	Std. dev
Non-aged								
T1-PEF	25.04.2023	27.04.2022	-	-	-	-	15	0,9
T2-PEF	25.04.2023	27.04.2022	-	-	-	-	41	0,9
T3-PEF	25.04.2023	27.04.2022	-	-	-	-	19	1,6
T1-ROM	25.04.2023	27.04.2022	-	-	-	-	19	1,3
T2-ROM	25.04.2023	27.04.2022	-	-	-	-	36	2,6
T3-ROM	25.04.2023	27.04.2022	-	-	-	-	14	2,2
Aged								
T1-PEF	14.04.2023	-	02.06.2023	14.04.2023	26.05.2024	6 weeks	24	0,9
T2-PEF	14.04.2023	-	02.06.2023	14.04.2023	26.05.2024	6 weeks	46	0,8
T3-PEF	14.04.2023	-	02.06.2023	14.04.2023	26.05.2024	6 weeks	24	3,4
T1-ROM	14.04.2023	-	02.06.2023	17.04.2024	30.05.2024	6 weeks	13	1,8
T2-ROM	14.04.2023	-	02.06.2023	17.04.2024	30.05.2024	6 weeks	29	6,7
T3-ROM	14.04.2023	-	02.06.2023	17.04.2024	30.05.2024	6 weeks	11	0,8

Appendix C - Permeability measurement data

Permeability measurements, non-aged condition:

T1-PEF-A1

	Measured airflow				Corrected				Average	
ΔP (Pa)	V_sys (ml/min)		V_tot (ml/min)		V_0,sys (ml/min)		V_0,tot (ml/min)		V_0,sys,avg	V_0,tot,avg
	1st series	2nd series	1st series	2nd series	1st series	2nd series	1st series	2nd series		
10	44,4	41,1	390	400	44,011	40,740	386,582	396,494	42,375	391,538
15	69,2	68,7	660	680	68,594	68,098	654,216	674,040	68,346	664,128
22	109	114	850	890	108,045	113,001	842,551	882,200	110,523	862,375
32	166	173	1070	1110	164,545	171,484	1060,623	1100,272	168,015	1080,447
46	242	236	1380	1420	239,879	233,932	1367,906	1407,555	236,905	1387,730
68	359	355	1780	1770	355,854	351,889	1764,400	1754,488	353,871	1759,444
100	510	520	2240	2230	505,530	515,443	2220,369	2210,456	510,487	2215,413

Laboratory conditions		
Temperature	21,9	°C
RH	19,5	%
Atm pressure	100	kPa
ρ_0	1,1988	
ρ_w	630,4328877	
ρ	1,177879571	
Corr. factor	0,991236025	

T1-PEF-A2

	Measured airflow				Corrected				Average	
ΔP (Pa)	V_sys (ml/min)		V_tot (ml/min)		V_0,sys (ml/min)		V_0,tot (ml/min)		V_0,sys,avg	V_0,tot,avg
	1st series	2nd series	1st series	2nd series	1st series	2nd series	1st series	2nd series		
10	31,2	31,7	550	560	30,927	31,422	545,180	555,092	31,174	550,136
15	68	67,3	790	820	67,404	66,710	783,076	812,814	67,057	797,945
22	130	125	1100	1070	128,861	123,905	1090,360	1060,623	126,383	1075,491
32	176	165	1400	1260	174,458	163,554	1387,730	1248,957	169,006	1318,344
46	249	209	1640	1430	246,818	207,168	1625,627	1417,468	226,993	1521,547
68	352	331	1940	1790	348,915	328,099	1922,998	1774,312	338,507	1848,655
100	500	480	2230	2190	495,618	475,793	2210,456	2170,807	485,706	2190,632

Laboratory conditions		
Temperature	21,9	°C
RH	19,5	%
Atm pressure	100	kPa
ρ_0	1,1988	
ρ_w	630,4328877	
ρ	1,177879571	
Corr. factor	0,991236025	

T1-PEF-A3

	Measured airflow				Corrected				Average	
ΔP (Pa)	V_sys (ml/min)		V_tot (ml/min)		V_0,sys (ml/min)		V_0,tot (ml/min)		V_0,sys,avg	V_0,tot,avg
	1st series	2nd series	1st series	2nd series	1st series	2nd series	1st series	2nd series		
10	16,9	17,2	490	450	16,752	17,049	485,706	446,056	16,901	465,881
15	23	22,9	670	500	22,798	22,699	664,128	495,618	22,749	579,873
22	37,6	37,2	820	710	37,270	36,874	812,814	703,778	37,072	758,296
32	56,8	55,9	1070	890	56,302	55,410	1060,623	882,200	55,856	971,411
46	83,1	83,4	1230	1070	82,372	82,669	1219,220	1060,623	82,520	1139,921
68	113	114	1390	1330	112,010	113,001	1377,818	1318,344	112,505	1348,081
100	157	152	1500	1440	155,624	150,668	1486,854	1427,380	153,146	1457,117

Laboratory conditions		
Temperature	21,9	°C
RH	19,5	%
Atm pressure	100	kPa
ρ_0	1,1988	
ρ_w	630,4328877	
ρ	1,177879571	
Corr. factor	0,991236025	

T1-PEF-B

	Measured airflow				Corrected				Average	
ΔP (Pa)	V_sys (ml/min)		V_tot (ml/min)		V_0,sys (ml/min)		V_0,tot (ml/min)		V_0,sys,avg	V_0,tot,avg
	1st series	2nd series	1st series	2nd series	1st series	2nd series	1st series	2nd series		
10	24,5	25,3	29,2	31,7	24,285	25,078	28,944	31,422	24,682	30,183
15	44,3	43,6	55,7	53,2	43,912	43,218	55,212	52,734	43,565	53,973
22	65,5	68,6	72,9	71,3	64,926	67,999	72,261	70,675	66,462	71,468
32	84,3	85,5	108	106	83,561	84,751	107,053	105,071	84,156	106,062
46	110	110	137	122	109,036	109,036	135,799	120,931	109,036	128,365
68	149	151	189	178	147,694	149,677	187,344	176,440	148,685	181,892
100	209	212	255	262	207,168	210,142	252,765	259,704	208,655	256,235

Laboratory conditions		
Temperature	21,9	°C
RH	19,5	%
Atm pressure	100	kPa
ρ_0	1,1988	
ρ_w	630,4328877	
ρ	1,177879571	
Corr. factor	0,991236025	

T1-PEF-C

	Measured airflow				Corrected				Average	
ΔP (Pa)	V_sys (ml/min)		V_tot (ml/min)		V_0,sys (ml/min)		V_0,tot (ml/min)		V_0,sys,avg	V_0,tot,avg
	1st series	2nd series	1st series	2nd series	1st series	2nd series	1st series	2nd series		
10	139	145	159	154	137,782	143,729	157,607	152,650	140,756	155,128
15	203	207	219	211	201,221	205,186	217,081	209,151	203,203	213,116
22	311	302	332	309	308,274	299,353	329,090	306,292	303,814	317,691
32	470	470	480	490	465,881	465,881	475,793	485,706	465,881	480,749
46	640	640	670	680	634,391	634,391	664,128	674,040	634,391	669,084
68	940	920	990	980	931,762	911,937	981,324	971,411	921,850	976,367
100	1470	1390	1510	1430	1457,117	1377,818	1496,766	1417,468	1417,468	1457,117

Laboratory conditions		
Temperature	21,9	°C
RH	19,5	%
Atm pressure	100	kPa
ρ_0	1,1988	
ρ_w	630,4328877	
ρ	1,177879571	
Corr. factor	0,991236025	

T1-PEF-D1

	Measured airflow				Corrected				Average	
ΔP (Pa)	V_sys (ml/min)		V_tot (ml/min)		V_0,sys (ml/min)		V_0,tot (ml/min)		V_0,sys,avg	V_0,tot,avg
	1st series	2nd series	1st series	2nd series	1st series	2nd series	1st series	2nd series		
10	117	124	339	337	115,892	122,826	335,790	333,809	119,359	334,799
15	190	189	415	430	188,201	187,210	411,070	425,928	187,706	418,499
22	269	273	570	570	266,453	270,415	564,603	564,603	268,434	564,603
32	377	379	870	890	373,430	375,411	861,762	881,573	374,421	871,667
46	510	500	1170	1250	505,171	495,266	1158,921	1238,164	500,218	1198,543
68	750	750	1680	1700	742,898	742,898	1664,092	1683,903	742,898	1673,997
100	1040	1050	2290	2300	1030,152	1040,058	2268,316	2278,221	1035,105	2273,269

Laboratory conditions		
Temperature	22,3	°C
RH	19,5	%
Atm pressure	100	kPa
ρ_0	1,1988	
ρ_w	648,3904354	
ρ	1,176204672	
Corr. factor	0,990531025	

T1-PEF-D2

	Measured airflow				Corrected				Average	
ΔP (Pa)	V_sys (ml/min)		V_tot (ml/min)		V_0,sys (ml/min)		V_0,tot (ml/min)		V_0,sys,avg	V_0,tot,avg
	1st series	2nd series	1st series	2nd series	1st series	2nd series	1st series	2nd series		
10	322	323	420	420	318,951	319,942	416,023	416,023	319,446	416,023
15	420	410	530	510	416,023	406,118	524,981	505,171	411,070	515,076
22	590	540	690	720	584,413	534,887	683,466	713,182	559,650	698,324
32	670	680	920	930	663,656	673,561	911,289	921,194	668,608	916,241
46	890	910	1190	1240	881,573	901,383	1178,732	1228,258	891,478	1203,495
68	1150	1190	1500	1600	1139,111	1178,732	1485,797	1584,850	1158,921	1535,323
100	1460	1520	2180	2270	1446,175	1505,607	2159,358	2248,505	1475,891	2203,932

Laboratory conditions		
Temperature	22,3	°C
RH	19,5	%
Atm pressure	100	kPa
ρ_0	1,1988	
ρ_w	648,3904354	
ρ	1,176204672	
Corr. factor	0,990531025	

T1-PEF-D3

	Measured airflow				Corrected				Average	
ΔP (Pa)	V_sys (ml/min)		V_tot (ml/min)		V_0,sys (ml/min)		V_0,tot (ml/min)		V_0,sys,avg	V_0,tot,avg
	1st series	2nd series	1st series	2nd series	1st series	2nd series	1st series	2nd series		
10	44	43	149	257	43,583	42,593	147,589	254,566	43,088	201,078
15	89	91	376	510	88,157	90,138	372,440	505,171	89,148	438,805
22	129	125	550	940	127,779	123,816	544,792	931,099	125,797	737,946
32	186	188	830	1270	184,239	186,220	822,141	1257,974	185,229	1040,058
46	278	281	1350	1550	275,368	278,339	1337,217	1535,323	276,853	1436,270
68	420	430	1750	1850	416,023	425,928	1733,429	1832,482	420,976	1782,956
100	580	580	2200	2320	574,508	574,508	2179,168	2298,032	574,508	2238,600

Laboratory conditions		
Temperature	22,3	°C
RH	19,5	%
Atm pressure	100	kPa
ρ_0	1,1988	
ρ_w	648,3904354	
ρ	1,176204672	
Corr. factor	0,990531025	

T2-PEF-A

	Measured				Corrected				Average	
ΔP (Pa)	V_sys (ml/min)		V_tot (ml/min)		V_0,sys (ml/min)		V_0,tot (ml/min)		V_0,sys,avg	V_0,tot,avg
	1st series	2nd series	1st series	2nd series	1st series	2nd series	1st series	2nd series		
10	147	119	138	140	145,712	117,957	136,791	138,773	131,834	137,782
15	165	155	184	201	163,554	153,642	182,387	199,238	158,598	190,813
22	287	255	290	270	284,485	252,765	287,458	267,634	268,625	277,546
32	394	389	411	405	390,547	385,591	407,398	401,451	388,069	404,424
46	520	510	530	540	515,443	505,530	525,355	535,267	510,487	530,311
68	790	790	800	810	783,076	783,076	792,989	802,901	783,076	797,945
100	1150	1130	1160	1150	1139,921	1120,097	1149,834	1139,921	1130,009	1144,878

Laboratory conditions		
Temperature	21,9	°C
RH	19,5	%
Atm	100	kPa
ρ_0	1,1988	
ρ_w	630,4328877	
ρ	1,177879571	
Corr. factor	0,991236025	

T2-PEF-B

	Measured				Corrected				Average	
ΔP (Pa)	V_sys (ml/min)		V_tot (ml/min)		V_0,sys (ml/min)		V_0,tot (ml/min)		V_0,sys,avg	V_0,tot,avg
	1st series	2nd series	1st series	2nd series	1st series	2nd series	1st series	2nd series		
10	155	159	167	189	153,642	157,607	165,536	187,344	155,624	176,440
15	190	203	217	211	188,335	201,221	215,098	209,151	194,778	212,125
22	268	274	302	298	265,651	271,599	299,353	295,388	268,625	297,371
32	430	420	450	450	426,231	416,319	446,056	446,056	421,275	446,056
46	550	590	690	700	545,180	584,829	683,953	693,865	565,005	688,909
68	880	850	900	910	872,288	842,551	892,112	902,025	857,419	897,069
100	1170	1200	1230	1250	1159,746	1189,483	1219,220	1239,045	1174,615	1229,133

Laboratory conditions		
Temperature	21,9	°C
RH	19,5	%
Atm	100	kPa
ρ_0	1,1988	
ρ_w	630,4328877	
ρ	1,177879571	
Corr. factor	0,991236025	

T2-PEF-C1

	Measured				Corrected				Average	
ΔP (Pa)	V_sys (ml/min)		V_tot (ml/min)		V_0,sys (ml/min)		V_0,tot (ml/min)		V_0,sys,avg	V_0,tot,avg
	1st series	2nd series	1st series	2nd series	1st series	2nd series	1st series	2nd series		
10	63	59	134	126	62,448	58,483	132,826	124,896	60,465	128,861
15	121	117	231	265	119,940	115,975	228,976	262,678	117,957	245,827
22	169	179	410	420	167,519	177,431	406,407	416,319	172,475	411,363
32	274	255	690	700	271,599	252,765	683,953	693,865	262,182	688,909
46	375	306	900	830	371,714	303,318	892,112	822,726	337,516	857,419
68	560	490	1190	1130	555,092	485,706	1179,571	1120,097	520,399	1149,834
100	720	630	1460	1400	713,690	624,479	1447,205	1387,730	669,084	1417,468

Laboratory conditions		
Temperature	21,9	°C
RH	21,3	%
Atm	100	kPa
ρ_0	1,1988	
ρ_w	688,6266927	
ρ	1,177619298	
Corr. factor	0,991126504	

T2-PEF-C2

	Measured				Corrected				Average	
ΔP (Pa)	V_sys (ml/min)		V_tot (ml/min)		V_0,sys (ml/min)		V_0,tot (ml/min)		V_0,sys,avg	V_0,tot,avg
	1st series	2nd series	1st series	2nd series	1st series	2nd series	1st series	2nd series		
10	207	204	295	375	205,186	202,212	292,415	371,714	203,699	332,064
15	359	378	550	630	355,854	374,687	545,180	624,479	365,270	584,829
22	510	502	850	920	505,530	497,600	842,551	911,937	501,565	877,244
32	740	730	1280	1290	733,515	723,602	1268,782	1278,694	728,558	1273,738
46	1050	1000	1690	1620	1040,798	991,236	1675,189	1605,802	1016,017	1640,496
68	1460	1440	2260	2150	1447,205	1427,380	2240,193	2131,157	1437,292	2185,675
100	2190	2230	3030	2980	2170,807	2210,456	3003,445	2953,883	2190,632	2978,664

Laboratory conditions		
Temperature	21,9	°C
RH	21,3	%
Atm	100	kPa
ρ_0	1,1988	
ρ_w	688,6266927	
ρ	1,177619298	
Corr. factor	0,991126504	

T2-PEF-C3

	Measured				Corrected				Average	
ΔP (Pa)	V_sys (ml/min)		V_tot (ml/min)		V_0,sys (ml/min)		V_0,tot (ml/min)		V_0,sys,avg	V_0,tot,avg
	1st series	2nd series	1st series	2nd series	1st series	2nd series	1st series	2nd series		
10	149	153	263	270	175,504	180,216	309,782	318,027	177,860	313,905
15	281	281	378	390	330,984	330,984	445,238	459,373	330,984	452,306
22	410	410	740	750	482,931	482,931	871,631	883,410	482,931	877,520
32	630	640	960	970	742,064	753,843	1130,764	1142,543	747,954	1136,654
46	770	770	1370	1340	906,967	906,967	1613,695	1578,359	906,967	1596,027
68	1110	1100	1860	1850	1307,446	1295,668	2190,856	2179,077	1301,557	2184,967
100	1730	1740	2510	2530	2037,732	2049,510	2956,478	2980,035	2043,621	2968,257

Laboratory conditions		
Temperature	22,2	°C
RH	21,5	%
Atm	100	kPa
ρ_0	1,1988	
ρ_w	709,8951244	
ρ	1,176328112	
Corr. factor	0,990583001	

T3-PEF-A

	Measured				Corrected				Average	
ΔP (Pa)	V_sys (ml/min)		V_tot (ml/min)		V_0,sys (ml/min)		V_0,tot (ml/min)		V_0,sys,avg	V_0,tot,avg
	1st series	2nd series	1st series	2nd series	1st series	2nd series	1st series	2nd series		
10	129	115	2370	2730	127,869	113,992	2349,229	2706,074	120,931	2527,652
15	187	145	3310	4100	185,361	143,729	3280,991	4064,068	164,545	3672,529
22	249	210	4230	5180	246,818	208,160	4192,928	5134,603	227,489	4663,765
32	339	298	6330	6650	336,029	295,388	6274,524	6591,720	315,709	6433,122
46	440	418	7720	8110	436,144	414,337	7652,342	8038,924	425,240	7845,633
68	650	630	8040	8300	644,303	624,479	7969,538	8227,259	634,391	8098,398
100	910	870	8900	8800	902,025	862,375	8822,001	8722,877	882,200	8772,439

Laboratory conditions		
Temperature	21,9	°C
RH	19,5	%
Atm	100	kPa
ρ_0	1,1988	
ρ_w	630,4328877	
ρ	1,177879571	
Corr. factor	0,991236025	

T3-PEF-B

	Measured				Corrected				Average	
ΔP (Pa)	V_sys (ml/min)		V_tot (ml/min)		V_0,sys (ml/min)		V_0,tot (ml/min)		V_0,sys,avg	V_0,tot,avg
	1st series	2nd series	1st series	2nd series	1st series	2nd series	1st series	2nd series		
10	18,3	19,2	98	101	18,140	19,032	97,141	100,115	18,586	98,628
15	26,5	26,3	148	149	26,268	26,070	146,703	147,694	26,169	147,199
22	45	46,1	217	211	44,606	45,696	215,098	209,151	45,151	212,125
32	58,7	59	317	306	58,186	58,483	314,222	303,318	58,334	308,770
46	87,2	87,1	407	419	86,436	86,337	403,433	415,328	86,386	409,380
68	121	117	630	650	119,940	115,975	624,479	644,303	117,957	634,391
100	159	158	930	960	157,607	156,615	921,850	951,587	157,111	936,718

Laboratory conditions		
Temperature	21,9	°C
RH	19,5	%
Atm	100	kPa
ρ_0	1,1988	
ρ_w	630,4328877	
ρ	1,177879571	
Corr. factor	0,991236025	

T3-PEF-C

	Measured				Corrected				Average	
ΔP (Pa)	V_sys (ml/min)		V_tot (ml/min)		V_0,sys (ml/min)		V_0,tot (ml/min)		V_0,sys,avg	V_0,tot,avg
	1st series	2nd series	1st series	2nd series	1st series	2nd series	1st series	2nd series		
10	90	92	179	186	89,211	91,194	177,431	184,370	90,202	180,901
15	117	121	267	266	115,975	119,940	264,660	263,669	117,957	264,164
22	149	150	430	430	147,694	148,685	426,231	426,231	148,190	426,231
32	163	167	590	610	161,571	165,536	584,829	604,654	163,554	594,742
46	221	230	880	890	219,063	227,984	872,288	882,200	223,524	877,244
68	367	348	1350	1330	363,784	344,950	1338,169	1318,344	354,367	1328,256
100	500	510	2030	1910	495,618	505,530	2012,209	1893,261	500,574	1952,735

Laboratory conditions		
Temperature	21,8	°C
RH	19,9	%
Atm	100	kPa
ρ_0	1,1988	
ρ_w	638,8554206	
ρ	1,178241237	
Corr. factor	0,991388192	

T1-ROM-A

	Measured				Corrected				Average	
ΔP (Pa)	V_sys (ml/min)		V_tot (ml/min)		V_0,sys (ml/min)		V_0,tot (ml/min)		V_0,sys,avg	V_0,tot,avg
	1st series	2nd series	1st series	2nd series	1st series	2nd series	1st series	2nd series		
10	119	124	276	281	117,957	122,913	273,581	278,537	120,435	276,059
15	193	201	377	375	191,309	199,238	373,696	371,714	195,273	372,705
22	304	300	570	559	301,336	297,371	565,005	554,101	299,353	559,553
32	456	449	880	880	452,004	445,065	872,288	872,288	448,534	872,288
46	770	770	1310	1300	763,252	763,252	1298,519	1288,607	763,252	1293,563
68	1190	1200	1990	2000	1179,571	1189,483	1972,560	1982,472	1184,527	1977,516
100	1660	1680	2870	2870	1645,452	1665,277	2844,847	2844,847	1655,364	2844,847

Laboratory conditions		
Temperature	21,6	°C
RH	19,5	%
Atm	100	kPa
ρ_0	1,1988	
ρ_w	617,2601662	
ρ	1,179137405	
Corr. factor	0,991765145	

T1-ROM-B

	Measured				Corrected				Average	
ΔP (Pa)	V_sys (ml/min)		V_tot (ml/min)		V_0,sys (ml/min)		V_0,tot (ml/min)		V_0,sys,avg	V_0,tot,avg
	1st series	2nd series	1st series	2nd series	1st series	2nd series	1st series	2nd series		
10	99	106	267	231	98,132	105,071	264,660	228,976	101,602	246,818
15	183	190	410	389	181,396	188,335	406,407	385,591	184,866	395,999
22	287	288	650	630	284,485	285,476	644,303	624,479	284,980	634,391
32	400	420	850	790	396,494	416,319	842,551	783,076	406,407	812,814
46	720	720	1410	1400	713,690	713,690	1397,643	1387,730	713,690	1392,687
68	1050	1130	1980	2000	1040,798	1120,097	1962,647	1982,472	1080,447	1972,560
100	1500	1490	3070	3020	1486,854	1476,942	3043,095	2993,533	1481,898	3018,314

Laboratory conditions		
Temperature	21,7	°C
RH	19,5	%
Atm	100	kPa
ρ_0	1,1988	
ρ_w	621,6232505	
ρ	1,178717967	
Corr. factor	0,991588736	

450

T2-ROM-A

	Measured				Corrected				Average	
ΔP (Pa)	V_sys (ml/min)		V_tot (ml/min)		V_0,sys (ml/min)		V_0,tot (ml/min)		V_0,sys,avg	V_0,tot,avg
	1st series	2nd series	1st series	2nd series	1st series	2nd series	1st series	2nd series		
10	122	120	213	209	120,931	118,948	211,133	207,168	119,940	209,151
15	192	188	363	368	190,317	186,352	359,819	364,775	188,335	362,297
22	322	325	640	630	319,178	322,152	634,391	624,479	320,665	629,435
32	490	500	880	890	485,706	495,618	872,288	882,200	490,662	877,244
46	700	710	1090	1070	693,865	703,778	1080,447	1060,623	698,821	1070,535
68	980	980	1670	1650	971,411	971,411	1655,364	1635,539	971,411	1645,452
100	1470	1460	2490	2510	1457,117	1447,205	2468,178	2488,002	1452,161	2478,090

Laboratory conditions		
Temperature	21,6	°C
RH	18,7	%
Atm	100	kPa
ρ_0	1,1988	
ρ_w	591,9366722	
ρ	1,17925078	
Corr. factor	0,991812823	

T2-ROM-B

	Measured				Corrected				Average	
ΔP (Pa)	V_sys (ml/min)		V_tot (ml/min)		V_0,sys (ml/min)		V_0,tot (ml/min)		V_0,sys,avg	V_0,tot,avg
	1st series	2nd series	1st series	2nd series	1st series	2nd series	1st series	2nd series		
10	136	135	236	241	134,808	133,817	233,932	238,888	134,312	236,410
15	206	215	329	338	204,195	213,116	326,117	335,038	208,655	330,577
22	374	383	590	580	370,722	379,643	584,829	574,917	375,183	579,873
32	510	510	890	890	505,530	505,530	882,200	882,200	505,530	882,200
46	750	690	1270	1290	743,427	683,953	1258,870	1278,694	713,690	1268,782
68	930	900	1700	1730	921,850	892,112	1685,101	1714,838	906,981	1699,970
100	1390	1360	2070	2110	1377,818	1348,081	2051,859	2091,508	1362,950	2071,683

Laboratory conditions		
Temperature	21,6	°C
RH	18,7	%
Atm	100	kPa
ρ_0	1,1988	
ρ_w	591,9366722	
ρ	1,17925078	
Corr. factor	0,991812823	

T3-ROM-A

	Measured				Corrected				Average	
ΔP (Pa)	V_sys (ml/min)		V_tot (ml/min)		V_0,sys (ml/min)		V_0,tot (ml/min)		V_0,sys,avg	V_0,tot,avg
	1st series	2nd series	1st series	2nd series	1st series	2nd series	1st series	2nd series		
10	142	138	550	550	140,756	136,791	545,180	545,180	138,773	545,180
15	203	199	840	850	201,221	197,256	832,638	842,551	199,238	837,594
22	335	333	1090	1290	332,064	330,082	1080,447	1278,694	331,073	1179,571
32	510	500	1600	1620	505,530	495,618	1585,978	1605,802	500,574	1595,890
46	720	730	1960	2010	713,690	723,602	1942,823	1992,384	718,646	1967,604
68	1010	1000	2580	2490	1001,148	991,236	2557,389	2468,178	996,192	2512,783
100	1530	1510	3530	3550	1516,591	1496,766	3499,063	3518,888	1506,679	3508,976

Laboratory conditions		
Temperature	21,6	°C
RH	19,5	%
Atm	100	kPa
ρ_0	1,1988	
ρ_w	617,2601662	
ρ	1,179137405	
Corr. factor	0,991765145	

T3-ROM-B

	Measured				Corrected				Average	
ΔP (Pa)	V_sys (ml/min)		V_tot (ml/min)		V_0,sys (ml/min)		V_0,tot (ml/min)		V_0,sys,avg	V_0,tot,avg
	1st series	2nd series	1st series	2nd series	1st series	2nd series	1st series	2nd series		
10	90	96	370	390	89,211	95,159	366,757	386,582	92,185	376,670
15	149	157	580	540	147,694	155,624	574,917	535,267	151,659	555,092
22	247	256	710	700	244,835	253,756	703,778	693,865	249,296	698,821
32	377	384	1270	1250	373,696	380,635	1258,870	1239,045	377,165	1248,957
46	580	580	1600	1610	574,917	574,917	1585,978	1595,890	574,917	1590,934
68	790	800	2470	2440	783,076	792,989	2448,353	2418,616	788,033	2433,484
100	1290	1280	3540	3570	1278,694	1268,782	3508,976	3538,713	1273,738	3523,844

Laboratory conditions		
Temperature	21,6	°C
RH	19,8	%
Atm	100	kPa
ρ_0	1,1988	
ρ_w	626,7564764	
ρ	1,17909489	
Corr. factor	0,991747265	

NT-ROM-A (substrate leakage)

	Measured				Corrected				Average	
ΔP (Pa)	V_sys (ml/min)		V_tot (ml/min)		V_0,sys (ml/min)		V_0,tot (ml/min)		V_0,sys,avg	V_0,tot,avg
	1st series	2nd series	1st series	2nd series	1st series	2nd series	1st series	2nd series		
10	23	26	156	152	22,798	25,772	154,633	150,668	24,285	152,650
15	30	29	225	224	29,737	28,746	223,028	222,037	29,241	222,532
22	53	55	346	344	52,536	54,518	342,968	340,985	53,527	341,976
32	77	81	540	550	76,325	80,290	535,267	545,180	78,308	540,224
46	112	110	790	810	111,018	109,036	783,076	802,901	110,027	792,989
68	154	160	1090	1100	152,650	158,598	1080,447	1090,360	155,624	1085,403
100	197	201	1710	1700	195,273	199,238	1695,014	1685,101	197,256	1690,057

Laboratory conditions		
Temperature	21,9	°C
RH	19,5	%
Atm	100	kPa
ρ_0	1,1988	
ρ_w	630,4328877	
ρ	1,177879571	
Corr. factor	0,991236025	

NT-ROM-B (substrate leakage)

	Measured				Corrected				Average	
ΔP (Pa)	V_sys (ml/min)		V_tot (ml/min)		V_0,sys (ml/min)		V_0,tot (ml/min)		V_0,sys,avg	V_0,tot,avg
	1st series	2nd series	1st series	2nd series	1st series	2nd series	1st series	2nd series		
10	22	19	152	150	25,877	22,348	178,783	176,431	24,112	177,607
15	30	31	198	205	35,286	36,462	232,889	241,122	35,874	237,005
22	41	44	257	266	48,224	51,753	302,285	312,870	49,989	307,578
32	66	68	356	361	77,630	79,982	418,729	424,610	78,806	421,669
46	96	96	500	490	112,916	112,916	588,102	576,340	112,916	582,221
68	149	153	740	740	175,254	179,959	870,391	870,391	177,607	870,391
100	196	201	1150	1170	230,536	236,417	1352,635	1376,159	233,477	1364,397

Laboratory conditions		
Temperature	22,1	°C
RH	21,6	%
Atm	100	kPa
ρ_0	1,1988	
ρ_w	708,2084616	
ρ	1,176734068	
Corr. factor	0,990753913	

Permeability measurements, aged condition:

T1-PEF-A

	Measured airflow				Corrected				Average	
ΔP (Pa)	V_sys (ml/min)		V_tot (ml/min)		V_0,sys (ml/min)		V_0,tot (ml/min)		V_0,sys,avg	V_0,tot,avg
	1st series	2nd series	1st series	2nd series	1st series	2nd series	1st series	2nd series		
10	580	600	25800	25000	573,748	593,533	25521,901	24730,524	583,640	25126,213
15	1020	1040	38900	35800	1009,005	1028,790	38480,696	35414,111	1018,897605	36947,403
22	1380	1410	47100	47700	1365,125	1394,802	46592,308	47185,841	1379,963261	46889,074
32	1900	1930	58400	57800	1879,520	1909,196	57770,505	57176,972	1894,358168	57473,739
46	2440	2500	67300	66900	2413,699	2473,052	66574,572	66178,883	2443,375809	66376,727
68	3490	3500	80200	79900	3452,381	3462,273	79335,522	79038,756	3457,327309	79187,139
100	4800	4900	97400	97500	4748,261	4847,183	96350,123	96449,045	4797,721731	96399,584

Laboratory conditions		
Temperature	22,5	°C
RH	34,6	%
Atm pressure	100	kPa
ρ_0	1,1988	
ρ_w	1166,713574	
ρ	1,173095496	
Corr. factor	0,989220975	

T1-PEF-B

	Measured airflow				Corrected				Average	
ΔP (Pa)	V_sys (ml/min)		V_tot (ml/min)		V_0,sys (ml/min)		V_0,tot (ml/min)		V_0,sys,avg	V_0,tot,avg
	1st series	2nd series	1st series	2nd series	1st series	2nd series	1st series	2nd series		
10	360	370	910	940	356,845	366,757	902,025	931,762	361,801	916,893
15	510	510	1470	1440	505,530	505,530	1457,117	1427,380	505,5303729	1442,248
22	710	730	2080	2100	703,778	723,602	2061,771	2081,596	713,6899382	2071,683
32	1080	1090	2640	2670	1070,535	1080,447	2616,863	2646,600	1075,491087	2631,732
46	1560	1550	3420	3420	1546,328	1536,416	3390,027	3390,027	1541,372019	3390,027
68	2260	2270	4470	4430	2240,193	2250,106	4430,825	4391,176	2245,149597	4411,000
100	3100	3290	5780	5820	3072,832	3261,167	5729,344	5768,994	3166,999101	5749,169

Laboratory conditions		
Temperature	21,9	°C
RH	19,5	%
Atm pressure	100	kPa
ρ_0	1,1988	
ρ_w	630,4328877	
ρ	1,177879571	
Corr. factor	0,991236025	

T1-PEF-C

	Measured airflow				Corrected				Average	
ΔP (Pa)	V_sys (ml/min)		V_tot (ml/min)		V_0,sys (ml/min)		V_0,tot (ml/min)		V_0,sys,avg	V_0,tot,avg
	1st series	2nd series	1st series	2nd series	1st series	2nd series	1st series	2nd series		
10	240	260	1900	1880	237,897	257,721	1883,348	1863,524	247,809	1873,436
15	550	560	3320	3350	545,180	555,092	3290,904	3320,641	550,135994	3305,772
22	960	960	5280	5330	951,587	951,587	5233,726	5283,288	951,5865843	5258,507
32	1500	1530	7000	7030	1486,854	1516,591	6938,652	6968,389	1501,722578	6953,521
46	2220	2200	8900	8880	2200,544	2180,719	8822,001	8802,176	2190,631616	8812,088
68	3210	3240	11200	11100	3181,868	3211,605	11101,843	11002,720	3196,736181	11052,282
100	4490	4510	13800	13700	4450,650	4470,474	13679,057	13579,934	4460,562114	13629,495

Laboratory conditions		
Temperature	21,9	°C
RH	19,5	%
Atm pressure	100	kPa
ρ_0	1,1988	
ρ_w	630,4328877	
ρ	1,177879571	
Corr. factor	0,991236025	

T2-PEF-A

	Measured airflow				Corrected				Average	
ΔP (Pa)	V_sys (ml/min)		V_tot (ml/min)		V_0,sys (ml/min)		V_0,tot (ml/min)		V_0,sys,avg	V_0,tot,avg
	1st series	2nd series	1st series	2nd series	1st series	2nd series	1st series	2nd series		
10	410	400	810	800	406,407	396,494	802,901	792,989	401,451	797,945
15	720	730	1170	1180	713,690	723,602	1159,746	1169,659	718,6461183	1164,702
22	1130	1170	1680	1690	1120,097	1159,746	1665,277	1675,189	1139,921429	1670,233
32	1810	1840	2410	2410	1794,137	1823,874	2388,879	2388,879	1809,005746	2388,879
46	2660	2640	3270	3300	2636,688	2616,863	3241,342	3271,079	2626,775467	3256,210
68	3850	3800	4520	4510	3816,259	3766,697	4480,387	4470,474	3791,477797	4475,431
100	5190	5210	6130	6170	5144,515	5164,340	6076,277	6115,926	5154,427331	6096,102

Laboratory conditions		
Temperature	21,9	°C
RH	19,5	%
Atm pressure	100	kPa
ρ_0	1,1988	
ρ_w	630,4328877	
ρ	1,177879571	
Corr. factor	0,991236025	

T2-PEF-B

	Measured airflow				Corrected				Average	
ΔP (Pa)	V_sys (ml/min)		V_tot (ml/min)		V_0,sys (ml/min)		V_0,tot (ml/min)		V_0,sys,avg	V_0,tot,avg
	1st series	2nd series	1st series	2nd series	1st series	2nd series	1st series	2nd series		
10	360	350	2890	2910	356,845	346,933	2864,672	2884,497	351,889	2874,584
15	690	690	4990	5040	683,953	683,953	4946,268	4995,830	683,9528574	4971,049
22	1020	1000	7200	7130	1011,061	991,236	7136,899	7067,513	1001,148386	7102,206
32	1570	1540	9400	9320	1556,241	1526,503	9317,619	9238,320	1541,372019	9277,969
46	2330	2270	12400	12300	2309,580	2250,106	12291,327	12192,203	2279,842858	12241,765
68	3200	3230	16600	16500	3171,955	3201,692	16454,518	16355,394	3186,823821	16404,956
100	4460	4430	21500	21400	4420,913	4391,176	21311,575	21212,451	4406,044132	21262,013

Laboratory conditions		
Temperature	21,9	°C
RH	19,5	%
Atm pressure	100	kPa
ρ_0	1,1988	
ρ_w	630,4328877	
ρ	1,177879571	
Corr. factor	0,991236025	

T1-ROM-A

	Measured airflow				Corrected				Average	
ΔP (Pa)	V_sys (ml/min)		V_tot (ml/min)		V_0,sys (ml/min)		V_0,tot (ml/min)		V_0,sys,avg	V_0,tot,avg
	1st series	2nd series	1st series	2nd series	1st series	2nd series	1st series	2nd series		
10	157	158	690	700	155,624	156,615	683,953	693,865	156,120	688,909
15	275	270	1230	1250	272,590	267,634	1219,220	1239,045	270,1118169	1229,133
22	430	421	1820	1860	426,231	417,310	1804,050	1843,699	421,7709288	1823,874
32	570	560	2560	2610	565,005	555,092	2537,564	2587,126	560,0483543	2562,345
46	810	800	3520	3550	802,901	792,989	3489,151	3518,888	797,9450003	3504,019
68	1190	1210	5030	5110	1179,571	1199,396	4985,917	5065,216	1189,48323	5025,567
100	1850	1880	7460	7250	1833,787	1863,524	7394,621	7186,461	1848,655187	7290,541

Laboratory conditions		
Temperature	21,9	°C
RH	19,5	%
Atm pressure	100	kPa
ρ_0	1,1988	
ρ_w	630,4328877	
ρ	1,177879571	
Corr. factor	0,991236025	

T1-ROM-B

	Measured airflow				Corrected				Average	
ΔP (Pa)	V_sys (ml/min)		V_tot (ml/min)		V_0,sys (ml/min)		V_0,tot (ml/min)		V_0,sys,avg	V_0,tot,avg
	1st series	2nd series	1st series	2nd series	1st series	2nd series	1st series	2nd series		
10	198	202	420	430	196,265	200,230	416,319	426,231	198,247	421,275
15	309	315	690	720	306,292	312,239	683,953	713,690	309,2656399	698,821
22	450	470	1130	1190	446,056	465,881	1120,097	1179,571	455,9685716	1149,834
32	690	700	1800	1840	683,953	693,865	1784,225	1823,874	688,9090376	1804,050
46	930	950	2680	2710	921,850	941,674	2656,513	2686,250	931,7618637	2671,381
68	1350	1420	4220	4260	1338,169	1407,555	4183,016	4222,665	1372,861895	4202,841
100	2140	2190	6230	6270	2121,245	2170,807	6175,400	6215,050	2146,025995	6195,225

Laboratory conditions		
Temperature	21,9	°C
RH	19,5	%
Atm pressure	100	kPa
ρ_0	1,1988	
ρ_w	630,4328877	
ρ	1,177879571	
Corr. factor	0,991236025	

T2-ROM-A

	Measured airflow				Corrected				Average	
ΔP (Pa)	V_sys (ml/min)		V_tot (ml/min)		V_0,sys (ml/min)		V_0,tot (ml/min)		V_0,sys,avg	V_0,tot,avg
	1st series	2nd series	1st series	2nd series	1st series	2nd series	1st series	2nd series		
10	135	137	420	430	133,817	135,799	416,319	426,231	134,808	421,275
15	269	277	660	660	266,642	274,572	654,216	654,216	270,6074349	654,216
22	415	419	960	1000	411,363	415,328	951,587	991,236	413,3454225	971,411
32	570	580	1230	1270	565,005	574,917	1219,220	1258,870	569,9607145	1239,045
46	790	810	1750	1730	783,076	802,901	1734,663	1714,838	792,9888202	1724,751
68	1250	1240	2640	2660	1239,045	1229,133	2616,863	2636,688	1234,088851	2626,775
100	1970	2010	3730	3710	1952,735	1992,384	3697,310	3677,486	1972,55969	3687,398

Laboratory conditions		
Temperature	21,9	°C
RH	19,5	%
Atm pressure	100	kPa
ρ_0	1,1988	
ρ_w	630,4328877	
ρ	1,177879571	
Corr. factor	0,991236025	

T2-ROM-B

	Measured airflow				Corrected				Average	
ΔP (Pa)	V_sys (ml/min)		V_tot (ml/min)		V_0,sys (ml/min)		V_0,tot (ml/min)		V_0,sys,avg	V_0,tot,avg
	1st series	2nd series	1st series	2nd series	1st series	2nd series	1st series	2nd series		
10	327	298	390	399	324,134	295,388	386,582	395,503	309,761	391,043
15	400	410	630	620	396,494	406,407	624,479	614,566	401,4505902	619,523
22	550	530	980	980	545,180	525,355	971,411	971,411	535,2674536	971,411
32	740	770	1510	1490	733,515	763,252	1496,766	1476,942	748,3831991	1486,854
46	980	1030	2130	2100	971,411	1020,973	2111,333	2081,596	996,1922054	2096,464
68	1490	1480	3030	3110	1476,942	1467,029	3003,445	3082,744	1471,985498	3043,095
100	2230	2300	4260	4320	2210,456	2279,843	4222,665	4282,140	2245,149597	4252,403

Laboratory conditions		
Temperature	21,9	°C
RH	19,5	%
Atm pressure	100	kPa
ρ_0	1,1988	
ρ_w	630,4328877	
ρ	1,177879571	
Corr. factor	0,991236025	

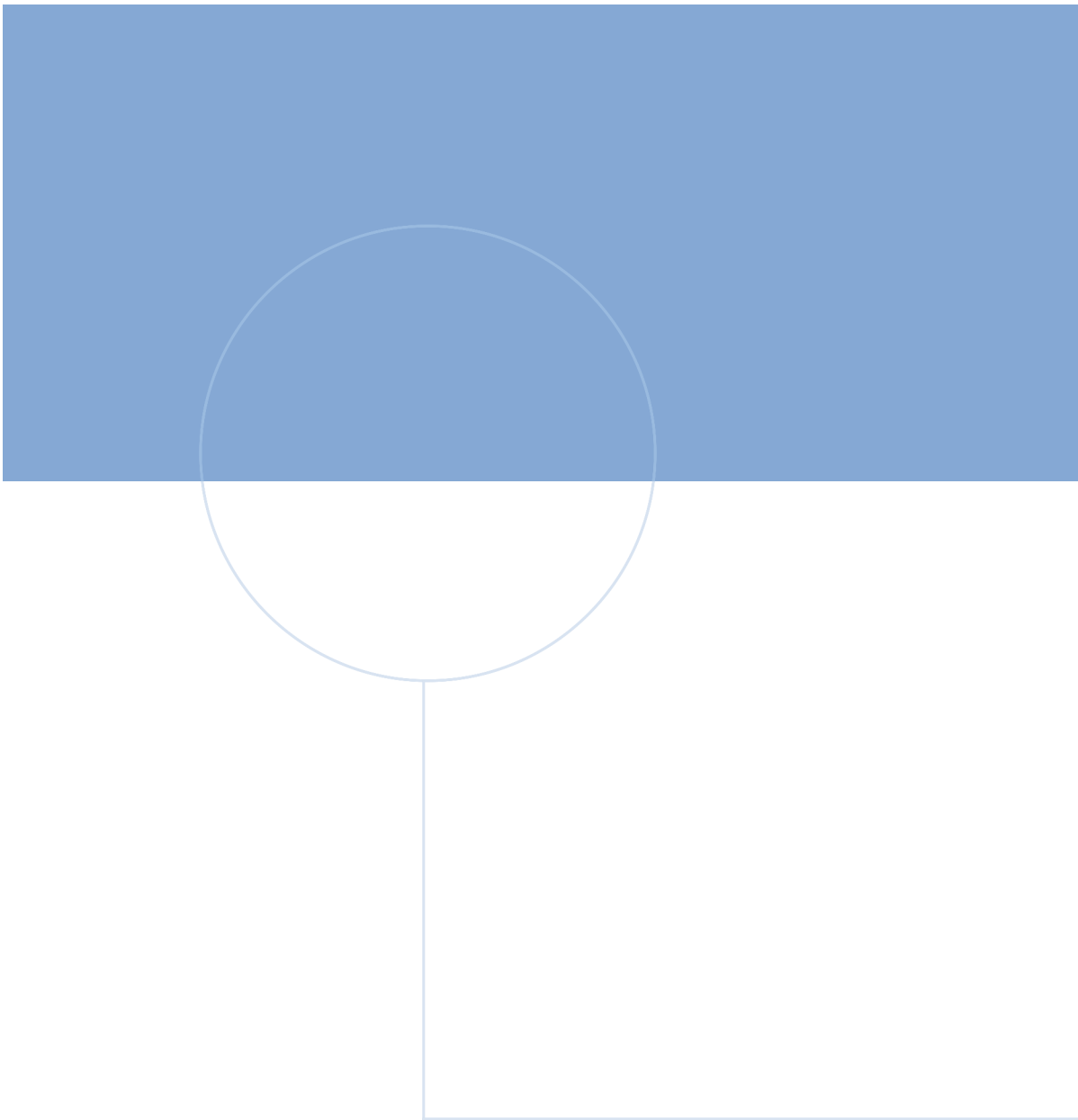

NTNU
Norwegian University of
Science and Technology

SINTEF